# DISSERTATION

Fakultät für Medizin

Institut für Medizinische Mikrobiologie, Immunologie und Hygiene

**Triggers of anti-CNS autoimmunity in the mouse model of Multiple Sclerosis**

Pushpalatha Palle

Vollständiger Abdruck der von der Fakultät für Medizin der Technischen Universität München zur Erlangung des akademischen Grades eines

**Doktors der Naturwissenschaften (Dr. rer. nat)**

genehmigten Dissertation.

Vorsitzender:

Prof. Dr. Thomas Korn

Prüfer der Dissertation:

1. apl. Prof. Dr. Clarissa Prazeres da Costa

2. Prof. Dr. Martin Klingenspor

Die Dissertation wurde am 28.07.2016 bei der Technischen Universität München eingereicht und durch die Fakultät für Medizin am 15.02.2017 angenommen.

## STATUTORY DECLARATION

I hereby declare that I have authored this thesis independently, that I have not used other than the declared sources / resources and that I have explicitly marked all material which has been quoted either literally or by content from the used sources.

# Contents

## Contents

# List of Figures

# List of Tables

# Abbreviations

| | |
|---|---|
| APCs | Antigen presenting cells |
| BBB | Blood Brain Barrier |
| BCR | B cell receptors |
| BMS | Benign MS |
| cDCs | Conventional DCs |
| CFA | Complete freund adjuvant |
| CNS | Central Nervous System |
| CTLA4 | Cytotoxic T-lymphocyte-associated protein 4 |
| DAMPs | Danger-associated molecular patterns |
| DCs | Dendritic cells |
| DN | Double negative |
| DP | Double positive |
| EAE | Experimental Autoimmune Encephalomyelitis |
| EBV | Epstein barr virus |
| ER | Endoplasmic Reticulum |
| FB | Follicular B |
| HHV-6 | Human herpesvirus 6 |
| HLA | Human leukocyte antigen |
| HRP | Horseradish peroxidase |
| HSCs | Hematopoietic stem cells |
| ICAM1 | Intercellular Adhesion Molecule 1 |
| IKK | I kappa B kinase |
| IL-1R | Interleukin 1 receptor |
| IRAK | Interleukin-1 Receptor-Associated Kinase |
| IκBα | Inhibitor of kappa B |

| | |
|---|---|
| LFB | Luxol fast blue |
| LRPs | Leucine rich repeats |
| MAL | MyD88-adaptor-like protein |
| MAPK | Mitogen-activated protein kinases |
| MBP | Myelin basic protein |
| mDCs | Myeloid DCs |
| MHC | Major Histocompatibility complex |
| MOG | Myelin oligodendrocyte glycoprotein |
| MS | Multiple Sclerosis |
| MyD88 | Myeloid differentiation primary response gene 88 |
| MZB | Splenic marginal zone B |
| NK | Natural killer |
| NLRs | NOD-like receptors |
| NOD | Nucleotide oligomerization domain |
| OD | Optical Density |
| OPC | Oligodendrocyte precursor cell |
| PAMPs | Pathogen associated molecular patterns |
| PB | Permeabilization buffer |
| PBMCs | Peripheral blood mononuclear cell |
| PCR | Polymerase Chain Reaction |
| pDCs | Plasmacytoid DCs |
| PIP2 | Phosphatidylinositol 4, 5-bisphosphate |
| PLP | Proteolipid protein |
| poly (I:C) | Polyinosinic:polycytidylic acid |
| PPMS | Primary Progressive MS |
| PPR | Pattern recognition receptors |
| PRMS | Progressive Relapsing MS |
| PT | Pertussis toxin |
| qPCR | quantitative-PCR/real-time PCR |

| | |
|---|---|
| RIG | Retinoic acid-inducible gene I |
| RIP-1 | Receptor-interacting protein |
| RLRs | RIG-like receptors |
| RRMS | Relapsing-remitting MS |
| SARM | Sterile α- and armadillo-motif-containing protein |
| SH2D2A | SH2 Domain Containing 2A |
| SLE | Systemic lupus erythematosus |
| SNS | Single nucleotide polymorphisms |
| SPMS | Secondary Progressive MS |
| SPMS | Single positive |
| TAB2 | TAK1 binding protein 2 |
| TAB3 | TAK1 binding protein 3 |
| TAK1 | Transforming growth factor beta-activated kinase 1 |
| TCR | T cell receptor |
| Th | T helper cells |
| TICAM2 | TIR domain containing molecule 2 |
| TIR | Toll/IL-1R |
| TIRAP | TIR-domain-containing adaptor protein |
| TLRs | Toll-like receptors |
| TRAF6 | Tumor necrosis factor receptor associated factor |
| TRAM | TRIF-related adaptor molecule |
| Tregs | Regulatory T cells |
| TRIF | TIR domain containing IFN β inducing |
| Wt | Wild type |

# ABSTRACT

Multiple sclerosis (MS) is an auto inflammatory disorder of the central nervous system (CNS) involving demyelination of axons. Infectious agents have been strongly implicated in the pathogenesis of MS. Also, studies from the animal model of MS, namely experimental autoimmune encephalomyelitis (EAE), have shown a prominent role for gut flora in disease induction, thus suggesting that pattern recognition receptors (PRRs) that recognize pathogen associated molecular patterns (PAMPs) might play a crucial role in EAE. Toll like receptors (TLRs) are the prominent PRRs of the innate immune system and therefore, we sought to investigate their role in EAE using *TLR9*$^{-/-}$, *TLR3*$^{-/-}$, *TLR379*$^{-/-}$ and *TLR23479*$^{-/-}$ mice. *TLR9*$^{-/-}$ , *TLR379*$^{-/-}$ and *TLR23479*$^{-/-}$ were all susceptible to EAE induction and further they exhibited more severe clinical symptoms in comparison to Wt controls. However, histological analysis of sick *TLR9*$^{-/-}$, *TLR379*$^{-/-}$ , *TLR23479*$^{-/-}$ and Wt mice at the peak of the disease revealed comparable extent of demyelination and infiltration by T cells in the CNS of TLR deficient and Wt control mice. On other hand, *TLR3*$^{-/-}$ mice exhibited low disease incidence and almost complete resistance to EAE induction. Because signaling through TLRs 3,4,7 and 9 leads to interferon beta production, which has been reported to be beneficial in EAE, we analyzed the relative mRNA expression of interferon beta levels during the initiation phase and the effector phase of EAE in *TLR23479*$^{-/-}$ and did not observe major differences when compared to Wt controls. Also, relative mRNA expression of pro-inflammatory cytokines remained comparable between *TLR23479*$^{-/-}$ and Wt mice during the course of EAE. Finally, we observed that TLR9 which recognizes *CpG DNA of mycobacterial components in* CFA is dispensable for EAE induction. Taken together, we observed that deficiency of TLR3 but not TLR 9 confers protection from developing EAE clinical signs. In contrast, combined deficiency of TLR3 along with TLRs 2, 4, 7 and 9 does not confer resistance to disease induction as *TLR23479*$^{-/-}$ mice were highly susceptible to disease induction.

# Zusammenfassung

Multiple Sklerose (MS) ist eine chronisch-entzündliche Erkrankung des zentralen Nervensystems (ZNS), welche zu Entmarkung der Axone führt. Infektionserreger werden mit der Krankheitsentstehung von MS stark in Verbindung gebracht. Zusätzlich zeigten Studien am Tiermodel experimentelle autoimmune Enzephalomyelitis (EAE), dass auch die Darmflora eine prominente Rolle in der Krankheitsinduktion spielt. Dies legt nahe, dass sogenannte Mustererkennungsrezeptoren, die zur Erkennung von Pathogen-assoziierten molekularen Mustern dienen, an der Auslösung der Erkrankung beteiligt sein könnten. Toll-like-Rezeptoren (TLRs) sind bekannte Mustererkennungsrezeptoren des angeborenen Immunsystems, deren Rolle in EAE mit Hilfe von *TLR9*$^{-/-}$, *TLR3*$^{-/-}$, *TLR379*$^{-/-}$ und *TLR23479*$^{-/-}$ Mäuse untersucht werden soll. *TLR9*$^{-/-}$, *TLR379*$^{-/-}$ und *TLR23479*$^{-/-}$ Mäuse waren alle empfänglich für die Induktion von EAE und entwickelten darüber hinaus stärkere klinische Symptome im Vergleich zu Wildtyp-Mäusen. Die histologische Untersuchung von erkrankten *TLR9*$^{-/-}$, *TLR379*$^{-/-}$, *TLR23479*$^{-/-}$ und Kontrollmäusen zum Zeitpunkt des Höhepunktes der Krankheit zeigte eine vergleichbare Entmarkung der Axone und Infiltration von T-Zellen in das ZNS von TLR-defizienten- und Wildtyp-Kontrollmäusen. Im Gegensatz dazu, zeigten *TLR3*$^{-/-}$ Mäuse eine fast komplette Resistenz der EAE-Induktion sowie eine deutlich abgeschwächte Symptomatik in den wenigen positiven Fällen. Auf Grund dessen, dass die Aktivierung von TLR-3,-4,-7 und -9 zu Interferon-beta Produktion führt, wurde die relative mRNA Expression von Interferon-beta während der Initiations- und Effektorphase von EAE in *TLR23479*$^{-/-}$ Mäusen gemessen und es konnten keine Unterschiede zu Wildtyp-Kontrollen festgestellt werden. Ebenso zeigte sich die relative mRNA Expression von pro-inflammatorischen Zytokinen im Krankheitsverlauf von EAE zwischen *TLR23479*$^{-/-}$ und Wildtyp-Mäusen vergleichbar. Schließlich, beobachteten wir, dass TLR 9, welches CpG DNA von mykobakteriellen Komponenten in CFA erkennt, für die Induktion von EAE unwichtig ist. Zusammenfassend, zeigten wir, dass der Verlust von TLR 3, nicht aber TLR 9, zu einem Schutz vor der Entwicklung von klinischen Symptomen von EAE führt. Im Gegensatz dazu, führte der kombinierte Verlust von TLR 3 zusammen mit TLR 2, 4, 7 und 9 nicht zu einer Resistenz der Krankheitsinduktion, da *TLR23479*$^{-/-}$ Mäuse sehr empfänglich für die Induktion der Krankheit waren.

# 1 Introduction

## 1.1 Immune system

The immune system has evolved to provide defense against the infectious agents by mounting an effective response. This response against invading pathogens is a complex reaction and involves many different cells and organs. Based on the type of immune response, cells involved, specificity and if the immunity is short lived or long lasting, the immune system can be broadly classified into innate immune system and adaptive immune system (Parkin and Cohen, 2001; Storey and Jordan, 2008). In addition to this, anatomical and physiological barriers exist that primarily act as first defense line of immune system (Turvey and Broide, 2010).

## 1.2 Anatomical and physiological barriers:

Anatomical barriers include skin and mucosal surfaces that act as first line of defense preventing entry of infectious agents. Skin forms a strong barrier preventing entry of microbes and when the epithetical surface of skin is broken it leads to infection. Similarly, mucus entraps microbes and mucociliary mechanisms expel microbes. Physiological barriers include low stomach pH and body temperature which inhibit the growth of microbes. Also, many antimicrobial enzymes such as lysozyme in tears and other secreted body fluids such as saliva, sebum from skin prevent the survival and growth of microbes (Turvey and Broide, 2010). When these first line of defenses are encroached, the innate immune system comes in to play.

## 1.3 Innate immune system

Innate immune responses can act fast and they operate with mechanisms that are germline encoded and exist even before an invasion by a harmful microbe. These mechanisms are operated by pattern recognition receptors (PRRs) of innate immune arm that recognize specific pathogen-associated molecular patterns(PAMPs) and danger-associated molecular patterns (DAMPs) (Mogensen, 2009). These responses provide specificity though to a lesser extent in comparison to the adaptive immune system. Toll-like receptors (TLRs), NOD (nucleotide oligomerization domain) - like

receptors (NLRs) and RIG (retinoic acid-inducible gene I) - like receptors (RLRs) are the major PRRs of innate immune system (Thompson et al., 2011). PRRs are expressed by innate immune cells, which are of both hematopoietic and non-hematopoietic origin. These includes macrophages, dendritic cells (DCs), granulocytes (neutrophils, eosinophils, and basophils), natural killer (NK) cells and epithelial cells of skin and respiratory and gastrointestinal tracts (Turvey and Broide, 2010). In addition, the innate immune system is also comprised of humoral elements such as complement proteins, C-reactive protein and defensins (Riera Romo et al., 2016).

In the context of this literature review, only TLRs are being discussed.

### 1.3.1 Toll-like Receptors

Toll-like receptors, one of the germ line encoded PRRs recognize PAMPs of various microbes and aid innate immune system in clearing foreign infectious pathogens (Mogensen, 2009). They not only play a role in activating innate immune system but also promote adaptive immune responses (Hou et al., 2008) which is discussed in later sections. So far, 10 TLRs (1-10) have been identified in humans and 13 TLRs (1-13) in mice with TLR10 being non-functional (Lee et al., 2012). TLRs are expressed on both immune cells such as antigen presenting cells (APCs), B cells, T cells and also on non-immune cells such as epithelial cells (Sato et al., 2009). TLRs 1,2,4,5 and 6 are transmembrane proteins expressed on cell surface whereas TLRs 3,7,8,9,11 and 12 are found intracellularly within cell compartments such as endosomes and lysosomes (Lee and Barton, 2014).

#### 1.3.1.1 TLR ligands

Ligands for most of the TLRs are known. TLR1 recognizes triacyl lipopeptides, TLR2 recognizes a broad range of PAMPs such as lipoproteins, peptidoglycan, porins, zymosan and endogenous ligands such as heat shock protein 70. TLR4 recognizes LPS, TLR5 recognizes flagellin and TLR6 recognizes diacyl lipopeptides (Akira and Takeda, 2004). TLR3 recognizes double stranded RNA, TLR7 and 8 recognize single stranded RNA and TLR9 recognizes CpG DNA (Akira and Takeda, 2004). TLR11 and TLR12 both recognize profilin from toxoplasma gondii (Yarovinsky et al., 2005) (Koblansky et al., 2013). TLR13 recognizes bacterial 23S rRNA (Oldenburg et al., 2012).

#### 1.3.1.2 TLR structure and signaling

TLRs are type 1 transmembrane proteins characterized by an extracellular domain and a cytoplasmic domain. Extracellular domains of all TLRs consists of leucine rich repeats (LRPs) comprised of a β strand and α helix connected by loops forming a horseshoe shaped structure (Akira and Takeda, 2004; Botos et al., 2011). Cytoplasmic region of all TLRs share homology with that of type 1 Interleukin 1 receptor (IL1R) and hence referred to as Toll/IL-1R (TIR) domain. Upon ligand binding TLRs either form homodimers or heterodimers to initiate the downstream signaling. TLR2 forms heterodimers with either TLR1 or TLR6, TLR8 forms hetero dimer either with TLR7 or TLR9 (Watters et al., 2007). TLR5 forms heterodimers with TLR4 (Buchholz and Bauer, 2010). Other TLRs are presumed to form homodimers.

Upon ligand binding, TLRs recruit adaptor proteins via homotypical interaction between TIR domains of TLRs and TIR domains found in adaptor proteins (Botos et al., 2011). TLR signaling pathways utilize five adaptor proteins. These include Myeloid differentiation primary response gene 88 (MyD88), TIR domain containing IFN β inducing adaptor protein (TRIF, also called as TICAM1, TIR domain containing adaptor molecule 1), TIRAP (TIR-domain-containing adaptor protein), TIRAP is also called as MyD88-adaptor-like protein (MAL), TRIF-related adaptor molecule (TRAM) which is also known as TIR domain containing molecule 2 (TICAM2) and Sterile ∝- and armadillo-motif-containing protein (SARM) (O'Neill and Bowie, 2007).

All TLRs utilize MyD88 for their downstream signaling except for TLR 3 which utilizes TRIF. TLR4 can utilize both MyD88 and TRIF (Troutman et al., 2012). An overview of TLR signaling is depicted in Fig 1.

##### 1.3.1.2.1 MyD88-dependent Pathway

After ligand binding most TLRs recruit the MyD88 adaptor protein via homotypic interaction between TIR domains. Recruitment of MyD88 leads to recruitment of IRAK (*Interleukin-1 Receptor-Associated Kinase*) family members. This leads to complex formation between MyD88 with IRAK kinase family members. This complex is termed as Myddosome (Kawasaki and Kawai, 2014). During this recruitment and complex formation process, IRAK4 activates IRAK1 by phosphorylation. After being phosphorylated both IRAK1 and IRAK4 leave MyD88 complex and

associate with TRAF6 (Tumor necrosis factor receptor associated factor) and leading to ubiquitination of TRAF6. After ubiquitination, TRAF6 forms a complex with TAK1 (Transforming growth factor beta-activated kinase 1), a MAPKKK family member and its regulatory subunits TAB2 (TAK1 binding protein 2) and TAB3 (TAK1 binding protein 3) inducing TAK1 activation. Following activation, TAK1 can lead to two different signaling pathways, one being nuclear factor-kappaB (NF-□B) pathway and other MAPK (Mitogen-activated protein kinases) pathway. TAK1 couples to IKK (I kappa B kinase) complex and phosphorylates IKKβ thus activating it, which in turn phosphorylates NF-κB inhibitory protein IκBα (inhibitor of kappa B) leading to its degradation. NF-κB can then translocate into nucleus where it induces the gene expression of proinflammatory cytokines (Akira and Takeda, 2004; Kawasaki and Kawai, 2014).

In addition, TLR2 and TLR4 require MAL which acts as connecting bridge to recruit MyD88 to the plasma membrane (O'Neill and Bowie, 2007). Mal has a TIR domain in its C terminal, through which it interacts with TLRs and MyD88. In N-terminal, it has phosphatidylinositol 4, 5-bisphosphate (PIP2)-binding domain that targets MAL to membrane where it recruits MyD88 for initiating MyD88-dependent signaling pathway (Sheedy and O'Neill, 2007).

#### 1.3.1.2.2 MyD88 independent TRIF pathway

As mentioned TLR3 utilizes TRIF for its downstream signaling instead of MyD88 and TLR4 can utilize both MyD88 and TRIF (Troutman et al., 2012). Ligand binding activates these TLRs to recruit TRIF through TIR domain. TRIF then interacts with TRAF6 and TRAF3 (Kawai and Akira, 2010). TRIF contains a TRAF6- binding motif in its N-terminal (O'Neill and Bowie, 2007) and upon association with TRIF, TRAF 6 then recruits RIP -1 (receptor-interacting protein). TRAF6 and RIP-1 together activate TAK1 leading to the activation of MAPK and NF-κB. TRAF3 interacts and activates TBK1 and IKKi which in turn activates IRF3 by phosphorylation. Phosphorylation of IRF3 induces its dimerization and translocation to the nucleus where it promotes the expression of type I interferon genes (Kawai and Akira, 2010; Kawasaki and Kawai, 2014). In addition, TLR4 needs TRAM which acts as a bridge to recruit TRIF to TLR4 (Sheedy and O'Neill, 2007).

SARM is another adaptor molecule involved in TLR signaling. SARM can interact directly with TRIF and inhibit TRIF-dependent activation of transcription factors and does not affect MyD88-dependent pathway (O'Neill and Bowie, 2007). In steady state, expression levels of SARM are low but ligand activation of TLRs 3 and 4 results in an increase of SARM protein levels correlating with increased expression of TRIF. It has been suggested that SARM inhibits TRIF signaling by preventing the recruitment of downstream signaling proteins to TRIF (Carty et al., 2006; O'Neill and Bowie, 2007).

An overview of MyD88 dependent and independent TLR signaling pathway is depicted in Figure 1.

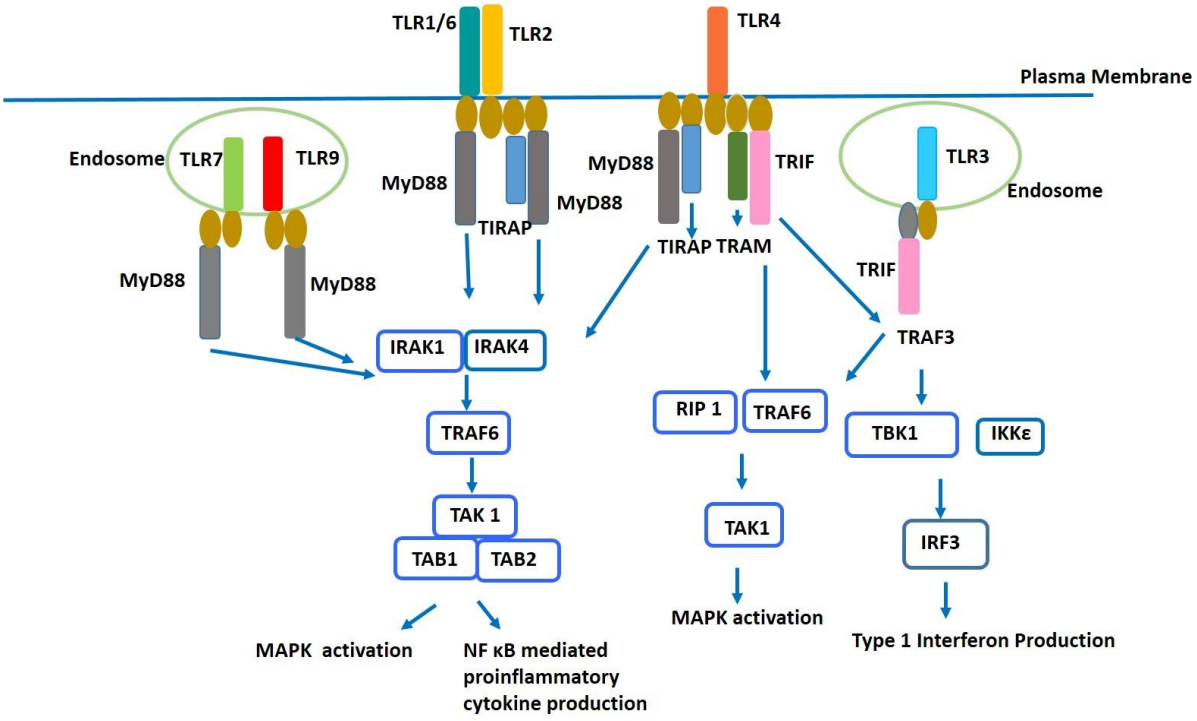


**Figure 1. An overview of TLR signaling pathway.**

Figure depicts an overview of TLR signaling pathway. There are 1-10 TLRs in humans and 1-13 TLRs in mice. All TLRs except TLR3 utilize MyD88 for downstream signaling. TLR4 is capable of utilizing both MyD88 and TRIF for its downstream signaling. TLR signaling results in the induction of proinflammatory cytokines as well as induction of type I interferons. Figure is modified from (O'Neill et al., 2013).

TLRs not only play an important role in defining adaptive immune responses, which is being discussed in the following section with brief introduction to adaptive immune system.

### 1.3.2 Adaptive immune system

The Adaptive immune system is highly specific in nature and is comprised of specialized cells, T and B cells (Medzhitov and Janeway, 2000). The adaptive immune system is characterized by both its ability to discriminate between self and non-self-antigens and immunological memory (Litman et al., 2010).

#### 1.3.2.1 T cells

T cells are the key players of adaptive immune system orchestrating various cell mediated responses to clear an infection. T cells recognize antigens presented on major histocompatibility complex (MHC) molecules with the help of the T cell receptor (TCR). This recognition and binding of TCR to antigen-bound MHC complexes initiates signaling events that lead to the activation of T cells resulting in their proliferation, production of proinflammatory cytokines and migration of these T cells to places of infection, where they perform effector functions (Pennock et al., 2013). Based on this effector functions that a T cell executes, it can be further categorized into three major subtypes. These are T helper cells (Th), T killer or cytotoxic cells and regulatory T cells (Tregs) which has immunosuppressive capacity (Corthay, 2009).

#### 1.3.2.2 B cells

B cells develop from hematopoietic stem cells (HSCs) in the bone marrow (Pieper et al., 2013). B cells recognize antigens with the help of B cell receptor (BCR). Once a naïve B cell encounters foreign antigen by binding to BCR, it differentiates in to short lived plasma cell and long lived memory cell (Nothelfer et al., 2015). Plasma B cells make antibodies that neutralize toxins besides activating complement system and aiding in opsonization of bacteria for phagocytosis (Parkin and Cohen, 2001). Memory B cells carry immunological memory and are reactivated upon secondary infection and differentiate into plasma cells (Nothelfer et al., 2015). B cells can further also act as an APC by internalizing the antigens (Kuokkanen et al., 2015).

### 1.3.3 Toll like receptors are involved in crucial interplay between Innate and Adaptive immune system

For a naïve T cell to confer adaptive immunity, it has to polarize towards the effector phenotype after being presented with antigen in conjunction with MCH class II by APCs such as DCs (Iwasaki and Medzhitov, 2004). In steady state DCs are in immature state but for efficient antigen presentation to T cells, their maturation is important. TLR signaling can induce maturation of DCs, which is characterized by upregulation of expression of co-stimulatory molecules involved in activating T cells (Werling and Jungi, 2003). TLR signaling in DCs not only promotes their maturation but also promotes DCs migration to lymph nodes where they present naïve T cell with captured antigen (Mogensen, 2009). Thus DC mediated T cell activation is dependent on TLR signaling. Moreover, TLR signaling in DCs also induces production of cytokines and chemokines such as IL12 which controls T helper cell differentiation towards Th1 phenotype (Netea et al., 2005). TLRs can also directly activate T cells independent of DCs (Rahman et al., 2009) .

### 1.3.4 Autoimmunity and role of Toll like Receptors in Autoimmunity

Immune responses may not always be protective in nature. It can be detrimental when an immune response is aimed at self-antigens instead of foreign pathogens. Though normally the immune system is programmed to tolerate self-antigens, this process is not foolproof. Tolerance to self-antigens is very important and loss of this tolerance leads to autoimmunity. Autoimmunity can be defined as condition in which the immune system recognizes self-antigens and initiates an autoimmune attack leading to inflammation and destruction of self-tissues (Kamradt and Mitchison, 2001). During the process of immune development, immune cells that recognize self-antigens are eliminated leaving behind only immune cells which are tolerant to self-antigens (Rioux and Abbas, 2005). Tolerance to self-antigens can be achieved either through central tolerance or peripheral tolerance. Central tolerance occurs in thymus for T cells and in bone marrow for B cells and is characterized by apoptosis of immature lymphocytes that recognize self-antigens (Kamradt and Mitchison, 2001; Rioux and Abbas, 2005). During the development of T cells in the thymus, a T cell is presented with self-antigen and the ability of T cell receptor (TCR)

to bind either strongly or weakly determines if it undergoes negative selection or positive selection (Ohashi, 2002). When a TCR interaction with self-antigen loaded on to a MHC class I or II is very strong, it undergoes negative selection and those T cells undergo apoptosis or become T regulatory cells (Klein et al., 2014). On the other hand, if this interaction is weak, it promotes the survival of mature T cell that which is tolerant to self-antigens (Ohashi, 2002). In peripheral tolerance, mature self-reactive lymphocytes that recognizes self-antigens are either killed or subjected to anergy (a state of functionally disabled) or suppressed by regulatory T cells (Rioux and Abbas, 2005).

Though it is not precisely known what leads to the activation of self-reactive lymphocytes triggering an autoimmune condition, it is widely suggested that the genetic variants and environmental factors such as infectious agents play a significant role (Ercolini and Miller, 2009). Many different mechanisms have been described as possible ways by which pathogens/infectious agents can trigger an autoimmune condition. Molecular mimicry and bystander activation are two such mechanisms. In both these mechanisms, TLRs play a critical role in initiating autoimmunity. According to the molecular mimicry hypothesis, viral or bacterial antigens that share structural similarity to self-antigens can activate auto reactive T cells leading to their activation and expansion (Cusick et al., 2012) (Figure 2). Bystander activation as a potential mechanism causing autoimmune condition has received considerable support from data emerging from various autoimmune models (Fujinami et al., 2006). Bystander activation assumes that during a viral infection, a nonspecific activation of self-reactive T cells that is independent of specific TCR stimulation can occur resulting in the damage to the self-tissues causing the release of self-antigens and thus initiating autoimmune response (Sfriso et al., 2010; Vanderlugt and Miller, 2002) (Figure 3).

In both molecular mimicry and bystander activation, the first step is that the foreign antigens from pathogens have to be recognized and captured by the APCs to be presented to autoreactive T cell. This first step of recognition is mediated by PRRs such as TLRs. TLR mediated APCs activation and their migration to lymph nodes where they present antigen to auto reactive T cell in addition to virus specific T cells resulting in the production of proinflammatory cytokines . Thus activation of TLRs by PAMPs can lead to bystander activation of auto reactive T cells (Mills, 2011).

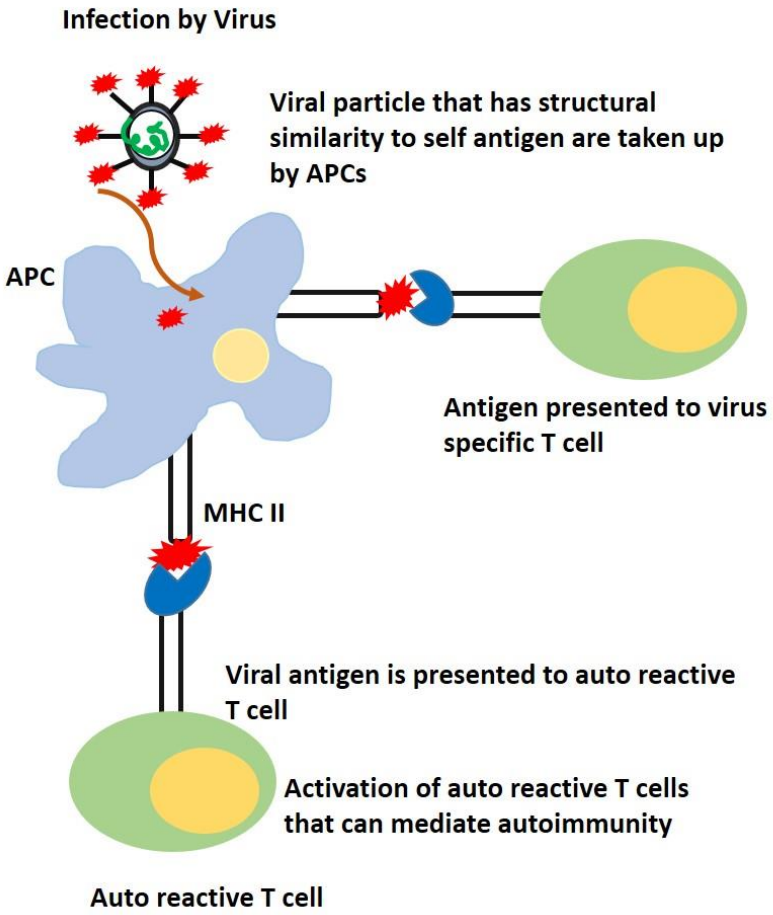


**Figure 2. Depicting the mechanism of molecular mimicry.**

Figure depicts the mechanism of molecular mimicry. Molecular mimicry suggests that autoreactive T cells can be activated by foreign pathogen antigens which share structural similarity with that of self-antigens. Figure is modified from (Munz et al., 2009).

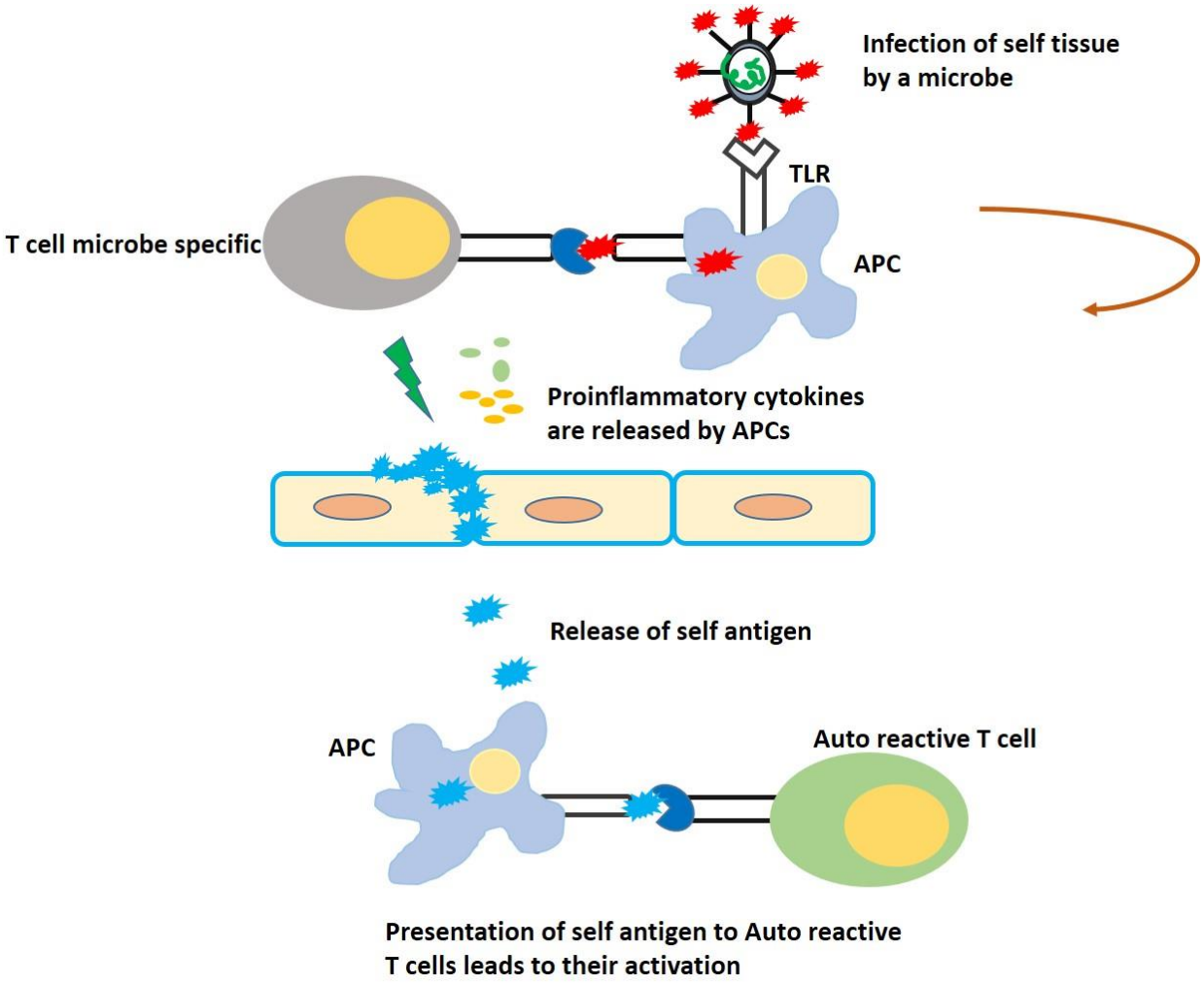


**Figure 3. Mechanism of Bystander Activation.**

Infection by a virus can result in the activation of antigen presenting cells (APCs). Activated APCs present viral antigen to virus specific T cells resulting in an inflammatory situation which also involves production of proinflammatory cytokines. This can lead to bystander destruction of uninfected tissue and thus leading to release of self-antigens, which can then be presented by APCs to autoreactive T cell. Figure modified from (Munz et al., 2009).

## 1.4 Multiple Sclerosis:

Multiple Sclerosis (MS) is a demyelinating disorder of the central nervous system. It is inflammatory and autoimmune in nature with unknown etiology. In MS, autoreactive T cells attack myelinated axons in the CNS destroying the myelin sheath and thus causing axonal loss (Goldenberg, 2012). MS affects more than 2.5 million people worldwide. It is the most common

cause of disability among adults (Haussleiter et al., 2009). Clinically MS is characterized by the formation of lesions in CNS with marked inflammation and destruction of myelin sheath (Weiner and Selkoe, 2002).

Diagnosis of MS is based on the clinical history of at least two attacks, lesion formation in CNS, presence of oligoclonal immunoglobulins bands in cerebrospinal fluid (Goldenberg, 2012). Symptoms of MS include weakness, neurological deficits, sensory disturbances, changes in vision, changes in bladder and bowel functions (Loma and Heyman, 2011; Noseworthy et al., 2000).

### 1.4.1 Clinical course of MS:

Depending on the course of disease MS is classified into four types. They are relapsing-remitting MS (RRMS), secondary progressive MS (SPMS), primary progressive MS (PPMS) and progressive relapsing MS (PRMS)(Goldenberg, 2012). RRMS is the most common form of MS and is characterized by attacks (episodes of neurological symptoms) also called relapses or exacerbations, followed by absence of symptoms, a phase called remission. During remission, symptoms may reappear or disappear altogether. Majority of patients with RRMS eventually develop SPMS and in SPMS, disease progression is steady with or without any relapses. PPMS affects 15% of MS patients and symptoms worsen from the start. It is characterized by steady deterioration of neurological function (Fitzner and Simons, 2010). PRMS is the rarest form of MS. It is characterized by superimposed relapses. The nature of the disease is progressive deterioration from onset (McKay et al., 2015).

Diagnosis of MS is performed taking many factors into consideration. Most common ones include examination of CSF for oligoclonal IgG band, MRI imaging of CNS and conducting evoked potential electrophysiological studies (Hurwitz, 2009).

### 1.4.2 Disease Pathology of MS:

MS is an autoimmune condition in which myelin components are wrongly attacked by the self-reactive T cells resulting in CNS demyelination (Lassmann et al., 2007; Racke, 2009). Plaque

formation consisting of inflammatory demyelinating regions in CNS forms the highlight of MS disease pathology. Histopathological examinations of human MS brains reveal that these plagues are characterized by myelin loss and influx of inflammatory immune cells (mostly T cells, monocytes and macrophages) into CNS (Frohman et al., 2006).

It is widely believed that this self-reactive T cells get activated in the periphery and cross the blood brain barrier (BBB) and attack myelin sheath (Figure 3). Under normal healthy conditions, T cells and other immune cells cannot infiltrate CNS by crossing through intact BBB but once activated self-reactive T cells are able to upregulate adhesion molecules and interact with endothelial cells of the BBB and gain access to CNS (Engelhardt, 2006). Once in CNS, T cells are further activated by residential microglial cells and subsequently cause CNS damage by attacking myelin sheath (Goverman, 2009).

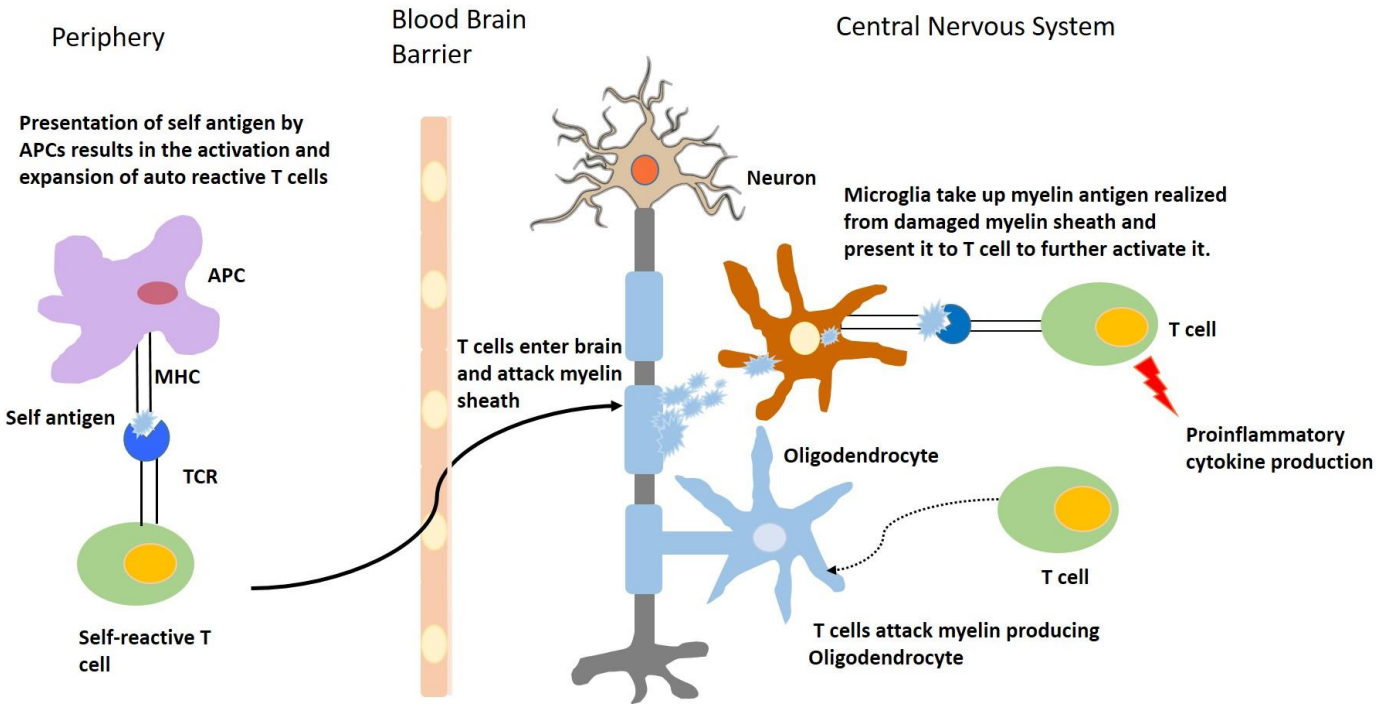


**Figure 4. An overview of MS immunopathology.**

Myelin specific autoreactive T cells once activated in periphery can migrate into brain by crossing the blood brain barrier. Once inside the brain, they attack the myelin sheath resulting in further release of myelin proteins as a consequence of tissue destruction. These myelin proteins can be then taken up by microglia, residential APCs in brain and present it back to T cells. The culmination of this process ultimately results in myelin loss and also death of oligodendrocytes that produce myelin. Figure modified from (Steinman and Zamvil, 2003).

### 1.4.3 Triggers of MS:

Though so far it is not known what exactly causes MS, many environmental factors and genetic factors have been suggested as possible triggers for MS some of which are discussed below.

#### 1.4.3.1 Genetic susceptibility:

The role of genetic factors in predisposing an individual to high risk of developing MS are well studied. Though MS occurs worldwide, its occurrence is more prevalent in northern Europe (Goldenberg, 2012) and North America and less prevalent in Asia and Africa (Trapp and Nave, 2008). This suggests that geographical location, genetic factors and ethnic background contributes to MS susceptibility. This notion is supported by experimental data from family aggregation and monozygotic twin studies. Familial recurrence rate of 15% (Compston and Coles, 2002) and an increased MS susceptibility in first degree relatives (Nielsen et al., 2005) have been reported. Moreover, twin studies suggest that MS susceptibility and concordance rate is higher in monozygotic twins than in dizygotic twins (Dyment et al., 2004).

Genome screening of MS patients identified a strong association of Human leukocyte antigen (HLA) class II haplotypes such as DR2/DQ6, DR3/DQ2, and DR4/DQ8 with MS. Apart from HLA class II genes, many other studies have reported an association between TCR β, *CTLA4* (Cytotoxic T-lymphocyte-associated protein 4), ICAM1 *(*Intercellular Adhesion Molecule 1), and SH2D2A *(*SH2 Domain Containing 2A) *a*nd an increased risk of MS susceptibility (Dyment et al., 2004).

#### 1.4.3.2 Environmental triggers:

Environmental triggers such as sunlight, smoking, diet and pathogens have been suggested as possible triggers for MS (O'Gorman et al., 2012). Deficiency of Vitamin D has been correlated with increased risk of multiple sclerosis. Having higher circulating levels of 1,25(OH)2D (active form of vitamin D) in women has been suggested to be protective against MS development as each 10 nmol/L increase of serum 1,25(OH)2D level was associated with a 19% reduction in the

likelihood of MS development (Kragt et al., 2009). Though MS affects people all over the world, its prevalence is higher in areas that are away from equator, areas that have less sunlight (main source of vitamin D in humans) which supports the concept of Vitamin D deficiency possibly posing higher MS risk (Simpson et al., 2011).

Smoking has been considered as another important risk factor for developing MS and that it worsens the MS clinical symptoms (Shirani and Tremlett, 2010). It has been suggested that smokers have 1.5 relative risk level of developing MS in comparison to nonsmokers (Wingerchuk, 2012).

Among environmental factors that are linked to MS as possible causative agents, infectious agents are highly discussed. Many research data suggests that infectious agents play a prominent role in triggering off MS. Though a clear association with one specific pathogen is not found, many pathogens have been associated with pathogenies of MS. These includes human herpesvirus 6 (HHV-6), Epstein Barr virus and Chlamydophila pneumoniae (Pawate and Sriram, 2010).

### 1.4.4 Animal models of Multiple Sclerosis:

Animal models of MS are needed not only to understand the complex immune-pathobiology underlying MS but also to find therapeutic cures that intervene with disease progression and aid repair mechanisms (Denic et al., 2011). There are many animal models of MS but most commonly studied models include Experimental autoimmune/allergic encephalomyelitis (EAE) model, toxin induced models of demyelination, virus induced chronic demyelinating models (Denic et al., 2011). Alongside these three commonly used models, transgenic mouse models of MS harboring T cells and B cells carrying specific receptors for myelin antigens (Scheikl et al., 2010) are also used to study different features of MS.

EAE is the most widely used animal model of MS and serves as valuable tool for studying CNS inflammation. EAE can be induced in susceptible mice strains either passively or actively. Active EAE can be induced by immunizing mice with subcutaneous injection of an emulsion containing equal amounts of complete freund adjuvant (CFA) which acts as adjuvant and synthetic peptides of myelin components such as myelin oligodendrocyte glycoprotein (MOG), myelin basic protein

(MBP) and proteolipid protein (PLP), followed by intraperitoneal injection of pertussis toxin (PT) (Denic et al., 2011). In C57BL/6 mice, $MOG_{35-55}$ peptide is used for immunization (Miller et al., 2010). Disease induction with active immunization involves two phases, the initial phase and the effector phase. The initial phase is marked by priming and activation of myelin antigen specific T cells in periphery. The effector phase is characterized by migration of these activated T cells into CNS by crossing BBB, with induction of inflammatory cytokines/chemokines by myelin specific T cells, entry of peripheral phagocytes into CNS followed by activation of CNS resident microglial cells (Constantinescu et al., 2011). Active immunization with myelin peptides results in activation and expansion of myelin specific T cells in the periphery. These activated T cells are capable of crossing the BBB and enter the CNS where they reencounter the myelin specific antigens and this reencounter results in T cell expansion in CNS which ultimately results in disease (Denic et al., 2011; Miller et al., 2010).

In passive or adoptive EAE, activated T cells are adoptively transferred from donor mice immunized with myelin peptide into naïve recipient mice. Therefore, adoptive transfer EAE is only characterized by effector phase in recipient mice (McCarthy et al., 2012).

Disease progression in immunized mice can follow either an acute/monophasic or chronic-progressive or relapsing-remitting form depending on the strain of the animal and immunization protocol. For example, immunization with $MOG_{35-55}$ peptide emulsified in CFA and PT results in monophasic or chronic form of EAE (Constantinescu et al., 2011) and immunization with antigen $PLP_{139-151}$ peptide emulsified in CFA and PT in SJL mice results in relapsing-remitting form of disease (Bittner et al., 2014).

Though EAE has been used for many years as animal model for human MS there is one major difference between MS and EAE. Disease induction in EAE requires immunization with myelin components and adjuvants in the form of CFA and PT but in humans that is not the case (Constantinescu et al., 2011; Gold et al., 2006). On other hand, there are many similarities between human MS and EAE model including lesions in the white matter of CNS associated with demyelination of axons, infiltration by T cells, macrophages and B cells and also oligoclonal IgG, found in both MS patients and EAE-induced sick mice (McCarthy et al., 2012).

In the following sections, the role of TLRs in both human MS disease and their requirement in EAE model are being discussed based on the results published by various research groups so far.

### 1.4.5 Toll like receptors in Multiple Sclerosis:

Recent studies have suggested an important role for TLRs in MS. TLRs are expressed on both immune and non-immune human cells such as:

**Table 1. Expression of TLRs by immune cells.**

| Cell Population | TLRs expressed |
|---|---|
| Monocytes | TLR1, TLR2, TLR4, TLR5, TLR6, TLR7, TLR8, TLR9 |
| Macrophages | TLR1, TLR2, TLR4, TLR5, TLR6, TLR7, TLR8, TLR9 |
| Dendritic cell types | TLR1, TLR2, TLR3, TLR4, TLR5, TLR7, TLR8, TLR9 |
| Mast cells | TLR6, TLR8 |
| B cells | TLR1, TLR3, TLR4, TLR6, TLR7, TLR9 |
| T cells | TLR4,TLR5 |

Note. Data source: (Miranda-Hernandez and Baxter, 2013)

Stimulation of TLRs with both external agents PAMPs and internal ligands in form of DAMPs has the potential to activate B and T cells of adaptive immune system. TLRs can contribute to autoimmune responses by inducing the production of proinflammatory cytokines (Fischer and Ehlers, 2008) and are capable of controlling autoimmune responses by inducing production of immunoregulatory components such as IFNβ (Noppert et al., 2007). There are many reasons that makes the study of TLRs in MS not only interesting but also important. One of them being that viral infections have always been associated with multiple sclerosis as possible triggers that give rise to autoimmune conditions (Kakalacheva et al., 2011). Epstein barr virus (EBV) has long been discussed as possible environmental trigger for MS initiation (Lunemann et al., 2007). This is

supported by data confirming high EBV seropositivity and higher serum anti-EBV antibody titres in MS patients in comparison to controls (Ludwin and Jacobson, 2011).

Among many mechanisms that were described as to how EBV can trigger MS, molecular mimicry and bystander activation are prominent. It is being postulated that EBV shares sequence homology with self-antigens in CNS and that an infection with EBV could result in cross reactivity between EBV antigens and self-antigens in CNS resulting in chain of immune reactions ultimately leading to activation of self-reactive lymphocytes (Cusick et al., 2012; Pender and Burrows, 2014). Also, EBV infection leading to bystander damage by $CD8^+$ T cells to CNS has been suggested to trigger off autoimmune response (Pender and Burrows, 2014). This body of evidence connecting MS with an infection brings TLRs to the forefront as TLRs are the most crucial players to instigate an autoimmune reaction by mechanisms such as molecular mimicry or by bystander activation (Fujinami et al., 2006).

Another strong factor connecting TLR signaling to MS is the key player IFNβ. Among many innate immune cells, pDCs are potent producers of type 1 interferons and are believed to play an important role triggering of autoimmune responses (Pradhan et al., 2012). Signaling through TLRs 3, 7 and 9 mostly leads to production of IFNβ, which has been found to be beneficial in treating MS patients. The role of TLRs and how their expression is modulated in response to IFNβ treatment in MS patients and how stimulation of PBMCs from MS patients with TLR ligands influences cytokine milieu is described below.

TLR1 expression is upregulated upon IFNβ treatment in MS patients (Singh et al., 2007) but otherwise not much is not known about TLR1 in MS. TLR2 is expressed by oligodendrocytes in CMS lesions contain hyaluronan deposits, which are known to inhibit oligodendrocyte precursor cell (OPC) maturation. It has been reported that hyaluronan mediated inhibition of OPC maturation is mediated through TLR2 (Sloane et al., 2010). Human dendritic cells from MS patients treated with IFNβ, when stimulated with TLR2 agonist Zymosan in presence of IFNβ in vitro study produced more IL10 which suppressed IL-23 and IL-1β production, both needed for Th17 polarization of T helper cells. (Sweeney et al., 2011).

Elevated expression of TLR3 was found in active MS lesions (Bsibsi et al., 2002). Peripheral blood mononuclear cell (PBMCs) from MS patients suffering from secondary progressive disease

pattern, when stimulated with TLR3 agonist polyinosinic:polycytidylic acid (poly I:C) produced higher levels of proinflammatory cytokines in comparison to healthy individuals. But when PBMCs from MS patients suffering from benign MS (BMS) were stimulated with TLR3 agonist poly (I:C), it resulted in the production of immunosuppressive molecules suggesting differential role for TLR3 in MS (Saresella et al., 2014).

High expression of TLR4 was reported in active MS lesions (Bsibsi et al., 2002). An increased expression of TLR4 and its endogenous ligand HMGB1 was observed in mononuclear cells of cerebrospinal fluid of MS patients in comparison to healthy controls (Andersson et al., 2008). A study involving 890 MS patients and 350 healthy controls investigating the role of Asp299Gly mutation in TLR4 receptor suggested no important role in MS (Kroner et al., 2005). Another study involving 362 MS patients and 467 healthy controls investigating the role of nine TLR4 single nucleotide polymorphisms (SNP) did not reveal any functional association with MS (Urcelay et al., 2007).

Not much is known about flagellin recognizing TLR5 in MS An association between rs5743810 polymorphism (Ser249Pro) of TLR6 and development of neutralizing antibodies against IFNβ after IFNβ therapy was found in male MS patients but not in female MS patients (Enevold et al., 2010). Plasmacytoid dendritic cells (pDCs) isolated from PBMCs of MS patients treated with IFNβ produced more IFNα upon in vitro stimulation with TLR7 ligand in comparison to pDCs from MS patients not treated with IFNβ. On other hand, TLR7 ligand stimulation of whole PBMCs from MS patients treated with IFNβ exhibited impaired IFNα production, an effect mediated by increased production of IL10 from monocytes in PBMCs (Severa et al., 2015).

TLR8 function is reported to be impaired in human MS patients. PBMCs from MS patients when stimulated with TLR8 ligand fail to induce functional IL12p40 protein production correlated with lower transcript levels of IL12β when compared to healthy controls. Also, unstimulated PBMCs from MS patients exhibit lower TLR8 mRNA expression (Johnson et al., 2013). TLR9 signaling through plasmacytoid dendritc cells (pDCs) results in type 1 interferon production. pDCs from untreated MS patients produce more IFNα in comparison to healthy controls and pDCs from IFNβ-treated MS patients produce less IFNα (Balashov et al., 2010). Also, IFNβ treatment inhibits TLR9 processing. Upon treatment with IFNβ, cleavage of the C terminal region of full length TLR9 is inhibited which is needed for its functionality (Balashov et al., 2010). Upon stimulation with TLR9

agonist, B cells from MS patients produce less IL10, an important immunosuppressive cytokine which correlate with decreased expression of TLR9 in B memory cells (Hirotani et al., 2010).Nothing is known about role of TLR10 in MS.

#### 1.4.5.1 Toll like receptors in EAE:

As mentioned in previous sections, EAE serves as an animal model for multiple sclerosis and is used since many years to understand the complex immunopathobiology lying behind MS. Recent studies have suggested an important role for gut flora in EAE. Mice reared in germ free conditions are resistant to EAE induction (Lee et al., 2011) suggesting an important role for gut flora in EAE. These brings TLRs to the forefront since TLRs are the prominent PRPs of innate immune system and recognize broad range of microbial components. So, understanding the role played by TLRs in EAE is crucial as it gives us insights into how innate immune system or gut flora could be important for priming of disease in EAE.

Moreover, adjuvants used for inducing EAE namely CFA and PT have microbial components which are recognized by TLRs. *Mycobacterium tuberculosis* present in CFA activates various TLRs such as TLR1,TLR2 and TLR 4 (Hansen et al., 2006). Also, TLR9 recognizes unmethylated CpG DNA which is abundant in Mycobacterium (Takeda et al., 2003) and TLR4 has been suggested to facilitate PT mode of action (Kerfoot et al., 2004). CFA and PT are crucial for inducing EAE in *C57BL/6* mice and because TLRs recognize many microbial components in these adjuvants, it is important to study the role of these TLRs in priming phase and in progression of disease in EAE and this could potentially lead to therapeutic drug development to be used later in human MS patients

Various groups have investigated the role of individual TLRs (1-9) in EAE model significant role has been found for some TLRs while some others were dispensable for EAE induction and disease progression.

*TLR1*$^{-/-}$ mice are susceptible to EAE but a significant role for TLR1 has not been reported so far. Though increased expression of TLR1 mRNA was observed in CNS during EAE disease course

(Prinz et al., 2006) but *TLR1*$^{-/-}$ mice both male and female genders developed similar EAE phenotype as that of wildtype controls (Miranda-Hernandez et al., 2011).

Many groups have investigated the role of TLR2 in EAE but results vary between the groups. One major factor that needs to be considered is that the immunization protocol used for induction varies between the groups. In EAE induced with $MOG_{35-55}$+CFA immunization on day 0 and day 7 post first immunization, *TLR2*$^{-/-}$ mice developed EAE disease course that was similar to that of wildtype mice suggesting a less prominent role for this TLR in EAE (Prinz et al., 2006). But in experiments conducted by Miranda et al., using same immunization protocol, *TLR2*$^{-/-}$ female mice exhibited less severe EAE clinical signs in comparison to the wildtype mice and *TLR2*$^{-/-}$ male mice exhibited symptoms similar to Wt mice. *TLR29*$^{-/-}$ double knockout mice both female and male mice developed less severe EAE clinical symptoms in comparison to Wt mice (Miranda-Hernandez et al., 2011). In $MOG_{35—55}$ + CFA, PT induced EAE with single immunization on day 0, *TLR2*$^{-/-}$ mice developed milder EAE symptoms in comparison to Wt (Shaw et al., 2011). In short, deficiency of TLR2 seems to confer protection from developing severe clinical signs in EAE model.

TLR3 expression was not upregulated in CNS during $MOG_{35-55}$ peptide induced EAE in *C57BL/6* mice (Prinz et al., 2006). So far, no group has reported about EAE in *TLR3*$^{-/-}$ mice on *C57BL/6* background. But stimulation with TLR3 agonist poly I:C reduces EAE clinical disease severity in SJL mice by inducing endogenous expression of interferon β and by peripheral induction of chemokine CCL2 (Touil et al., 2006).

The role of TLR4 in EAE model is extensively studied by various groups. But once again results vary between the research groups. As mentioned before some research groups have used $MOG_{35-55}$ peptide for EAE induction and immunized mice twice with MOG peptide on day 0 followed by second immunization on day 7, whereas others have used MOG protein for induction and only one time immunization on day 0. MOG protein induced immunization with single day 0 immunization induced EAE in *TLR4*$^{-/-}$ female mice resulted in severe form of disease in comparison to WT and purified T cells from *TLR4*$^{-/-}$ spleen showed increased mRNA expression of IL17 on day 10 post immunization. This correlated with decreased mRNA expression of IFNγ from purified T cells in immunized mice on day 10. Also, splenic myeloid dendritic cells *(*mDC*)* from *TLR4*$^{-/-}$ had higher mRNA expression for proinflammatory cytokines IL6 and IL23p40 on day 10 post immunization with MOG protein. Expression of IL17 or IFNγ in CNS during EAE

disease course was not discussed (Marta et al., 2008). In contradiction to this, in $MOG_{35-55}$ peptide induced EAE with single immunization on day 0, deletion of TLR4 had no influence on disease severity (Kerfoot et al., 2004). In $MOG_{35-55}$+CFA, PT induced EAE with double immunization on day 0 and day 7, *TLR4*$^{-/-}$ male and female mice exhibited similar disease pattern as that of Wt mice (Miranda-Hernandez et al., 2011). Finally, role of TLR4 remains controversial in EAE.

Not much is known about the role of TLR5 in EAE. TLR5 expression was not increased in CNS during EAE in *C57BL/6* mice (Prinz et al., 2006). Active EAE induction in *TLR6*$^{-/-}$ mice did not affect the disease severity. EAE induction in *TLR6*$^{-/-}$ mice followed similar disease pattern as in wildtype mice, suggesting less important role for this receptor in EAE model (Miranda-Hernandez et al., 2011).

Active EAE in *TLR7*$^{-/-}$ mice followed less severe disease pattern in comparison to wildtype mice. At the peak of disease, *TLR7*$^{-/-}$ mice exhibited reduced demyelination in the spinal cord and also exhibited reduced *in vitro* T cell proliferative responses to MOG peptide in comparison to wildtype mice. Furthermore, T cells from *TLR7*$^{-/-}$ mice produced more IL10 at peak of disease when compared to wildtype mice. Also, *TLR7*$^{-/-}$ mice had increased percentage of splenic T regulatory cells in *TLR7*$^{-/-}$ mice during EAE (Lalive et al., 2014) . Treatment with TLR7 agonist imiquimod reduced severity of EAE clinical signs in B6 mice when immunized with $MOG_{35-55}$ peptide. This effect was mediated by production of IFN β in periphery. (O'Brien et al., 2010). Similar results were also observed in SJL/J background. Treatment with TLR7 agonist 9-benzyl-8-hydroxy-2-(2-methoxyethoxy) adenine (called 1V136) reduced disease severity in SJL/J mice when immunized with $PLP_{139-151}$ peptide (Hayashi et al., 2012) leading to reduced cellular infiltration in spinal cord.

Not much is known about the role of TLR8 in EAE though increased expression of TLR8 mRNA was observed during MOG peptide-induced EAE (Prinz et al., 2006). TLR8 expression was downregulated in spinal cord during active EAE when mice were treated with 1,25-Dihydroxyvitamin D3 ($1,25(OH)_2D_3$) (Li et al., 2013) suggesting a possible mechanism by which Vitamin D could protect from EAE severity.

The role of TLR9 in EAE model has been studied by various groups with contradictory results: Once again the fact that different induction protocols were used makes it difficult to compare the results. In MOG peptide-induced EAE, with two times immunization on day 0 and day 7, EAE clinical signs were reduced in *TLR9*$^{-/-}$ female mice (Miranda-Hernandez et al., 2011; Prinz et al.,

2006) but male *TLR9*$^{-/-}$ mice displayed similar disease pattern as that of Wt mice (Miranda-Hernandez et al., 2011) whereas in EAE induced with recombinant rat MOG protein resulted in increased disease severity in *TLR9*$^{-/-}$ female mice (Marta et al., 2008) both these studies where done in *C57BL/6* background.

TLR10 is non-functional in mice and not much is known about the role of TLRs11, 12 and 13 in EAE.

Apart from individual function of TLRs in EAE, the role of adaptor proteins involved in TLR signaling namely MyD88 and TRIF have been extensively studied. These studies have shown a prominent role for both MyD88 and TRIF in EAE. Increased expression of MyD88 mRNA was observed during EAE disease course in *C57BL/6* mice with $MOG_{35-55}$ peptide induced disease (Prinz et al., 2006). *MyD88*$^{-/-}$ mice are resistant to EAE suggesting an indispensable role for this adaptor protein for EAE induction and disease progression ((Marta et al., 2008; Miranda-Hernandez et al., 2011; Prinz et al., 2006). EAE resistance in *MyD88*$^{-/-}$ mice was associated with low levels of inflammatory cytokines such as IL6, IL23 and IL17 (Marta et al., 2008; Prinz et al., 2006) and no infiltrating T cells were observed in CNS (Marta et al., 2008; Miranda-Hernandez et al., 2011).

All TLRs utilize the adaptor protein MyD88 for their downstream signaling except for TLR 3 and TLR4. TLR4 can utilize both MyD88 and TRIF adaptor proteins whereas TLR3 utilizes only TRIF for its downstream signaling (Akira and Takeda, 2004). Signaling through TRIF adaptor protein results in the production of IFNβ (Noppert et al., 2007) and IFNβ have been shown to be protective in MS (Weinstock-Guttman et al., 2008) . In accordance to this, mice deficient in TRIF adaptor protein develop severe EAE clinical signs in comparison to wildtype mice (Guo et al., 2008). *TRIF*$^{-/-}$ mice exhibited early onset of EAE clinical signs and increased infiltration of $CD4^+$ T cells in CNS on day 10 post EAE induction. Disease severity in *TRIF*$^{-/-}$ was characterized by increased production of IL17 from $CD4^+$ T cells in CNS than wildtype EAE induced controls. When co-cultured with LPS-stimulated macrophages, T cells from *TRIF*$^{-/-}$ exhibited increased production of IL17 suggesting that type 1 interferon production in macrophages is required to negatively control IL17 production. This data suggested a protective role for TRIF in EAE. Also, *IFNAR*$^{-/-}$ deficient mice developed severe form of EAE than induced Wt controls further suggesting a protective role for type 1 interferons in EAE model (Guo et al., 2008). TRIF signaling results in the

phosphorylation of IRF3, upon activation IRF3 translocates to the nucleus and activates the expression of IFNβ (Perry et al., 2005). *IRF3*$^{-/-}$ mice exhibited less severe disease symptoms in comparison to Wt mice (Fitzgerald et al., 2014). This finding is surprising as *TRIF*$^{-/-}$ and *IFNAR*$^{-/-}$ mice both develop severe form of EAE.

**Table 2 An overview of TLRs and adaptor proteins in active EAE model.**

| Genotype | Gender | Immunization Protocol | Disease Severity Compared to Wt | Reference |
|---|---|---|---|---|
| *TLR1*$^{-/-}$ | Female | Day 0: $MOG_{35-55}$+IFA+ heat killed M. tuberculosis H37RA,PT<br>Day 2: PT<br>Day 7: $MOG_{35-55}$+IFA+ heat killed M. tuberculosis | Similar | (Miranda-Hernandez et al., 2011) |
| | Male | Day0: $MOG_{35-55}$+IFA+ heat killed M. tuberculosis H37RA,PT<br>Day2: PT<br>Day 7: MOG35-55+IFA+ heat killed M. tuberculosis | Similar | (Miranda-Hernandez et al., 2011) |
| *TLR2*$^{-/-}$ | Female | Day0: $MOG_{35-55}$+CFA,PT<br>Day2: PT<br>Day7: $MOG_{35-55}$+CFA | Similar | (Prinz et al., 2006) |
| | | Day0: MOG35-55+CFA,PT<br>Day2: PT | Reduced | (Shaw et al., 2011) |
| | | Day0: $MOG_{35-55}$+IFA+ heat killed M. tuberculosis H37RA,PT<br>Day2: PT<br>Day 7: MOG35-55+IFA+ heat killed M. tuberculosis | Reduced | (Miranda-Hernandez et al., 2011) |

| | | | | |
|---|---|---|---|---|
| | Male | Day0: $MOG_{35-55}$+IFA+ heat killed M. tuberculosis H37RA,PT<br>Day2: PT<br>Day 7: $MOG_{35-55}$+IFA+ heat killed M. tuberculosis | Similar | (Miranda-Hernandez et al., 2011) |
| *TLR29*$^{-/-}$ | Female | Day0: $MOG_{35-55}$+IFA+ heat killed M. tuberculosis H37RA,PT<br>Day2: PT<br>Day 7: $MOG_{35-55}$+IFA+ heat killed M. tuberculosis | Reduced | (Miranda-Hernandez et al., 2011) |
| | Male | Day0: $MOG_{35-55}$+IFA+ heat killed M. tuberculosis H37RA,PT<br>Day2: PT<br>Day 7: $MOG_{35-55}$+IFA+ heat killed M. tuberculosis | Reduced | (Miranda-Hernandez et al., 2011) |
| *TLR3*$^{-/-}$ | None | None | Not known | None |
| *TLR4*$^{-/-}$ | Female | Day0: rat rMOG+CFA,PT<br>Day2: PT | Increased | (Marta et al., 2008) |
| | | Day0: $MOG_{35-55}$+IFA+ heat killed M. tuberculosis H37RA,PT<br>Day2: PT<br>Day 7: MOG35-55+IFA+ heat killed M. tuberculosis | Similar | (Miranda-Hernandez et al., 2011) |
| | | Day0: $MOG_{35-55}$+IFA+ heat killed M. tuberculosis H37RA,PT<br>Day2: PT | Similar | (Miranda-Hernandez et al., 2011) |

| | | | | |
|---|---|---|---|---|
| | Male | Day 7: $MOG_{35-55}$ +IFA+ heat killed M. tuberculosis | | |
| *TLR5*$^{-/-}$ | - | - | Not known | - |
| *TLR6*$^{-/-}$ | Female | Day0: $MOG_{35-55}$+IFA+ heat killed M. tuberculosis H37RA,PT<br>Day2: PT<br>Day7: $MOG_{35-55}$ +IFA+ heat killed M. tuberculosis | Similar | (Miranda-Hernandez et al., 2011) |
| | | Day0: rat rMOG+CFA,PT<br>Day2: PT | Similar | (Marta et al., 2008) |
| | Male | Day0: $MOG_{35-55}$+IFA+ heat killed M. tuberculosis H37RA,PT<br>Day2: PT<br>Day7: $MOG_{35-55}$ +IFA+ heat killed M. tuberculosis | Similar | (Miranda-Hernandez et al., 2011) |
| *TLR7*$^{-/-}$ | Female | Day0: $MOG_{35-55}$+CFA+PT<br>Day2: PT | Reduced | (Lalive et al., 2014) |
| *TLR8*$^{-/-}$ | None | None | Not Known | None |
| | Female | Day0: $MOG_{35-55}$+IFA+ heat killed M. tuberculosis H37RA,PT<br>Day2: PT<br>Day7: $MOG_{35-55}$+IFA+ heat killed M. tuberculosis | Reduced | (Miranda-Hernandez et al., 2011; Prinz et al., 2006) |
| | Female | Day0: $MOG_{35-55}$+CFA, PT<br>Day2:PT<br>Day7: $MOG_{35-55}$+CFA | Reduced | (Prinz et al., 2006) |

| | | | | |
|---|---|---|---|---|
| *TLR9*$^{-/-}$ | Female | Day0: rat rMOG+CFA,PT<br>Day2: PT | Increased | (Marta et al., 2008) |
| | Male | Day0: $MOG_{35-55}$+IFA+ heat killed M. tuberculosis H37RA,PT<br>Day2: PT<br>Day7: $MOG_{35-55}$+IFA+ heat killed M. tuberculosis | Reduced | (Miranda-Hernandez et al., 2011) |
| *TLR10*$^{-/-}$ | - | - | Not known | - |
| *TLR11*$^{-/-}$ | - | - | Not known | - |
| *TLR12*$^{-/-}$ | - | - | Not known | - |
| *MyD88*$^{-/-}$ | Female | Day0: rat rMOG+CFA,PT<br>Day2: PT | Resistant | (Marta et al., 2008) |
| | | Day0: $MOG_{35-55}$+CFA, PT<br>Day2:PT<br>Day7: $MOG_{35-55}$+CFA | Resistant | (Prinz et al., 2006) |
| | | Day0: $MOG_{35-55}$+IFA+ heat killed M. tuberculosis H37RA,PT<br>Day2: PT<br>Day7: $MOG_{35-55}$+IFA+ heat killed M. tuberculosis | Resistant | (Miranda-Hernandez et al., 2011) |
| | Male | Day0: $MOG_{35-55}$+IFA+ heat killed M. tuberculosis H37RA,PT<br>Day2: PT<br>Day7: $MOG_{35-55}$+IFA+ heat killed M. tuberculosis | Resistant | (Miranda-Hernandez et al., 2011) |
| | | Day 0: $MOG_{35-55}$+ CFA+PT | | |

| | | | | |
|---|---|---|---|---|
| *TRIF*$^{-/-}$ | Female | Day2: PT | Increased | (Guo et al., 2008) |
| *IFNAR*$^{-/-}$ | Female | Day 0: $MOG_{35-55}$+ CFA+PT<br>Day2: PT | Increased | (Guo et al., 2008) |

## 1.5 Summary and Project Aims

Recent studies have suggested an important role for TLR signaling in the pathogenesis of MS. Modulating TLR signaling could pave way for new therapeutics for treating human MS. For example, treating mice with TLR agonists such as poly I:C has been beneficial in the EAE model (Touil et al., 2006). Therefore, we sought to investigate the role of TLRs in EAE.

**AIM 1:** To decipher the requirement of TLR3 and TLR 9 in EAE using *TLR3*$^{-/-}$ and *TLR9*$^{-/-}$ mice.

TLR3 signaling through TRIF leads to IFNβ production, which is known to be beneficial in MS (Touil et al., 2006). Yet, there are no reports about the impact of TLR3 deficiency on active EAE. TLR9 recognizes CpG motifs which are abundant in DNA of *Mycobacterium tuberculosis* (Basu et al., 2012) present in CFA, which is necessary for successful active EAE induction in C57BL/6 background (Bittner et al., 2014). Therefore, we sought to investigate the requirement of TLR3 and TLR9 in EAE using *TLR3*$^{-/-}$ *and TLR9*$^{-/-}$ mice.

**AIM 2:** To decipher the requirement of endosomal TLRs 3, 7 & 9 in EAE using *TLR379*$^{-/-}$ mice.

Endosomal TLRs have been implicated in the disease pathology of many autoimmune disorders such as rheumatoid arthritis and lupus (Trivedi and Greidinger, 2009) but so far there are no reports on the combined role of endosomal TLRs in EAE model. Therefore, we sought to investigate the requirement of endosomal TLRs 3, 7 and 9 in EAE using *TLR379*$^{-/-}$ mice.

**AIM 3:** To decipher the combined deficiency of TLRs 2,3,4,7 and 9 in EAE using *TLR23479*$^{-/-}$ mice.

Further, we aimed to decipher the combined requirement of many TLRs for EAE induction using *TLR23479*$^{-/-}$ mice. TLR2 deficiency renders TLR1 and TLR6 non-functional due to requirement of heterodimer formation with TLR2, TLR8 is known to be non-functional in mice (Liu et al., 2010b) and TLR10 is non-existent in mice. Therefore, among TLRs1-13 in mice, *TLR23479*$^{-/-}$ mice offer deficiency of most TLRs giving an opportunity to decipher the requirement of TLR signaling for EAE induction.

# 2 MATERIALS AND METHODS

## 2.1 Mice

All mice used in this study were of C57BL/6 background. Mice were housed in SPF facilities at Technische Universität München and at Universität Zürich according to German and Swiss animal welfare laws. *TLR9*$^{-/-}$, *TLR379*$^{-/-}$ and *TLR2379*$^{-/-}$ were provided by Institute of Microbiology, Immunology and Hygiene. *TLR3*$^{-/-}$ (Alexopoulou et al., 2001) mice were provided by SWIMMR facility, University of Zurich. Homozygous *TLR379*$^{-/-}$ mice were generated by intercrossing *TLR3*$^{-/-}$ (Honda et al., 2003), *TLR7*$^{-/-}$ (Hemmi et al., 2002), *TLR9*$^{-/-}$ (Hemmi et al., 2000) which were on C57BL/6 background (Yu et al., 2012). Homozygous *TLR23479*$^{-/-}$ were generated by intercrossing *TLR2*$^{-/-}$ (Spiller et al., 2007), *TLR3*$^{-/-}$ (Honda et al., 2003), *TLR4*$^{-/-}$ (Hoshino et al., 1999), *TLR7*$^{-/-}$ (Hemmi et al., 2002), *TLR9*$^{-/-}$ (Hemmi et al., 2000) single knockouts (Conrad et al., 2009). C57BL/6 mice were purchased from Harlan.

### 2.1.1 Genotyping of mice

Genotypes of knockout mice were confirmed by polymerase chain reaction (PCR) using specific primers. Tail and ear biopsies were used for isolating the DNA. In brief, biopsies were digested using direct PCR lysis reagent (Peqlab, Cat # 31-301-C) which was supplemented with proteinase K (Thermofischer, Cat # AM2548) at a concentration of 1 mg/ml in 250 µl volume of lysis reagent and was incubated at 55°C overnight on a thermomixer (Eppendorf thermomixer, Cat # 05-400-203). Reaction was stopped by incubating further at 85° C for 45 minutes, inactivating proteinase K. 2µl of the crude lysate was directly used for the PCR analysis.

Unless stated otherwise below, PCR reaction was carried out in 25µl volume containing 12.5µl of Go taq green master mix (Promega, Cat # M7122), 2µl of crude DNA lysate, 1µl of each forward and reverse primers (final concentration of 1µM) (Eurofins Scientific) and 8.5µl of nuclease free $H_2O$ (Roth, Cat # T143.3). In case of *TLR4*$^{-/-}$ Wt PCR and *TLR7*$^{-/-}$ knockout PCR, PCR reaction was carried out in 25µl volume containing 12.5µl of dream taq buffer (Thermofischer Scientific, Cat # B65), 2µl of crude DNA lysate, 1µl of each forward and reverse primers (final concentration of 1µM) (Eurofins Scientific), 1µl dream taq polymerase (Thermofischer Scientific, Cat # EP0701) and 7.5µl of nuclease free $H_2O$.

PCR reactions were carried out using Bio-Rads C1000 Touch Thermocycler (Cat # 1851196 and PCR products were run on 1% agarose gel (Bioconcept, Cat # 7-01P02-R).

#### 2.1.1.1 PCR reaction for *TLR2*$^{-/-}$ genotyping

Spiller et al., generated *TLR2*$^{-/-}$ mice by disrupting open reading frame within exon 3 of *TLR2 gene by placing a* neomycin cassette (Spiller et al., 2007).

The mutant allele was detected using following primers:

5′-CTTCCTGAATTTGTCCAGTACAGG-3′

5′-GGGCCAGCTCATTCCTCCCACTCAT -3′

The Wt allele was detected using primers:

5′-TCGACCTCGATCAACAGGAGAAGGG-3′

5′-GGGCCAGCTCATTCCTCCCACTCAT -3′

PCR amplification was carried out by an initial step of denaturation at 94°C for 300 sec which was followed by 30 cycles of denaturation at 94°C for 60 sec, annealing at 59°C for 30 sec, and extension for 60 sec at 70°C, with a final extension at 72°C for 120 sec.

#### 2.1.1.2 PCR reaction for *TLR3*$^{-/-}$ genotyping in *TLR23479*$^{-/-}$

Honda et al., have generated *TLR3*$^{-/-}$ mice by replacing third and fourth exons of the coding region in *TLR3* gene with neomycin resistance gene cassette.

The mutant allele was detected using following primers:

5′-TCCAGACAATTGGCAAGTTATTCGCCC-3′

5′-ATCGCCTTCTATCGCCTTCTTGACGAG-3′

The Wt allele was detected using following primers:

5′-CCAGAGCCTGGGTAAGTTATTGTGCTG-3′

5′-TCCAGACAATTGGCAAGTTATTCGCCC-3′

PCR amplification was carried out by an initial step of denaturation at 94°C for 300 sec which was followed by 30 cycles of denaturation at 95°C for 30 sec, annealing at 67°C for 90 sec, and extension for 60 sec at 74°C, with a final extension at 72°C for 500 sec.

#### 2.1.1.3 PCR reaction for *TLR4*$^{-/-}$ genotyping

*TLR4*$^{-/-}$ mice were generated by replacing 2.4 kbp genomic DNA of *TLR4* gene (the transmembrane and cytoplasmic regions of TLR4) with neomycin resistance gene (Hoshino et al., 1999).

The mutant allele was detected using following primers:

5′-GTTTAGAGAATCTGGTGGCTGTGGAGAC-3′

5′-TGTTGGGTCGTTTGTTCGGATCCGTCG -3′

The Wt allele was detected using following primers:

5′-GTTTAGAGAATCTGGTGGCTGTGGAGAC-3

5′-TATATG CGGCCGCTCATCTGC TGTACTTTTTACAGCC-3′

PCR amplification for Wt allele was carried out by an initial step of denaturation at 95°C for 180 sec which was followed by 30 cycles of denaturation at 95°C for 30 sec, annealing at 60°C for 30 sec, and extension for 180 sec at 72°C, with a final extension at 72°C for 120 sec.

PCR amplification for mutant allele was carried out by an initial step of denaturation at 95°C for 180 sec which was followed by 30 cycles of denaturation at 95°C for 30 sec, annealing at 67°C for 60 sec, and extension for 180 sec at 74°C, with a final extension at 72°C for 120 sec.

#### 2.1.1.4 PCR reaction for *TLR7*$^{-/-}$ genotyping

*TLR7*$^{-/-}$ mice were generated by replacing 1.8kb fragment of *TLR7* gene with neomycin resistance gene cassette (Hemmi et al., 2002).

The mutated allele was detected using following primers:

5′-CCAGATACATCGCCTACCTACTAGACC-3′

5′-ATCGCCTTC TATCGCCTTCTTGACGAG-3′

The Wt allele was detected using following primers:

5′-ACGTGATTGTGGCGGTCAGAGGATAAC-3′

5′-CCAGATACATCGCCTACCTACTAGACC -3′

PCR amplification was carried out by an initial step of denaturation at 94°C for 180 sec which was followed by 35 cycles of denaturation at 94°C for 30 sec, annealing at 62°C for 60 sec, and extension for 90 sec at 72°C, with a final extension at 72°C for 120 sec.

#### 2.1.1.5 PCR reaction for *TLR9*$^{-/-}$ genotyping in *TLR23479*$^{-/-}$ as well for *TLR9*$^{-/-}$ single knockout

*TLR9*$^{-/-}$ mice were generated by disrupting the *TLR9* gene with homologous recombination (Hemmi et al., 2000).

The mutated allele was detected using following primers:

5′-GCAATGGAAAGGACTGTCCACTTTGTG-3′

5′-ATCGCCTTCTATCGCCTTCTTGACGAG-3′

The Wt allele was detected using following primers

5′ - GAAGGTTCTGGGCTCAATGGTCATGTG-3′

5′ - GCAATGGAAAGGACTGTCCACTTTGTG-3′

PCR amplification was carried out by an initial step of denaturation at 94°C for 300 sec which was followed by 30 cycles of denaturation at 95°C for 30 sec, annealing at 67°C for 90 sec and extension for 60 sec at 74°C, with a final extension at 72°C for 500 sec.

## 2.2 EAE

### 2.2.1 Induction of EAE

*TLR9*$^{-/-}$, *TLR3*$^{-/-}$, *TLR379*$^{-/-}$, *TLR23479*$^{-/-}$, *or* C57BL/6 (Wt) female mice were immunized subcutaneously with 200µg of $MOG_{35-55}$ peptide (Genscript, Cat # RP10245) emulsified in equal volumes of CFA containing *M. tuberculosis* H37Ra (Difco Laboratories) in both sides of abdominal flanks. Followed by intraperitoneal injection with 250ng of pertussis toxin (Sigma-Aldrich, Cat # P7208) at the time of immunization and 48 hours post immunization.

### 2.2.2 Clinical Scoring

Post immunization mice were observed daily for clinical symptoms. Mice were scored as follows: 0 - no clinical signs of EAE; 0.5- partial limp tail; 1- limp tail; 1.5- limp tail and hind limb weakness; 2- limp tail and one side partial hind limb paralysis; 2.5- limp tail and partial bilateral hind limb paralysis; 3- limp tail and complete bilateral hind limb paralysis; 3.5- limp tail and complete hind limb paralysis and unilateral forelimb paralysis; 4- total paralysis of both forelimbs and hind limbs; 5- death (Becher et al., 2002).

## 2.3 Preparation of Single cell Suspension from Organs/Tissues

### 2.3.1 Preparation of single cell suspension from spleen with mechanical and enzymatic homogenization

Mice were euthanized with $CO_2$ and spleen was dissected and was processed either by mechanical homogenization or by enzymatic digestion. In case of enzymatic digestion, spleen was finely cut into small pieces with scissors and transferred to 15ml falcon tubes containing 10ml of digestion cocktail. Digestion cocktail was prepared by adding Collagenase D (Roche Molecular Products) at 1mg/ml and DNase I (Roche Molecular Products) at 20 µg/mL to 10ml of RPMI media supplemented with 2% FCS. Cell suspension was further incubated at 37°C for 40 min with frequent resuspension. The reaction was stopped by adding 0.1ml of 0.5M EDTA and with incubation at 37°C for 5 min. At the end of incubation, the cell suspension was transferred to 50ml falcon tube and the volume was made up to 25ml with PBS. In case of mechanical digestion, spleen was placed in 70µm cell strainer (BD falcon, Cat #352350), placed on ice cold PBS (Gibco, Life technologies, Cat # 14190-094) in a petri dish. Tissue was homogenized with syringe plunger and cell suspension was transferred to 50ml falcon. From this step onwards, cell suspension obtained after enzymatic digestion and mechanical homogenization is processed similarly. Cell suspension is centrifuged at 1500 rpm for 5 min at 4°C. Supernatant was discarded and cell pellet was resuspended in 500µl of PBS, to which 1ml of 1X Red blood cell (RBC) lysis solution was added and incubated for 10 min on ice. After incubation, cell suspension was diluted with ice cold PBS to achieve final volume of 25ml, passed through cell strainer into new 50ml falcon tube and centrifuged at 1500rpm for 5 min at 4°C. Supernatant was discarded and cell pellet was suspended either in RPMI media (PAN biotech, Cat # P04-17500) containing 5% FCS or ice cold PBS (Gibco, Life technologies, Cat # 14190-094). Cells were then counted using Neubauer chamber (Bright-Line, Assistent) and used for FACS staining.

### 2.3.2 Preparation of single cell suspension from bone marrow:

Mice were euthanized with $CO_2$. Skin and muscle was removed from femur, tibia and hips. Femur was cut from tibia and each bone was flushed with ice cold PBS solution. Cell suspension was passed through 70µM strainer (BD) into 15ml falcon tube and centrifuged at 1500 rpm for 10 min 4°C. From this step onwards, sample was processed as described in section 2.3.1.

### 2.3.3 Preparation of single cell suspension from thymus:

Mice were euthanized with $CO_2$ and thymus was dissected and placed in a 70µM filter, placed in a petridish containing 14ml of ice cold PBS the tissue was homogenized using syringe plunger. In case of enzymatic digestion, tissue was processed in same way as described for spleen in section 1.3.1 except for RBC lysis step. Cell suspension was then transferred to 15ml falcon tube and was centrifuged at 1500 rpm for 5 min at 4°C and continued as described in section 2.3.1.

### 2.3.4 Isolation of mononuclear cells from CNS and spinal cord:

Mice were euthanized with $CO_2$ and perfused with ice cold PBS. Brain and spinal cord were dissected and placed on to a 70µM cell strainer in a petri dish containing 25 ml of ice cold PBS. Tissue was homogenized using syringe plunger and cell suspension was transferred to 50 ml falcon tube and centrifuged at 1500 rpm at 4°C for 10 minutes. Supernatant was discarded and the pellet was resuspended in 10.5 ml PBS and was transferred to oak ridge centrifuge tubes (Thermo Scientific, Nalgene, Cat # 3138-0030). Cell suspension was overlaid with 4.5 ml of percoll (GE healthcare, Catalogue number 17-0891-01) and centrifuged (Heraeus Multifuge X1R centrifuge, Cat-No: 75004250) at 108000 rpm at 4°C for 30 min without brakes. After centrifugation, 3 layers can be seen based on percoll gradient separation, with uppermost layer containing myelin and lowermost layer showing a RBC ring and a middle interphase containing mononuclear cells. Uppermost layer is discarded by gently pipetting out and the interphase is collected into 50ml falcon tube. Volume is made up to 40ml with ice cold PBS and centrifuged for 10 minutes at 1500 rpm at 4° C. Supernatant was discarded and pellet was resuspended in ice cold PBS and proceeded for flow cytometry staining.

### 2.3.5 Preparation of single cell suspension from Lymph nodes

Mice were euthanized with CO2. Lymph nodes were dissected and placed on to 70µM cell strainer (BD, Cat # 352350) in a petri dish containing ice cold PBS and were homogenized using syringe plunger. Cell suspension was processed as described in section 2.3.1 except for RBC lysis step.

## 2.4 Surface staining of antigens

1-2 million cells were used for flow cytometry analysis. Cells were transferred to V bottomed 96 well plate and were centrifuged at 1500 rpm for 5 minutes at 4 ° C. Prior to surface staining, cells were stained for viability with live/dead fixable aqua dead cell staining kit (Thermofisher Scientific Cat # L34957) for 15 minutes in dark on ice in a volume of 100µl. At the end of incubation, volume was made up to 200µl with ice cold PBS and centrifuged at 1500 rpm for 5 minutes at 4 ° C and supernatant was discarded. Surface antibody cocktail was added to the cell pellet, a volume of 50µl and cells were suspended by pipetting and incubated for 20 minutes on ice in dark. Finally volume was made up to 200µl with ice cold PBS (washing step) and centrifuged at 1500 rpm for 5 minutes at 4°C. Supernatant was discarded and washing step was repeated again and cell pellet was either resuspended in 250µl of FACS buffer for analysis or was proceeded for intracellular antigen staining.

## 2.5 Intracellular staining

Cells were stimulated with PMA (50ng/ml) and Ionomycin (1µl/ml) for 4.5 hours at 37 °C. After surface staining of antigens and live/dead staining, cells were fixed using BD Cytofix/Cytoperm ™ kit (BD Biosciences, Cat # 554722) and intracellular staining was performed according to the manufacturer's instructions in 96 V bottomed well plate. In brief, cells were fixed with 100µl of Cytoperm buffer and incubated for 20 minutes at room temperature. Following incubation, cells were washed with 1x perm buffer (provided as 10X with the kit & is diluted to 1x with distilled $H_20$), centrifuged for 5 mins at 1500 rpm at 4°C and supernatant was discarded. Wash step was repeated, followed by addition of antibodies dissolved in perm buffer and was incubated on ice for 20 minutes, following which washing step with perm buffer was repeated. Finally, pellet was resuspended in FACS buffer and samples were acquired on a flow cytometer.

## 2.6 Intranuclear staining:

Intranuclear staining was performed using FOXP3 ebiosciences staining kit (Cat # 00-5523-00) according to manufacturer's instructions in 96 V bottomed well plate. In short, after surface

staining of antigens and live/dead staining was performed, cells were fixed by adding 200µl of fixation solution, followed by 30 min incubation at room temperature. Cell samples were centrifuged for 5 min at 1500 rpm 4°C and supernatant was discarded. Cell pellet was washed further with 100µl of 1X permeabilization buffer (PB) (Provided as 10X with the kit, it is diluted to 1X with distilled $H_2O$) and centrifugation step was performed. After discarding supernatant, cells were washed again with PB and centrifuged. To the cell pellet, 50ul of FOXp3 flourochrome conjugated antibody dissolved in PB was added and incubated on ice for 30 mins, following which 200ul of PB was added and centrifugation step was repeated. Washing step with PB was repeated once again. Finally pellet was suspended in FACS buffer and samples were acquired with a flow cytometer.

## 2.7 *In vitro* T cell proliferation assay

Mice were immunized with $MOG_{35-55}$ peptide as described in section 2.2.1. On day 14, post immunization mice were sacrificed and spleen was dissected. Single cell suspension of spleen was prepared as described in section. 2x $10^5$ cells per well were plated in triplicates in 96 well round bottomed plates and were stimulated for 48 hours with 60µg/ml of $MOG_{35-55}$ peptide, 500ng/ml Phorbol 12-myristate 13-acetate (PMA) (Sigma, Cat # P1585) and 1µg/ml of Ionomycin (Molecular Probes ™, Cat # I24222) which served as positive control and media without any stimulant served as negative control. After 48 hours of stimulation, 1µCi [3H] thymidine (Hartmann Analytic, Cat # MT6031) was added per well and incubated for 24 hours. Later, thymidine incorporation was measured by beta scintillation counter (Matrix 96 Direct Beta counter, Packard).

## 2.8 *In vitro* stimulation of splenocytes with TLR agonists

Single cell suspension of splenocytes was prepared. Cells were counted and 1x $10^6$ cells were plated per well in triplicates in round bottomed 96 well plates in a volume of 100µl of RPMI media (PAN Biotech, Cat # P04-17500). TLR agonists dissolved in RPMI media were added to the cells making final volume to 200µl per well and media without agonists served as negative control.

TLR2 agonist HKLM was used at the concentration of 0.5µg/ml, TLR3 agonist poly (I:C) of high molecular weight at 10 µg/ml, TLR4 agonist LPS at 1µg/ml, TLR7 agonist ssRNA40 at 0.5 µg/ml and TLR9 agonist ODN1826 at 5µM (Invivogen Mouse TLR1-9 kit, Cat # tlrl-kit1mw). Upon addition of TLR agonists, cells were incubated at 37°C and culture supernatants were collected at 6, 12 and 24 hours post stimulation and sandwich ELISA was done to detect TNF α produced in response to TLR stimulation.

## 2.9 *In vitro* differentiation of naïve T cells:

For *in vitro* differentiation of naïve $CD4^+$ T cells into different Th subsets, spleen and total lymph nodes were dissected and homogenized to prepare single cell suspension. Total cell suspension was used to isolate naïve $CD4^+$ T cells using Miltenyi naïve $CD4^+$ T cell isolation kit (Cat # 130-104-453) according to the manufacturer's instructions. Cells were counted and diluted with the media to obtain the concentration of 4 $x10^6$ cells /ml of which 50ul were plated/well. Plates were prepared by coating 96 well round bottomed plates with plate bound 4µg/ml of anti-CD3 antibody (ebiosciences, Cat # 145-2C11), incubated overnight at 37°C followed by washing with PBS. Cell culture wells were further supplemented with 50ul of media containing skewing cytokines and 2µg/ml of soluble anti-CD28 antibody (Abcam, Cat # PV-1).Cytokines were added at the following concentration: Th0 - none, Th1 - IL-12 (10µg/ml), IL4 (20µg/ml), Th17 – IL-6 (25µg/ml), TGFβ (2.5µg/ml), IL4 (20µg/ml), IFNγ (20µg/ml), iTreg – TGFβ 2.5µg/ml, TR1- IL-27 (100µg/ml), TGFβ (2.5µg/ml). All cytokines were from R & D systems. Cells were cultured for 3 days at 37°C. Thereafter, cells were stimulated with PMA (50ng/ml)/Ionomycin (1µg/ml) for 4.5 hrs and later, stained for surface antigens followed by intracellular staining of cytokines.

## 2.10 **Isolation of cells from Immunization site**

Mice were immunized with MOG peptide as described in section 2.2.1. On Day 5, mice were euthanized with $CO_2$ and site of immunization was dissected. It was then placed on to 70µM cell strainer in a petri dish containing 20ml of ice cold PBS and slightly homogenized using syringe plunger and resultant cell suspension was transferred to 50ml falcon tube and the volume was

made up to 40ml with PBS followed by centrifugation at 1500 rpm for 10 min at 4°C. Supernatant was discarded and pellet was suspended in 40ml of ice cold PBS and centrifugation step was repeated. Pellet was resuspended in ice cold PBS and was either used for extracting RNA or flow cytometry staining.

## 2.11 Isolation of RNA, DNase treatment, cDNA preparation

Mice were euthanized with $CO_2$ and samples of interest namely cortex, spleen, cervical lymph nodes, inguinal lymph nodes and spinal cord were dissected out and were kept on ice. Less than 30 mg of tissue per sample was used for RNA extraction, as per Qiagen RNeasy Mini Kit recommendation (Cat # 74104). 10 µL of 2-Mercaptoethanol (Fluka, Cat# 63689) was added per 1 mL RTL buffer. 500 µL of $RTL^+$ was then added to each sample and pipetted up and down until a homogenate was obtained. The suspension was transferred to a QIA Shreder (QIAGEN Cat #79654) column and centrifuged at 10000 rpm for 5 min. 1 volume 70 % ethanol was added to each sample and was mixed well by pipetting up and down. 500 µL of this solution was added to an RNeasy spin column and was centrifuged for 1 min at 8000 rpm. The flow-through was discarded and the remaining 500 µL was added to the column and centrifuged as above. After discarding the flow-through, 700 µL of RW1 buffer was added to the column and samples were centrifuged at 8000 rpm for 1 min .The flow-through was discarded and 500 µL RPE buffer was added to the column, followed by centrifugation for 1 min at 8000 rpm. The column was transferred to a new 2 mL collection tube and the centrifugation step was repeated. The column was placed into a new 1.5 mL eppendorf tube and 30 µL RNase-free water was added to the center of the column without touching the membrane. Samples were centrifuged for 1 min at 8000 rpm.

Samples were further subjected to DNase treatment (Ambicon, Life Technologies # AM1907), according to the kit recommendations 0.1 µL buffer and 1 µL DNase was added for every 1 µL of RNA sample. In final, 3 µL buffer + 1 µL DNase were added to 30 µL of each sample, followed by incubation at $37^0$C for 30 minutes. 1.7 µL DNase inhibitor was added to each sample and was incubated at room temperature for 5 minutes with vortexing every minute, after which samples were centrifuged at 10000 rpm for 2 min. 30 µL sample was transferred to a fresh 1.5 mL eppendorf tube. RNA concentration was assessed by Nanodrop.

cDNA synthesis was carried out using iScript (Bio-Rad #1708891) kit. In brief, RNA was reverse-transcribed to cDNA as per kit recommendations: for each 20 µL of final reaction mix, 4 µL of master mix and 1 µL of transcriptase enzyme was added to template RNA for a final concentration of 5 ng/µL. Water was added to make a final volume of 20 µL.

Reaction was run in 96-well PCR plates (Thermo-Fischer) and on C1000 Touch Thermocycler (Bio-Rad), with the following PCR cycle: 25°C for 5 min; 42°C for 30 min; 85°C for 5 min.

### 2.11.1 Quantitative polymerase chain reaction (qPCR) analysis

For quantitative analysis of mRNA expression levels, 2 µL of each sample was added to 10 µL QuantiFast SYBR Green PCR buffer (QIAGEN, Cat. #204054), 6 µL Nuclease free water and 2 µL of QuantiTect Primer Assay (QIAGEN) primer of interest. Primers: Ifnb1 (QT00249662), Irf7 (QT00245266), Mx1 (QT01064231), CSF2 (QT00251286), IFNg1 (QT01038821), IL10 (QT00106169), IL17A1 (QT00103278) and Actb (QT00095242). qPCR was run in Framestar 384-well plates (4titude), 5 µL per well, 3 technical replicates per sample, on QuantStudio™ 6 & 7 Flex Real-Time PCR System (Applied Biosystems) with the following PCR cycle conditions: 95 $^0$C for 5 min; 95 $^0$C for 10 s, 60 $^0$C for 30 s for 40 cycles; followed by melting curve analysis: 40 $^0$C for 15 s; 60 $^0$C for 1 min, 95$^0$C for 15 s.

mRNA expression levels were calculated against those of a standard wild-type non-induced spleen sample, using Actb as the house keeping gene, according to the formula mRNA expression levels equals 2^-ΔΔCt. Only replicates that presented a single peak in the melting curve analysis were included in the analysis.

## 2.12 Measurement of IFN β expression in vivo

Δβ-luc reporter mice, in which luciferase activity is driven by IFNβ promoter were used for measuring IFNβ expression in vivo. This reporter mouse allows to visualize constitutive expression of IFNβ in several tissues (Lienenklaus et al., 2009). EAE was induced in Δβ-luc mice as described in section 2.2.1.

For detection of luciferase activity post immunization, *in vivo* imaging was done. In brief, mice were injected with 150 mg/kg of D-luciferin in PBS intraperitoneally and were anesthetized using Isofluran (Baxter) and monitored using an IVIS 200 imaging system (Calipers Life Sciences). Living Image 3.0 software (Calipers Life Sciences) was used to quantify photon influx (Lienenklaus et al., 2009).

## 2.13 Enzyme-linked immunosorbent assay (ELISA)

To determine the amount of TNF α produced in response to stimulation of splenocytes with TLR agonists in vitro, sandwich ELISA was performed using anti-mouse TNFα ready-set go kit from eBioscience (Cat # 88-7324-22). ELISA plates were prepared by coating the plate with capture antibody and were incubated at 4°C overnight. Plates were then washed with washing buffer and free binding sites were blocked with assay solution by incubating at room temperature for 1 h. Plate washing step was repeated, followed by the addition of standard and diluted samples to the plate with an overnight incubation at 4°C. Following washing, the biotin-conjugated detection antibody was added and incubated for 1 h at room temperature. Unbound antibodies were removed by washing and avidin- horseradish peroxidase (HRP) was added, followed by incubation for 30 min. After washing, substrate TMB (Tetramethyl benzidine) was added and the reaction was stopped after 15 min of adding 1 M $H_3PO_4$. The optical density (OD) was measured in the Sunrise ELISA microplate reader at 450 nm with 570 nm correction. After preparing a standard curve by plotting the OD of each standard versus its concentration, the protein concentration of the samples was calculated by comparing the optical density of the unknown samples to the standard curve.

## 2.14 Histology

Mice were sacrificed and perfused with freshly prepared 4% Paraformaldehyde. Spinal cords were carefully removed and fixed in 4% buffered formalin. Further, spinal cords were dissected and embedded in paraffin before proceeding with H&E staining and, Luxol fast blue to measure the degree of demyelination, MAC-3 staining was done (BD Pharmingen) for macrophages and microglia, CD3 (MCA1477 Serotec, Düsseldorf, Germany) for T cells, B220 (1 BD Pharmingen)

for B cells and APP (MAB348, Millipore) for indication of axonal damage. Spinal cord sections were evaluated using cell-P software (Olympus) (Prinz et al., 2006).

### 2.14.1 Statistical analysis of histology data

Normality test was done using Kolmogorov-Smirnov test. If normality was given, an unpaired *t*-test was applied. If the data did not meet the criteria of normality, the Mann-Whitney *U* test was applied. Differences were considered significant when the *P* value was <0.05.

## 2.15 Graphical software and statistical analysis of data

Microsoft Excel and Graphpad prism versions 5 and 6 were used for analyzing the data and making the graphs. Student t test was performed were applicable. Mann-Whitney *U* test was applied to EAE maximal scores between the groups and to area under curve.

## 2.16 Flow cytometry sample acquisition and data analysis

Samples were acquired on LSR II Fortessa and CyAn$^{TM}$ ADP flow cytometers. Flow cytometry data was analyzed using Flow Jo version 10.

**Table 3. List of antibodies for flow cytometry analysis**

| Antibody | Clone | Flurochrome | Catalogue number | Company |
|---|---|---|---|---|
| CD11b | M1/70 | PE<br>APC-Cy7 | 101207<br>101225 | BioLegend |
| CD4 | RM4-4 | PB<br>APC | 116007<br>100515 | BioLegend |
| CD8 | 53-6.7 | FITC<br>PE | 100705<br>100707 | BioLegend |
| CD11c | N418 | PE-CY7 | 117317 | BioLegend |
| Siglec H | 551 | PE | 129605 | BioLegend |
| BST2 | 927 | APC | 127015 | BioLegend |
| B220 | RA3-6B2<br>RA3-6B2 | FITC<br>APC | 103205<br>103211 | BioLegend |
| IL17 | TC11-18H10.1 | PE | 506903 | BioLegend |
| FOXP3 | 150D | PE | 320007 | BioLegend |
| IFNγ | XMG1.2<br>XMG1.2 | APC<br>PE-Cy7 | 505809<br>505825 | BioLegend |
| IL10 | JES5-16E3 | APC | 505009 | BioLegend |
| CD44 | IM7 | PE | 103007 | BioLegend |
| CD25 | 3C7 | APC-CY7 | 101909 | BioLegend |
| GR1 | RB6-8C5 | APC | 108407 | BioLegend |
| NK1.1 | PK136 | PE-CY7 | 108713 | BioLegend |
| CD3 | 17A2 | FITC | 100203 | BioLegend |
| CD5 | 53-7.3 | FITC | 100605 | BioLegend |
| CD23 | B3B4 | PE-CY7 | 101613 | BioLegend |

| | | | | |
|---|---|---|---|---|
| CD21 | 7E9 | APC | 123411 | BioLegend |
| CD19 | 6D5 | APC-CY7<br>FITC | 115529 | BioLegend |
| CD45 | 30-F11 | APC<br>APC-CY7 | 103111<br>103115 | BioLegend |
| IgM | RMM-1 | PE | 406507 | BioLegend |

# 3 RESULTS

## 3.1 *TLR9*$^{-/-}$ mice are susceptible to EAE

CFA used for EAE induction is composed of heat killed *Mycobacterium tuberculosis* and mineral oil. TLR9 recognizes CpG motifs present in the mycobacterial DNA (Basu et al., 2012). Many research groups have investigated the requirement of TLR9 for EAE induction and disease course but reports have been inconsistent (Details Table 2). Therefore, we investigated the impact of TLR9 deficiency on EAE disease course. Both *TLR9*$^{-/-}$ and Wt mice were immunized with MOG peptide as described in the methods section. We observed that both *TLR9*$^{-/-}$ and Wt mice were susceptible to EAE induction and clinical disease symptoms commenced around day 10 in both the groups. 100% disease incidence was observed in *TLR9*$^{-/-}$ group where as 80% disease incidence was seen in Wt control group (Table 4). *TLR9*$^{-/-}$ mice displayed trend of more severe disease symptoms over the course of EAE in comparison to the Wt mice (Fig 5). *TLR9*$^{-/-}$ mice exhibited maximum clinical scores around day 14 post immunization whereas for Wt controls maximum scores were observed around day 13 (Table 4). Median of maximal scores for *TLR9*$^{-/-}$ mice was 3.5 whereas for Wt mice it was 2.6 (Table 4). But the difference of median of maximal score was not significant between the groups (Mann-Whitney test, p value 0.1400).

Further, to assess the extent of demyelination, infiltration by T cells, B cells and macrophages during the disease progression, both *TLR9*$^{-/-}$ and Wt mice were killed at the peak of the disease and spinal cords were examined histologically. The extent of demyelination was comparable between Wt mice and *TLR9*$^{-/-}$ mice (Figure 7A and B). Infiltration by T cells, macrophages and B cells also remained comparable between the two groups (Figure 7 C, D, E, F, G and H). But higher amyloid precursor protein-positive (APP) axonal structures representing axonal damage were observed in *TLR9*$^{-/-}$ mice in comparison to the Wt mice (Figure 7 I and J). Histological analysis of sick mice CNS revealed no major difference between the two groups except for higher axonal damage seen in case of *TLR9*$^{-/-}$ mice. This taken together with the EAE clinical scoring clearly suggests that TLR9 is dispensable for EAE induction.

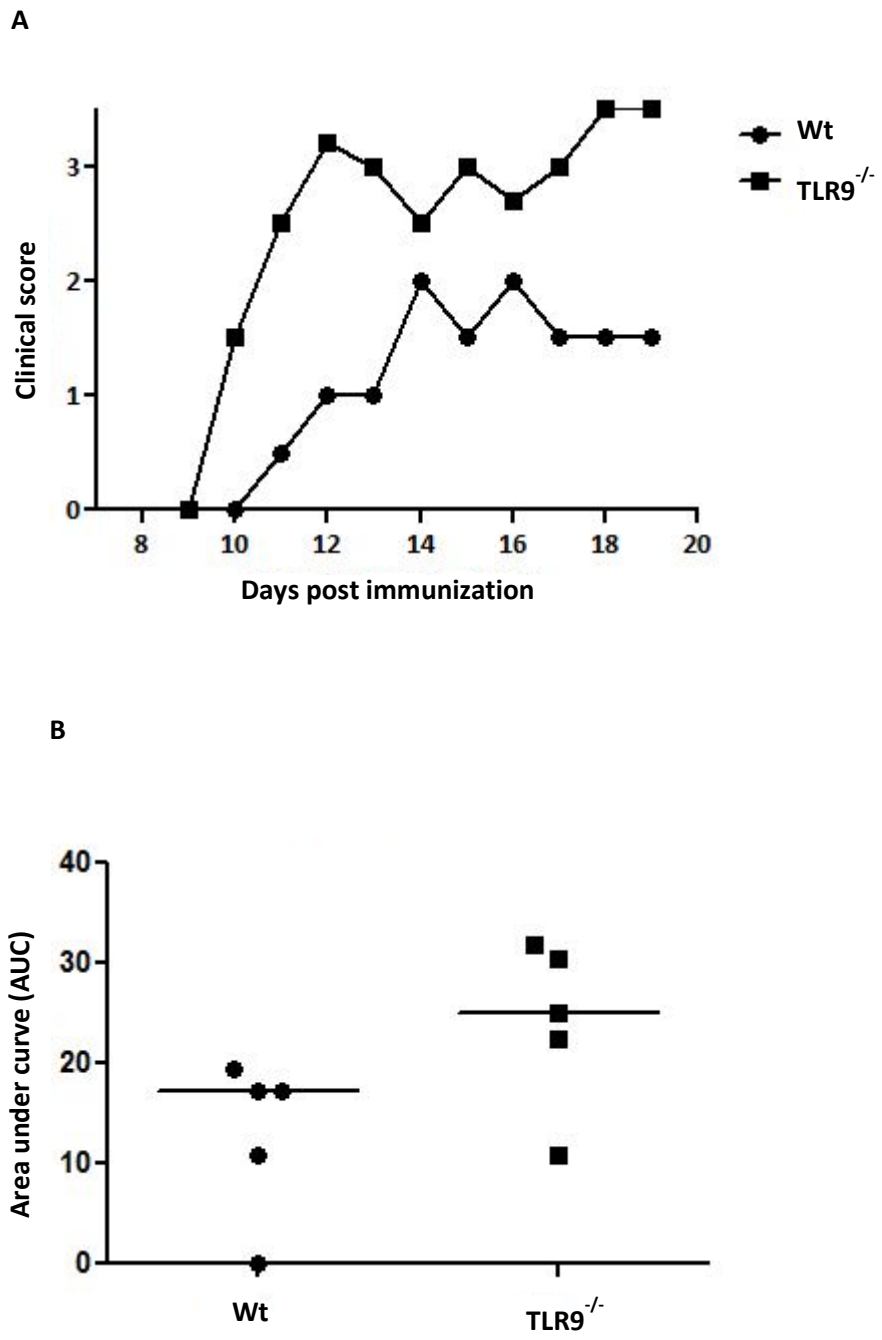


**Figure 5. Active EAE induction in *TLR9*$^{-/-}$** A) Both *TLR9*$^{-/-}$ (Squares) and Wt (dots) female mice, 5 mice per group were immunized with MOG peptide, CFA and PT. Mice were observed daily for EAE clinical symptoms. Each data point represents median of score per day from five mice per group. Out of 5 mice, in Wt group 4 mice developed EAE disease symptoms and in *TLR9*$^{-/-}$ group, all the 5 mice developed EAE clinical signs. B) Area under the curve (AUC) for each mouse was calculated during the EAE disease course and the middle line represents median. AUC was used to measure the overall disease severity

between Wt and *TLR9*$^{-/-}$ . Using Mann-Whitney U test, no significant difference was found between the groups in disease severity at $p<0.05$. Experiment was performed once.

**Table 4. Requirement of *TLR9*$^{-/-}$ in EAE** A) EAE was induced in both Wt and *TLR9*$^{-/-}$ female mice with 5 mice per group. In Wt group, only 4 mice developed EAE clinical signs out of 5 with disease incidence of 80% where as in *TLR9*$^{-/-}$ group, all the 5 mice developed EAE clinical signs with disease incidence of 100%. Mean day of disease onset was calculated by taking mean of the first day of disease onset. Mean day of maximum score was calculated by taking the mean of the day when each mouse displayed its maximum clinical score during EAE disease course. To calculate mean day of disease onset and mean day of maximum score, only sick mice were taken into consideration. B) Median of maximal score was calculated by taking maximum score displayed by each mouse during the EAE disease course. To calculate median of maximal score, only maximum score of sick mice was included.

**A**

| Genotype | Incidence % | Mean day of disease onset | Mean day of maximum score |
|---|---|---|---|
| ***TLR9*$^{-/-}$** | **100%** | **10** | **14** |
| **Wt** | **80%** | **10** | **13** |

**B**

| Genotype | Median of maximal score |
|---|---|
| ***TLR9*$^{-/-}$** | **3.5 (5/5)** |
| **Wt** | **2.6(4/5)** |

## 3.2 Endosomal TLRs are dispensable for EAE induction

Endosomal TLRs (3, 7, and 9) have been highly implicated in pathology of many autoimmune diseases. Endosomal TLRs are primarily expressed on DCs and their signaling in DCs results in the upregulation of IFN-inducible genes besides promoting recruitment of T helper cells and inducing B cell activation (Trivedi and Greidinger, 2009). So, we wanted to investigate the requirement of endosomal TLRs for active EAE induction using *TLR379*$^{-/-}$ mice. Active EAE was induced in *TLR379*$^{-/-}$ and Wt control female mice by immunizing with MOG peptide as described earlier and mice were observed daily post induction for EAE clinical symptoms. We observed that combined deficiencies of endosomal TLRs 3, 7 and 9 did not protect mice from developing EAE clinical signs. 100% disease incidence was observed in *TLR379*$^{-/-}$ group and Wt mice developed EAE clinical symptoms with 87% disease incidence (Table 5). Mean day of disease onset for Wt control group was day 10 post induction whereas *TLR379*$^{-/-}$ exhibited a delay of two days in disease onset (Table 5). This delay in disease onset was accompanied by more severe clinical signs in *TLR379*$^{-/-}$ in comparison to Wt controls (Figure 6 and Table 5). Median maximum score exhibited by *TLR379*$^{-/-}$ was 3.5 in comparison to 2.5 score exhibited by Wt controls (Table 5) and the difference of median maximum score between the groups was significant (Mann Whitney test, p value 0.0029)

Further, to assess the extent of demyelination, infiltration by T cells, B cells and macrophages during disease course, both *TLR379*$^{-/-}$ and Wt mice were sacrificed at the peak of the disease and spinal cords were examined histologically. Extent of demyelination was comparable between Wt and *TLR379*$^{-/-}$ mice (Figure 7 A and B). Infiltration by T cells, macrophages and B cells was slightly reduced in *TLR379*$^{-/-}$ in comparison to Wt mice (Figure 7 C, D, E, F, G and H). Axonal damage was slightly reduced in *TLR379*$^{-/-}$ when compared to Wt controls (Figure 7 I and J).

Though absence of endosomal TLRs3, 7 and 9 resulted in increased disease severity in comparison to Wt mice, histological analysis of sick mice CNS revealed no major difference between the two groups. This taken together with the EAE clinical scoring clearly suggests that the endosomal TLRs are dispensable for EAE induction.

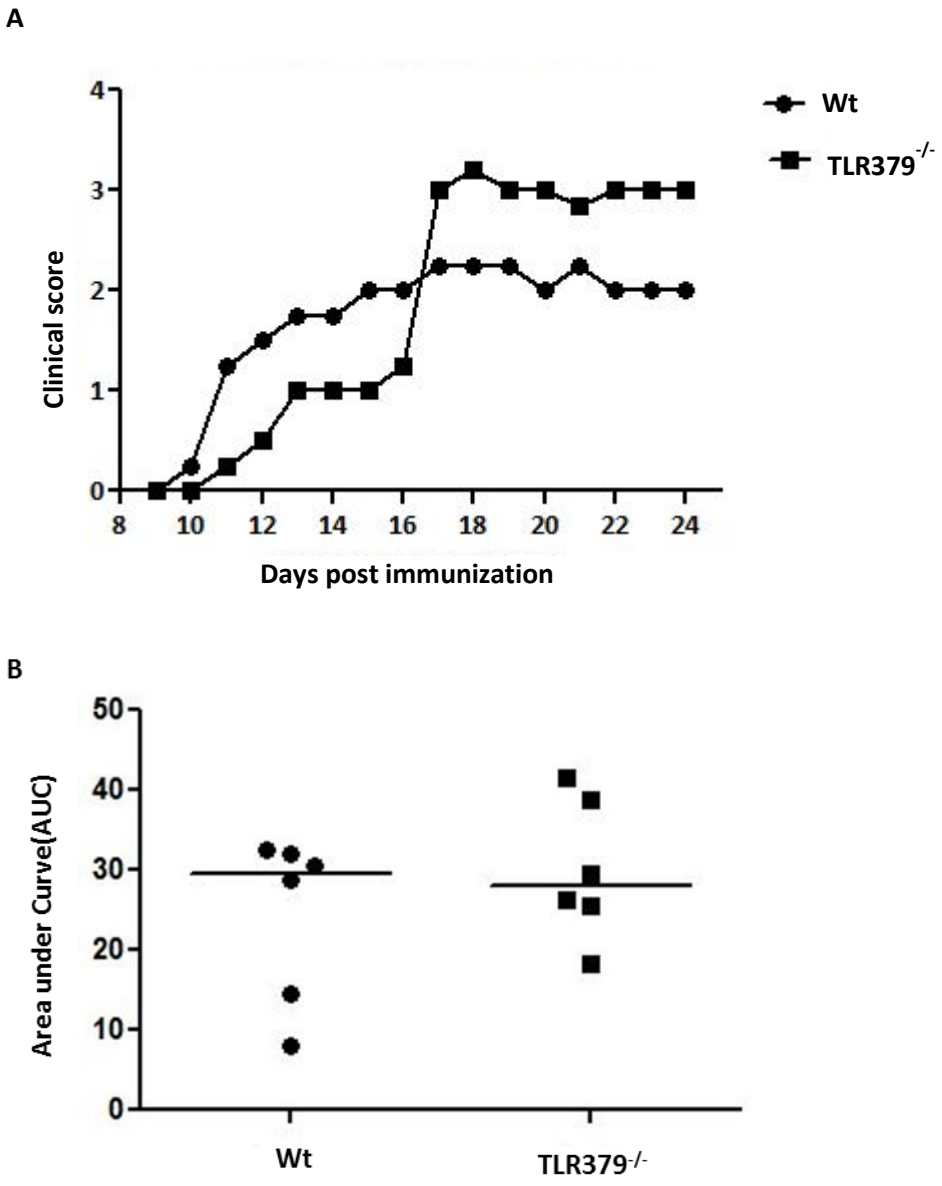


**Figure 6. Active EAE induction in *TLR379*$^{-/-}$.** A) Both *TLR379*$^{-/-}$ (squares) *and* Wt (dots) female mice, 6 mice per group were immunized with MOG peptide, PT , CFA and were scored daily for EAE clinical signs. Each data point represents median per day from six mice. All Wt and *TLR379*$^{-/-}$ mice developed EAE clinical signs with 100% disease incidence. B) Area under the curve (AUC) for each mouse was calculated during the EAE disease course and the middle line represents median. AUC was used to measure the overall disease severity between Wt and *TLR379*$^{-/-}$ .Using Mann-Whitney U test, no significant difference was found between the groups in disease severity. Experiment was performed thrice. Experimental repetition results are shown in appendix I.

**Table 5. Table summarizing the requirement of endosomal TLRs 3, 7 and 9 for active EAE induction.** A) Data pooled in from three independent experiments. In total, 16 mice were used for analysis per group (Wt and *TLR379*$^{-/-}$). In Wt group, out of 16 mice only 14 mice were sick with disease incidence of 87% and in *TLR379*$^{-/-}$ group all the 16 mice developed EAE with disease incidence of 100%. Mean day of disease onset was calculated by taking mean of the first day of disease onset. Mean day of maximum score was calculated by taking the mean of the day when each mouse displayed its maximum clinical score during EAE disease course. To calculate mean day of disease onset and mean day of maximum score, only sick mice were taken into consideration. B) Median of maximal score was calculated by taking maximum score displayed by each mouse during the EAE disease course. To calculate median of maximal score, only maximum score of sick mice was included.

**A**

| Genotype | Incidence % | Mean day of disease onset | Mean day of maximum score |
|---|---|---|---|
| **TLR379$^{-/-}$** | **100%** | **12** | **18** |
| **Wt** | **87%** | **10** | **14** |

**B**

| Genotype | Median of maximal score |
|---|---|
| **TLR379$^{-/-}$** | **3.5(16/16)** |
| **Wt** | **2.5 (14/16)** |

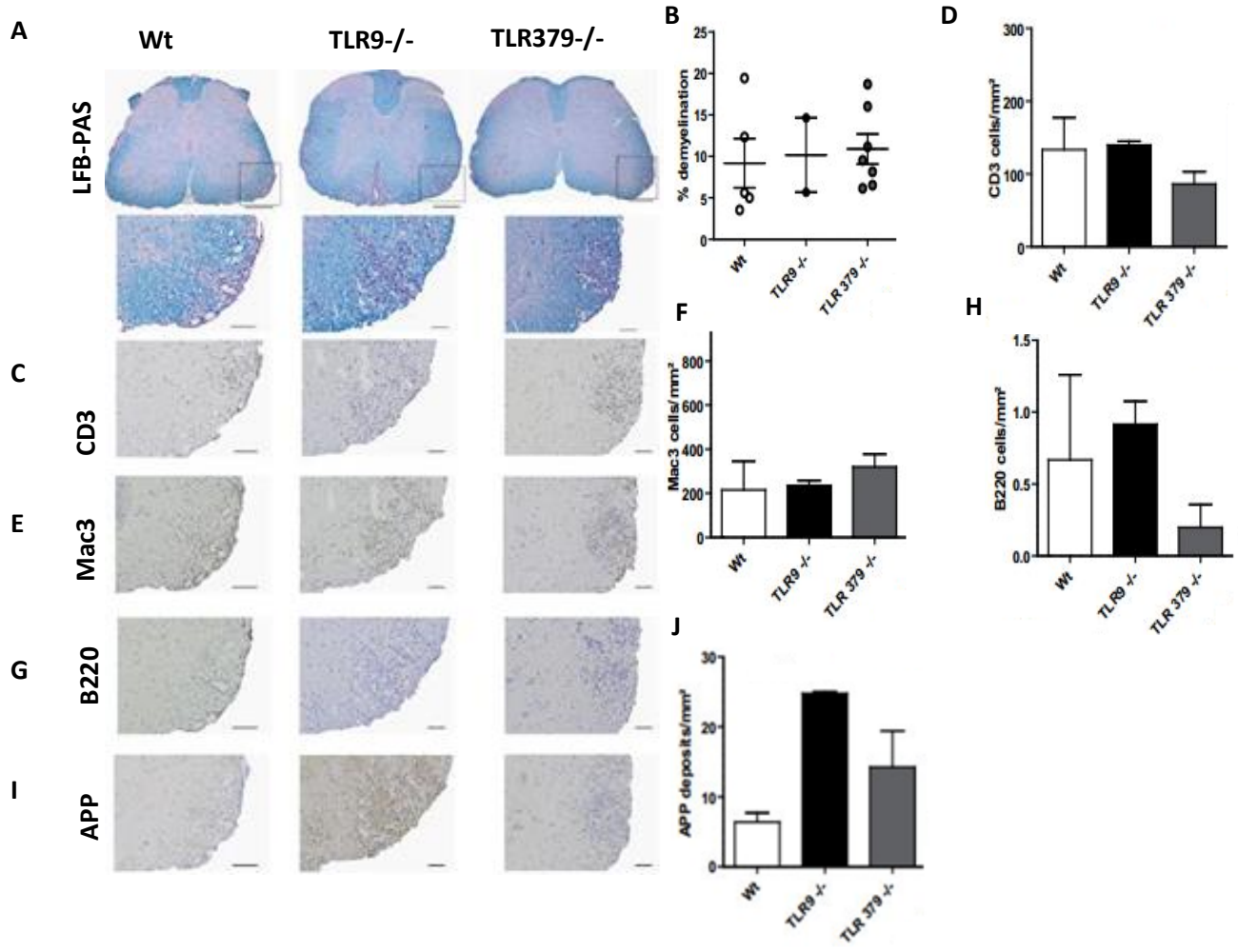


**Figure 7. Histological analysis of CNS tissue from *TLR9*$^{-/-}$ , *TLR379*$^{-/-}$ and Wt sick mice examined at the peak of the disease**.

Spinal cord sections were stained with Luxol fast blue (LFB) to assess the extent of demyelination (A), CD3 to assess T cell infiltration (C), Mac 3 for macrophage infiltration and microglial population (E), B220 for B cells (G) and amyloid precursor protein (APP) (I) to assess the extent of axonal damage. Scale bars shown are 100µm. On the right is the statistical quantification of extent of demyelination, cell infiltration and axonal damage (B, D, F, G, H, I). Data is expressed as mean ± SD.

## 3.3 Deciphering the role of combined deficiencies of TLRs 2, 3, 4, 7 and 9 in EAE

Next, we wanted to use a knockout model that would allow us to investigate the role of major number of TLRs in EAE giving us insights into requirement of the TLR signaling for EAE induction. For this, we have used *TLR23479*$^{-/-}$ mice. As mentioned earlier, in *TLR23479*$^{-/-}$ mice not

only TLR 2, 3 , 4, 7 and 9 signaling is disabled but also that of TLRs 1 and 6 because of their dependency on TLR2 for hetero dimer formation

### 3.3.1 Ex vivo stimulation of total splenocytes with TLR agonists

The *TLR23479*$^{-/-}$ mice genotype was initially confirmed by PCR typing for Wt allele and mutant allele. In order to further confirm the deficiencies of TLRs 2, 3,4,7,9 in *TLR23479*$^{-/-}$ mice, total splenocytes from *TLR23479*$^{-/-}$ and Wt mice were stimulated *ex vivo* with TLR agonists: HKLM (TLR2 agonist), poly (I:C) (TLR3 agonist), LPS (TLR4 agonist), ssRNA40 (TLR7 agonist) and ODN1826 (TLR9 agonist) for 24 h. Cell culture supernatants were collected at 24 h post stimulation and TNFα was measured by ELISA. Splenocytes from *TLR23479*$^{-/-}$ failed to respond to respective TLR ligands whereas splenocytes from Wt mice responded to TLR ligands by producing TNFα (Figure 8), thus confirming the deficiencies of TLRs 2,3,4,7 and 9 in *TLR23479*$^{-/-}$ mice.

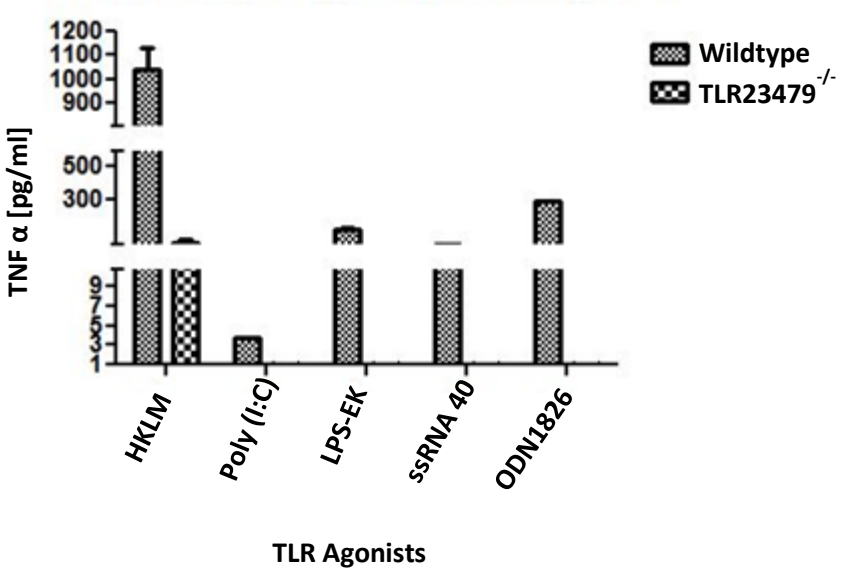


**Figure 8. Ex vivo stimulation of splenocytes from *TLR23479*$^{-/-}$ and Wt mice with TLR agonists.**

Splenocytes from *TLR23479*$^{-/-}$ and Wt mice were stimulated with TLR agonists: HKLM (TLR2 agonist) at $10^8$ cells/ml, poly (I: C) at 10 µg/ml (TLR3 agonist), LPS (TLR4 agonist) at 1µg/ml, ssRNA40 (TLR7 agonist) at 0.5 µg/ml and ODN1826 (TLR9 agonist) at 5µM for 24 h. Cell culture supernatants were harvested at 24 h post stimulation and production of TNFα was measured by ELISA. Data represents the means ± SEM from one experiment performed with n=3 mice per group.

### 3.3.2 Characterization of *TLR23479*$^{-/-}$ mice

We further characterized *TLR23479*$^{-/-}$ mice for any disparity in terms of various cellular compositions in organs thymus, spleen, bone marrow and CNS in comparison to Wt mice.

#### 3.3.2.1 Microglia population remained comparable between *TLR23479*$^{-/-}$ and Wt mice

Microglia express TLRs1-9 and TLR signaling in microglia is known to initiate immune responses in CNS (Olson and Miller, 2004). In order to assess the impact of deficiencies of TLRs 2, 3,4,7,9 on the frequency of microglial cells in the CNS, brain and spinal cords were dissected from *TLR23479*$^{-/-}$ mice and Wt mice in steady state and cells were stained with CD11b and CD45 antibodies and were analyzed by flow cytometry. Microglial cell population was identified by low expression of CD45 and CD11b high expression on cell surface. Microglial population size was comparable between *TLR23479*$^{-/-}$ mice and Wt (Figure 9). Moreover, recently it has been reported that TLRs 2, 3, 4, 7 and 9 are not required for microglial maturation and maintenance in steady state (Erny et al., 2015).

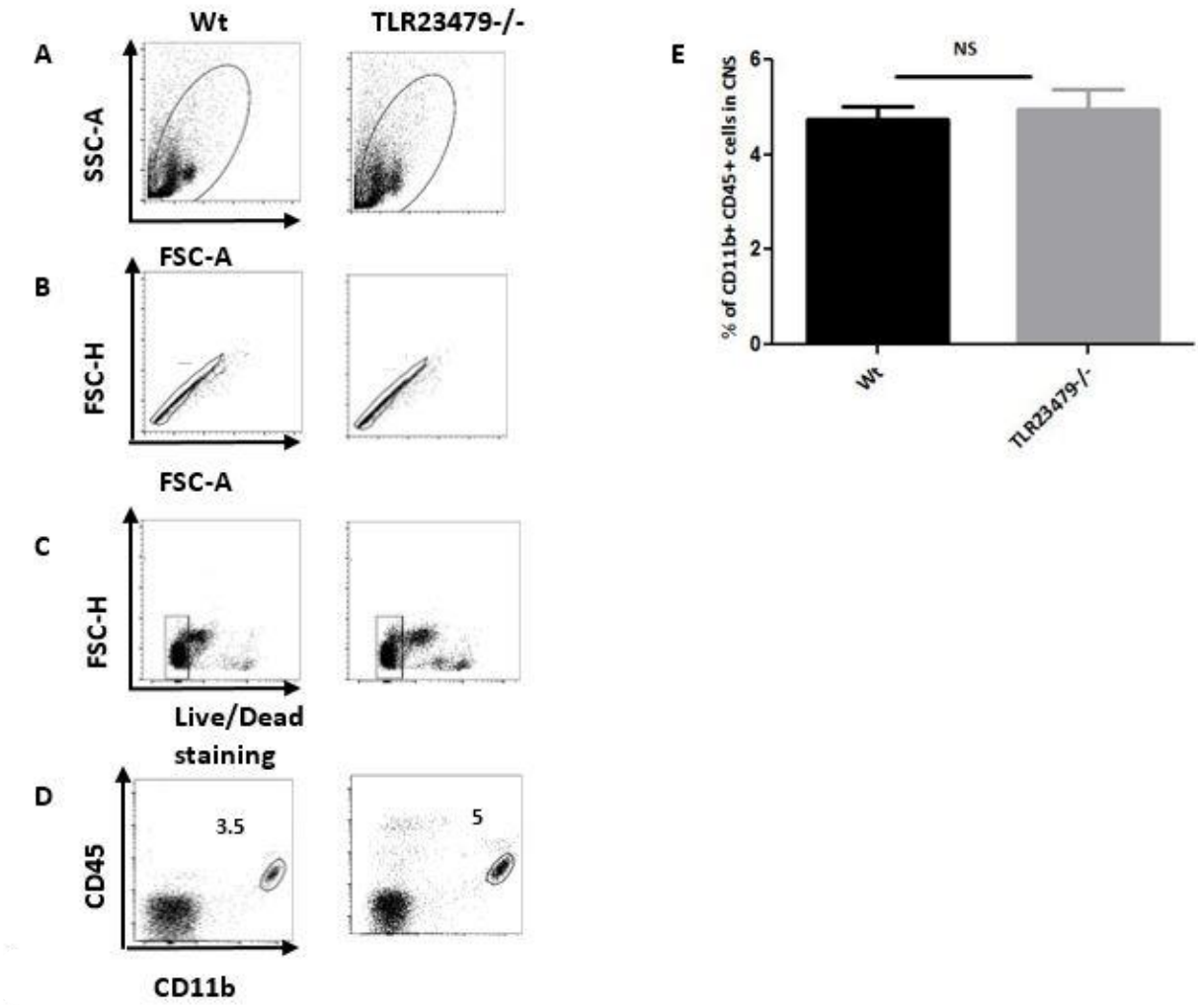


**Figure 9. FACS analysis of microglial population in the CNS of *TLR23479*$^{-/-}$ and Wt mice.** FACS analysis of mononuclear cells isolated from CNS, stained with CD45 and CD11b antibodies. A-C) Gating strategy used for selecting microglial cell population, doublets and dead cell exclusion. D) Microglial population was identified by CD11b$^{high}$ and CD45$^{low}$ expression. E) Data are the means of percentage of CD11b$^{high}$ CD45 $^{low}$ cells ± SEM and two tailed student's t test was performed to check the significance. Experiment was performed once with n= 4 per group.

### 3.3.2.2 *TLR23479*$^{-/-}$ mice have increased populations of CD4$^{+}$ and CD8$^{+}$ single positives and lower population of CD4$^{+}$ CD8$^{+}$ double positives in the thymus

We next wanted to investigate if combined deficiencies of TLRs 2,3,4,7 and 9 has an impact on T cell development in thymus. Double negative (DN), single positive (SP) CD4$^{+}$, SP CD8$^{+}$ and double positive (DP) cells as well as all the four double negative stages (DN1-4) were analyzed.

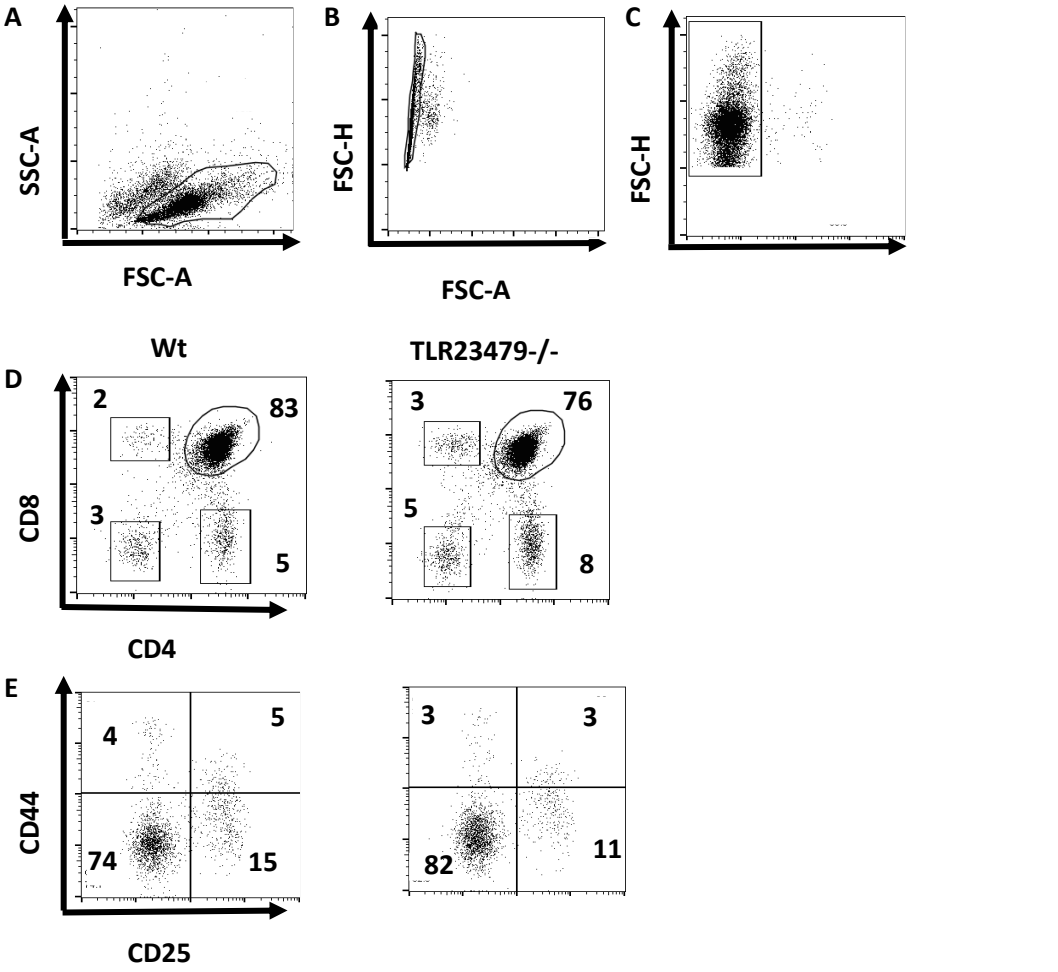
A
SSC-A
FSC-A
B
FSC-H
FSC-A
C
FSC-H
Wt
TLR23479-/-
D
CD8
CD4
2
83
3
5
3
76
5
8
E
CD44
CD25
4
5
74
15
3
3
82
11

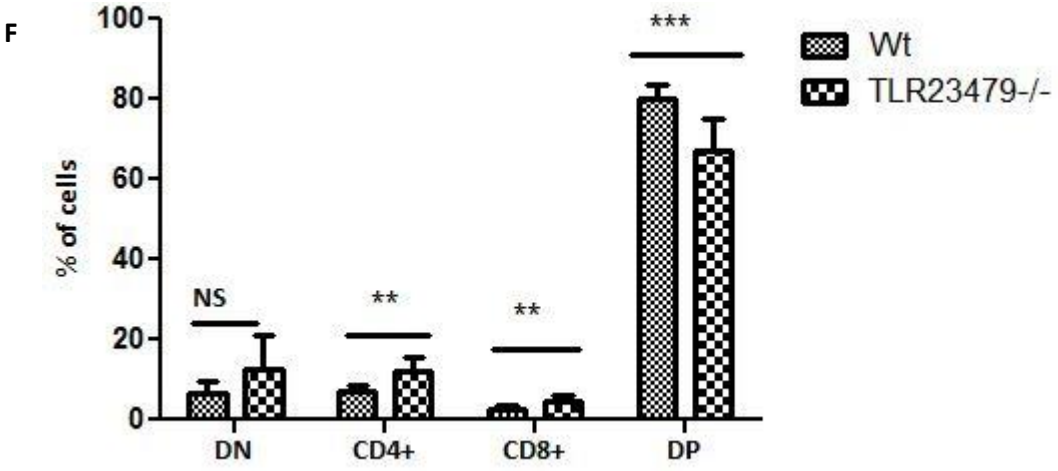
F
% of cells
100
80
60
40
20
0
NS
**
**
***
DN
CD4+
CD8+
DP
Wt
TLR23479-/-

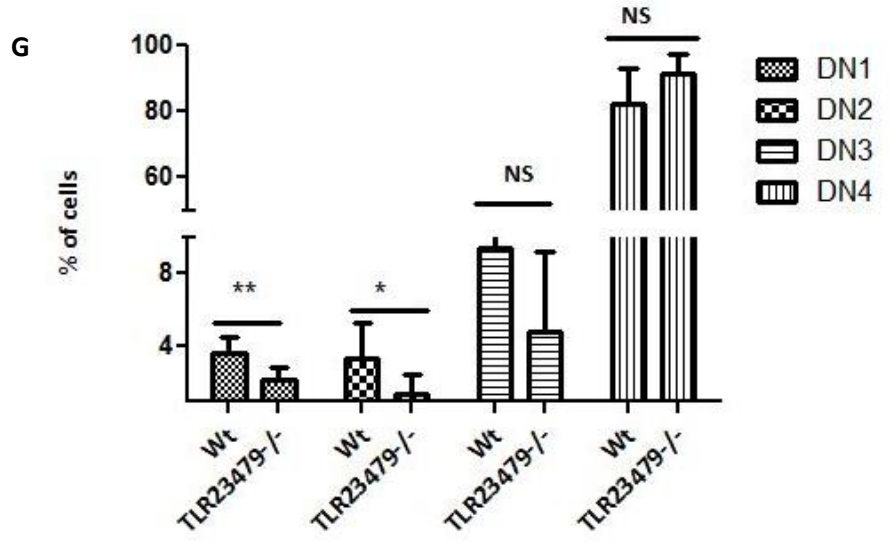


**Figure 10 . FACS analysis of different stages of T cell development in the thymus of *TLR23479*$^{-/-}$ and Wt mice.** A) Cells were gated for lymphocytes. B-C) Doublets and dead cells were excluded. D) Gating strategy for $CD4^+$, $CD8^+$, $CD8^+CD4^+$ DPs and $CD4^-CD8^-$ DNs. E) Gating strategy for DN stages, cells were pregated on $CD4^-CD8^-$ cells shown in D, all the four DN stages are shown. $CD44^+$ $CD25^-$ (DN1 stage) $CD44^+$ $CD25^+$ cells (DN2), $CD44^-CD25^+$ (DN3) and $CD44^-$ $CD25^-$ (DN4). F) Mean percentages of indicated populations ± SD, with n = 8 mice per group. Statistically significant difference was found between $CD4^+$ SP, $CD8^+$ SP, $CD4^+$ $CD8^+$ DPs of *TLR23479*$^{-/-}$ and Wt. G) Mean percentages of indicated populations ± SD with n = 7 mice per group. Statistically significant difference was found between DN1 and DN2 stages of *TLR23479*$^{-/-}$ and Wt Data is pooled from 3 independent experiments. For statistical significance, student t-test was performed, ** p <0.01, *** p<0.001.

We observed that *TLR23479*$^{-/-}$ mice exhibited slightly increased population of $CD4^+$ and $CD8^+$ SPs and a reduction in the $CD4^+CD8^+$ DPs in comparison to Wt mice (Figure 10F). A slight increase in the population size of double negative cells was observed in *TLR23479*$^{-/-}$ group in comparison to Wt mice (Figure 10F). Further analysis of DN stages (DN1-DN4) revealed significantly reduced fraction of cells in DN1, DN2 stages in *TLR23479*$^{-/-}$ group in comparison to Wt. A trend to lower fraction of cells in DN3 and DN4 stages was observed in *TLR23479*$^{-/-}$ group in comparison to Wt mice but the difference was statistically not significant (Figure 10G). Taken together, *TLR23479*$^{-/-}$ mice have higher population of $CD4^+$, $CD8^+$ SPs and lesser population of $CD4^+CD8^+$ DPs in thymus in comparison to Wt mice.

#### 3.3.2.3 *TLR23479*$^{-/-}$ mice have increased population of CD11b$^{+}$ GR1$^{+}$ cells in the spleen in comparison to Wt mice.

We analyzed the impact of absence of multiple TLRs on the frequency of various cell populations in the spleen of *TLR23479*$^{-/-}$ mice in comparison to Wt mice. We observed that *TLR23479*$^{-/-}$ had increased population of CD11b$^{+}$ GR1$^{+}$ granulocytes in comparison to Wt mice (Figure 11 A and B). There was no difference in the cell populations of NK1.1$^{+}$ natural killer cells (11 D and E), CD11c$^{+}$ DCs, pDCs and conventional DCs CD11c$^{+}$ CD4$^{+}$ and CD11c$^{+}$ CD4$^{+}$ cells between *TLR23479*$^{-/-}$ and Wt spleen. (Figure 12 A-F).

T and B cell populations were also analyzed. There was no difference in the population size of CD8$^{+}$ cells between *TLR23479*$^{-/-}$ and Wt mice groups but a slight reduction in population size of CD4$^{+}$ cells was observed in *TLR23479*$^{-/-}$ group but the difference was statistically not significant (Figure 13 A and B). Similarly, Treg population was comparable between the two groups (Figure 13 D and E). Splenic marginal zone B (MZB) cells and follicular B (FB) cells were also analyzed. Splenic MZB cells population was significantly higher in *TLR2379*$^{-/-}$ mice in comparison to Wt mice (13 B and C) whereas splenic FB cells population was slightly reduced in *TLR23479*$^{-/-}$ mice in comparison to Wt mice. Overall, *TLR23479*$^{-/-}$ mice displayed increased population of CD11b$^{+}$ GR1$^{+}$ granulocytes and MZB cells in the spleen in comparison to Wt whereas other cellular populations remained comparable between the two groups.

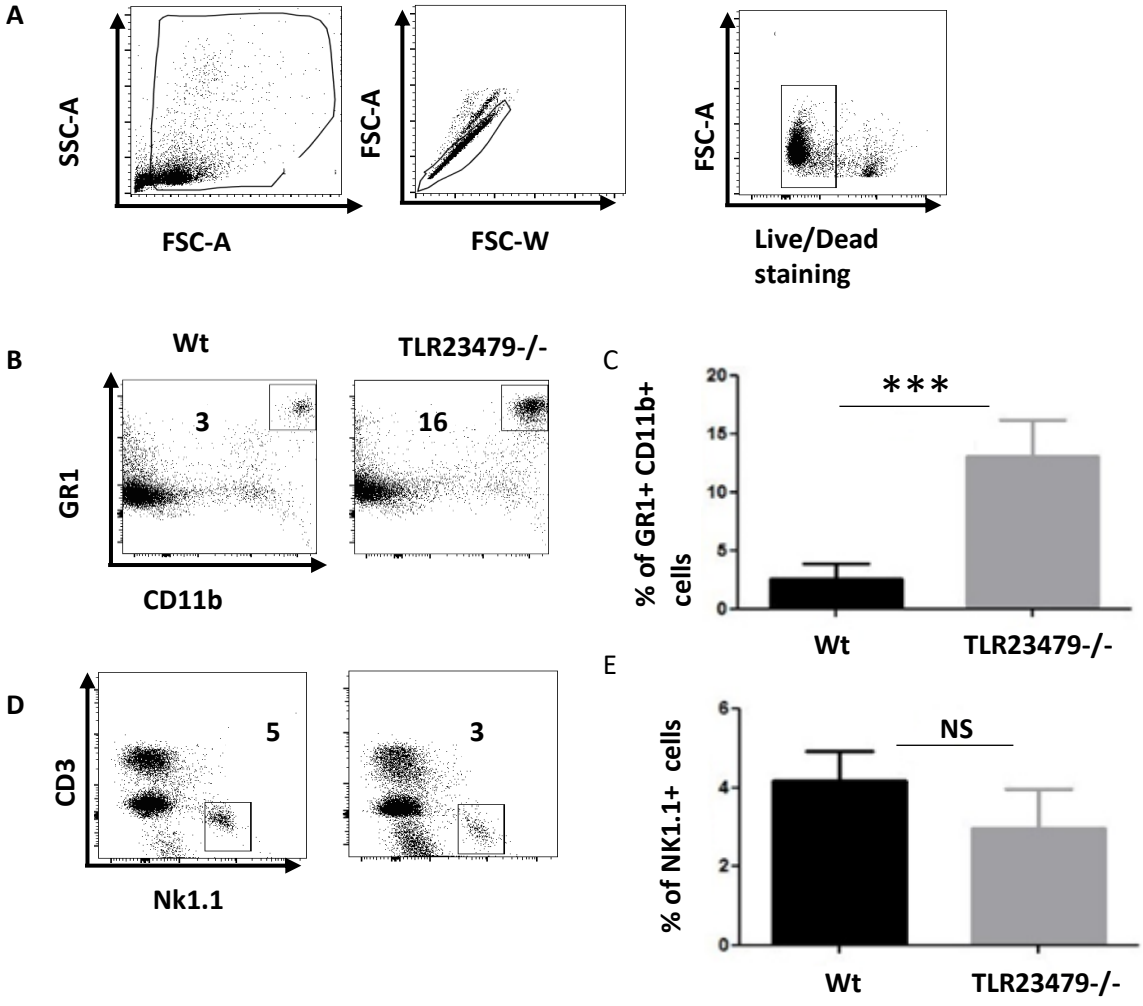


**Figure 11. FACS analysis of cell populations in the spleen of Wt and *TLR23479*$^{-/-}$ .** A) Gating strategy for selection of cells, doublets and dead cells exclusion. B) Higher population of CD11b$^{+}$GR1$^{+}$ granulocytes were observed in TLR23479$^{-/-}$ spleen in comparison to Wt mice. C) Mean percentages of indicated populations ± SD with n = 5 mice per group with significant difference. D) There was no difference in the population size of NK1.1$^{+}$ natural killer cells between the two groups. E) Mean percentages of indicated populations ± SD with n = 5 mice per group. No statistical significance was observed. Data is pooled from two independent experiments. For statistical significance, student t-test was performed, *** p<0.001.

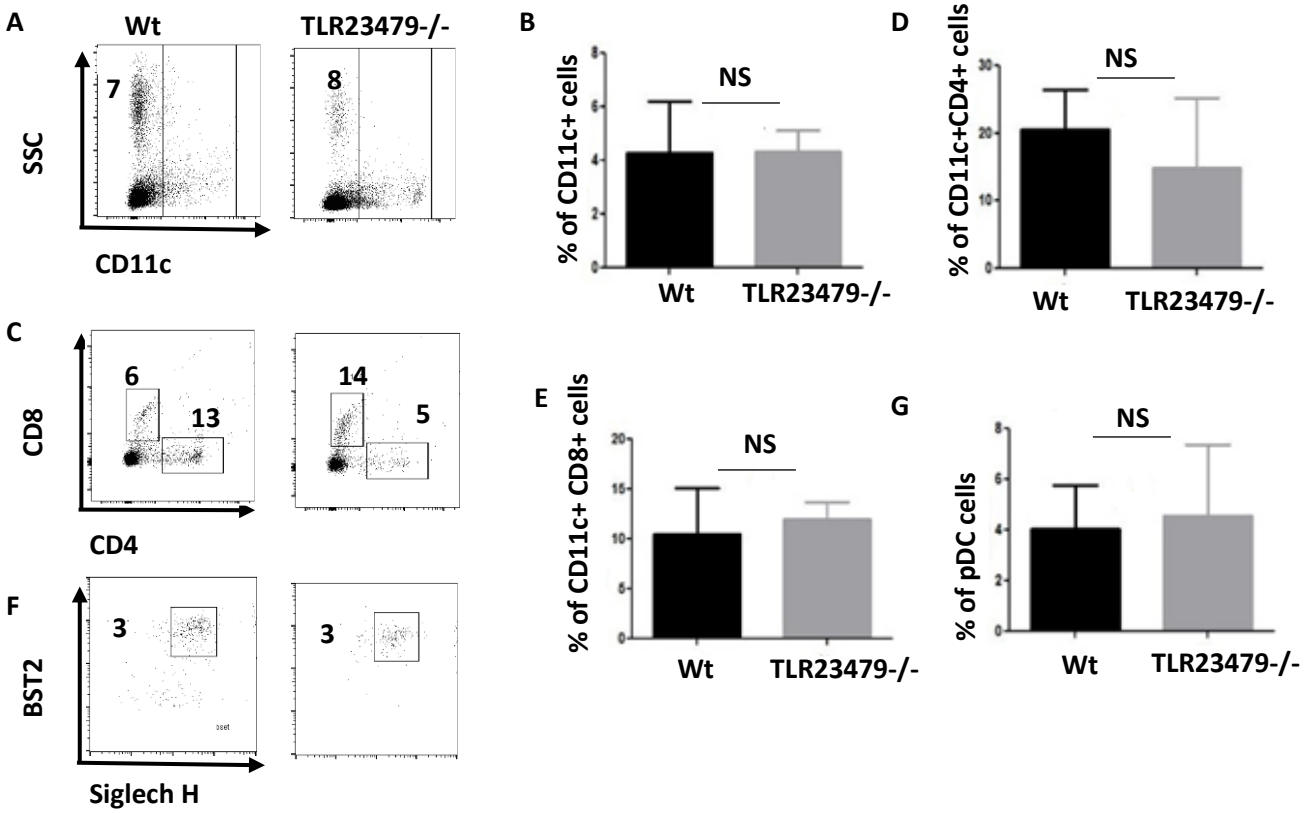


**.Figure 12. FACS analysis of dendritic cell populations in the spleen of Wt and *TLR23479*$^{-/-}$ mice.**

Gating strategy shown in figure 11 was used for selection of cells, duplets and dead cells exclusion. A) Comparable population of CD11c$^{+}$ cells were observed in *TLR23479*$^{-/-}$ spleen in comparison to Wt mice. B) Mean percentages of indicated populations ± SD with n = 5 mice per group. No significant difference was observed. C) Conventional dendritic cells (cDCs) namely CD11c$^{+}$ CD4$^{+}$ and CD11c$^{+}$ CD8$^{+}$ cells population size differed between *TLR23479*$^{-/-}$ and wild type mice. *TLR23479*$^{-/-}$ mice displayed higher fraction of CD11c$^{+}$ CD8$^{+}$ cDCs and lower fraction of CD11c$^{+}$ CD4$^{+}$ cDCs in comparison to the Wt. D and E) Mean percentages of indicated populations ± SD, n = 5 mice per group. No statistical significance was observed. F) Similar percentage of pDCs were observed between the two groups. For pDC selection, pregated CD11c$^{+}$ cells which expressed both Sigech H and BST2 were selected G) Mean percentages of indicated populations ± SD with n = 5 mice per group. No statistical significance was observed. Data is pooled from two independent experiments. For statistical significance, student t-test was performed.

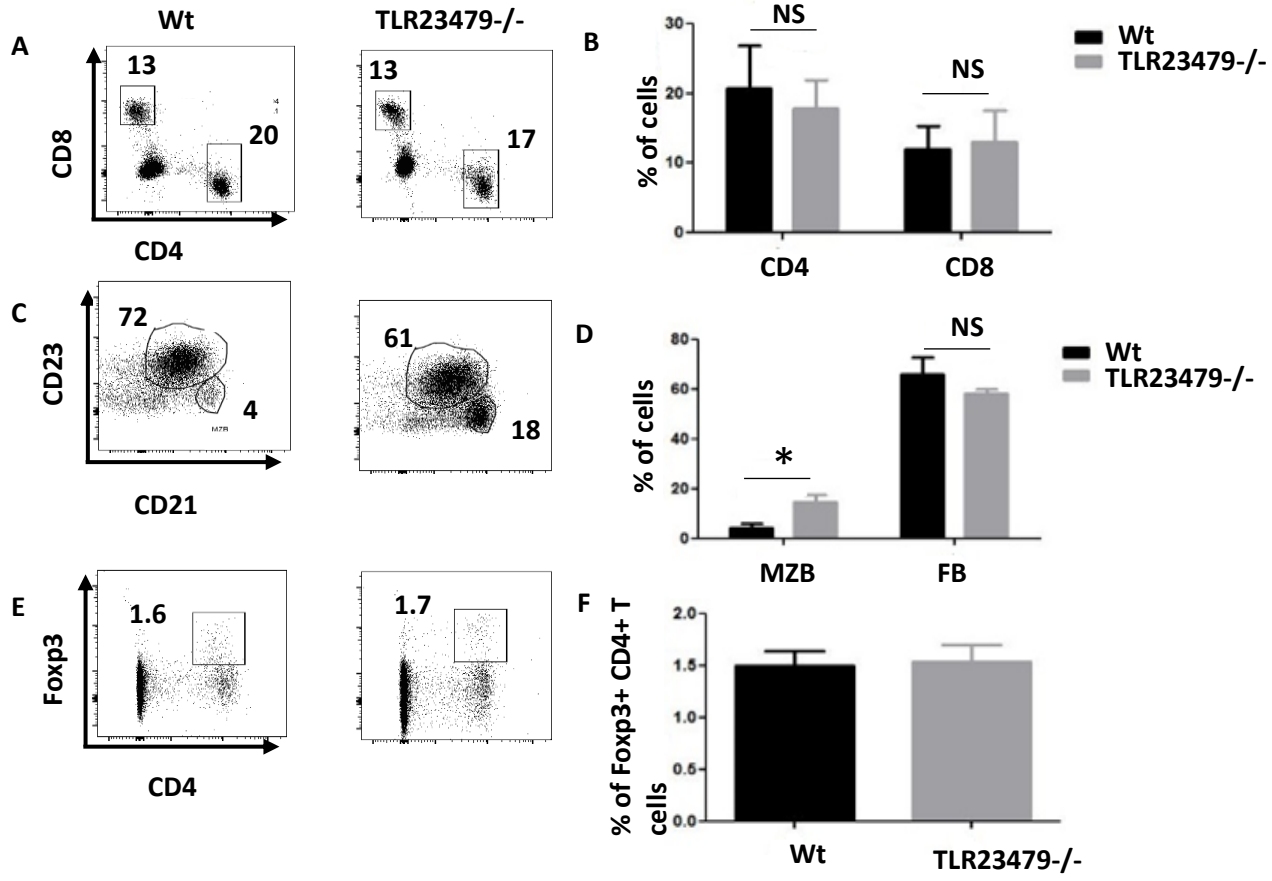


**Figure 13. FACS analysis of T and B cell populations in the spleen of Wt and *TLR23479*$^{-/-}$ mice**

Gating strategy shown in figure 11 was used for selection of cells, doublets and dead cells exclusion. A) Comparable population of CD8$^{+}$ cells were observed in *TLR23479*$^{-/-}$ and Wt spleen. Slight reduction was observed in the fraction of CD4$^{+}$ cells. B) Mean percentages of indicated populations ± SD with n = 5 mice per group. No significant difference was observed between population size of CD4$^{+}$ and CD8$^{+}$ T cells in the spleen between *TLR23479*$^{-/-}$ and Wt mice. C) Marginal zone B cells (MZBs) and follicular B (FB) cells were analyzed. MZBs and FB cells were identified based on the expression of CD21 and CD23. MZBs were gated on the basis of CD21$^{hi}$ expression and CD23$^{lo.}$ FB cells were identified as CD21$^{+}$ CD23$^{+}$ cells. D) Mean percentages of indicated populations ± SD with n = 5 mice per group. E) Similar population of Treg cells (gated as foxp3 expressing CD4$^{+}$ cells) were observed between the two groups. F) Mean percentages of indicated populations ± SD with n = 5 mice per group. Data is pooled from two independent experiments. For statistical significance, student t-test was performed, * $p<0.05$.

### 3.3.3 *TLR23479*$^{-/-}$ had increased population of CD11b$^{+}$ GR1$^{+}$ granulocytes in the bone marrow in comparison to Wt mice.

Cellular composition of various cell types in the bone marrow of *TLR23479*$^{-/-}$ and Wt mice were analyzed. *TLR23479*$^{-/-}$ mice exhibited significantly higher population of CD11b$^{+}$ GR1$^{+}$ granulocytes in comparison to Wt mice (Figure 14 A and B). The population of NK1.1$^{+}$ cells was also reduced in the *TLR23479*$^{-/-}$ group in comparison to the Wt (Figure 14 C and D) whereas populations of CD11c$^{+}$ dendritic cells as well as CD11c$^{+}$ Siglech$^{+}$ BST2$^{+}$ pDC remained comparable between *TLR23479*$^{-/-}$ and Wt groups (Figure 15 A-D). Further, there was no difference in the CD4$^{+}$ and CD8$^{+}$ lymphocyte populations between *TLR23479*$^{-/-}$ and Wt groups (Figure 16 B). However a reduction in the population size of CD19$^{+}$ B cells was observed in *TLR23479*$^{-/-}$ in comparison to Wt.

Over all, does not seem to be any major cellular discrepancies between *TLR23479*$^{-/-}$ and Wt mice except for slightly increased CD4$^{+}$, CD8$^{+}$ SPs in thymus and an increase in CD11b$^{+}$ GR1$^{+}$ population in spleen and bone marrow.

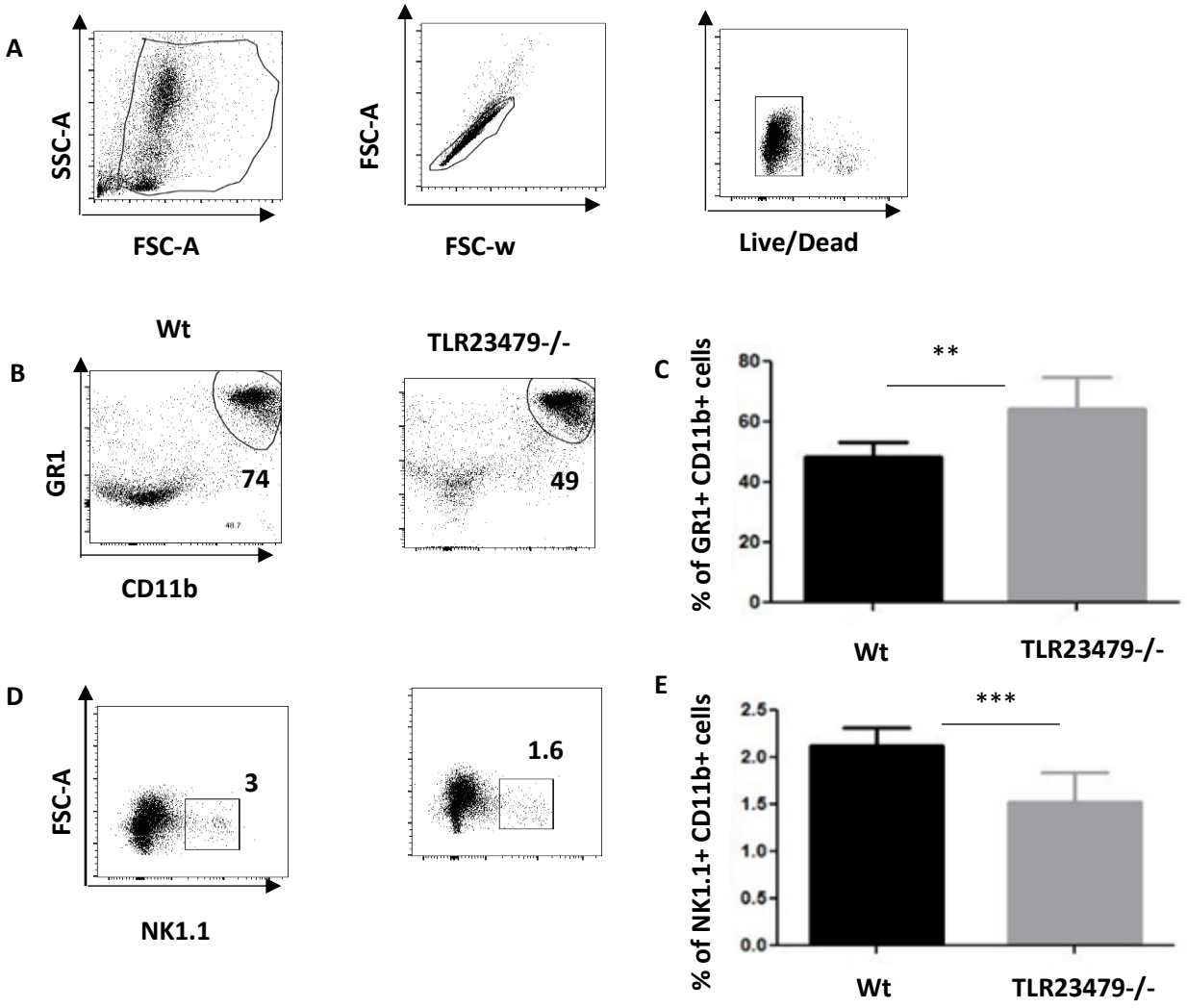


**Figure 14. FACS analysis of cell populations in the bone marrow of Wt and *TLR23479*$^{-/-}$**

A) Gating strategy for selection of cells, doublets and dead cells exclusion. B) Increased population of CD11b$^{+}$GR1$^{+}$ granulocytes were observed in *TLR23479*$^{-/-}$ bone marrow in comparison to Wt mice. C) Mean percentages of indicated populations ± SD, n = 5 mice per group with significant difference (unpaired two tailed student t-test, $p < 0.05$). D) There was significant reduction in the population of NK1.1$^{+}$ natural killer cells in *TLR23479*$^{-/-}$ bone marrow in comparison to Wt group. E) Mean percentages of indicated populations ± SD with n = 5 mice per group. A statistical significance was observed (unpaired two tailed student t-test, ** $p<0.01$, *** $p<0.001$)

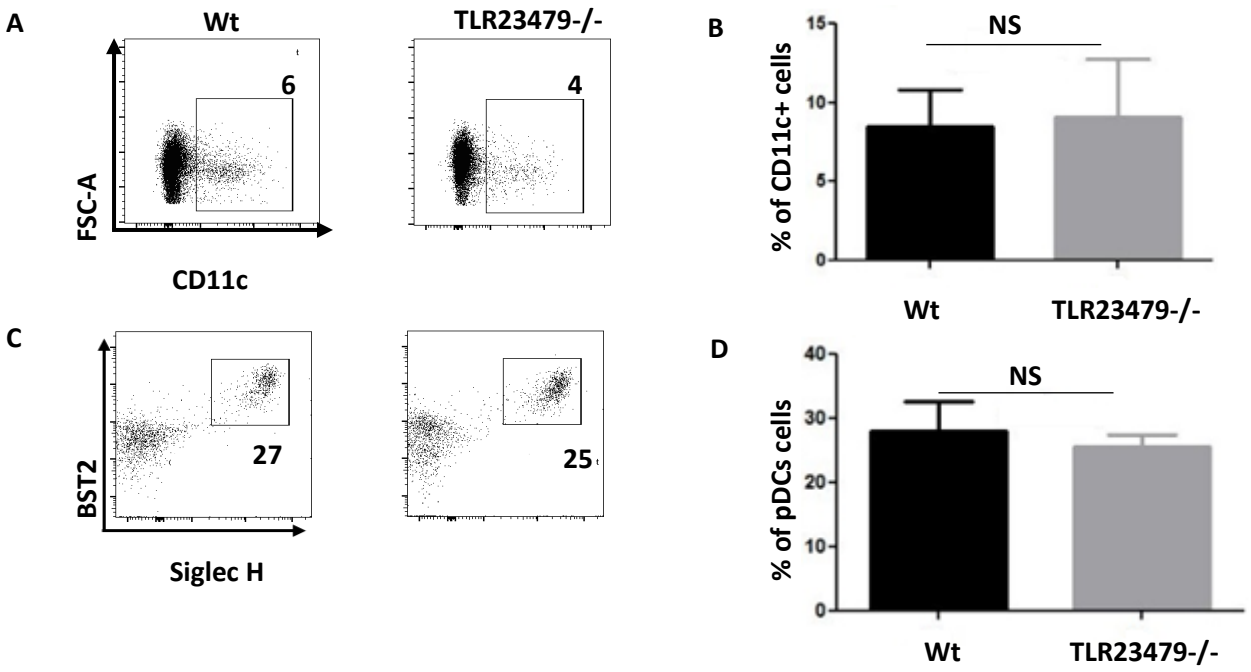


**Figure 15.FACS analysis of dendritic cell populations in the bone marrow of Wt and *TLR23479*$^{-/-}$ mice**

Gating strategy shown in figure 7 was used for selection of cells, doublets and dead cells exclusion. A) Comparable population of CD11c$^{+}$ cells were observed in *TLR23479*$^{-/-}$ and Wt bone marrow. B) Mean percentages of indicated populations ± SD with n = 5 mice per group. No significant difference was observed (unpaired two tailed student t-test, $p < 0.05$). C) Similar population size of pDCs were observed the two groups. For pDC selection, pregated CD11c$^{+}$ cells which expressed both Sigech H and BST2 were selected D) Mean percentages of indicated populations ± SD with n = 5 mice per group. No statistical significance was observed (unpaired two tailed student t-test, $p < 0.05$).

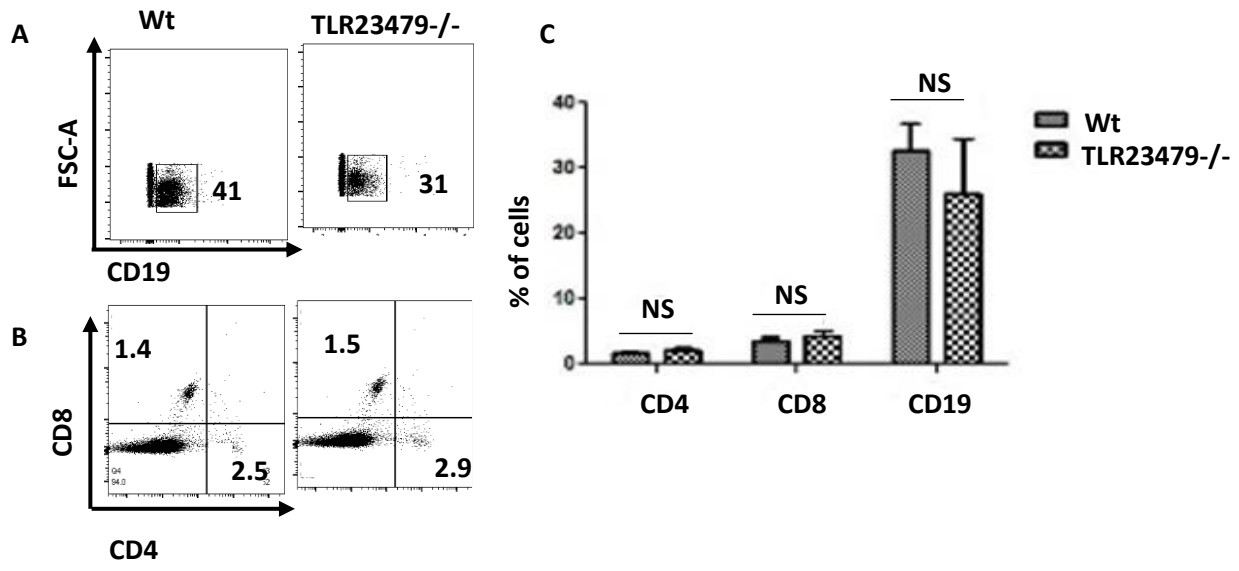


**Figure 16. FACS analysis of T and B cell populations in the bone marrow of Wt and *TLR23479*$^{-/-}$ mice.**

Gating strategy shown in figure 7 was used for selection of cells, doublets and dead cells exclusion. A) Population size of CD19$^{+}$ cells was reduced in *TLR23479*$^{-/-}$ bone marrow in comparison to Wt mice. B) Similar percentage of CD4$^{+}$ and CD8$^{+}$ T cells were observed between *TLR23479*$^{-/-}$ and Wt mice. C) Mean percentages of indicated populations ± SD with n = 5 mice per group. No significant difference was observed (unpaired two tailed student t-test, $p < 0.05$) between the population size of CD19$^{+}$ B cells, CD4$^{+}$ and CD8$^{+}$ T cells in the bone marrow of *TLR23479*$^{-/-}$ and Wt mice.

## 3.4 *TLR23479*$^{-/-}$ mice are susceptible to EAE induction

Next we wanted to investigate the impact of combined deficiencies of endosomal TLRs 3, 7, 9 and surface TLRs 2 and 4 on EAE induction and disease course, we immunized *TLR23479*$^{-/-}$ and Wt mice with MOG peptide and observed mice daily for EAE clinical signs. Disease onset for Wt mice was observed around day 9 and *TLR23479*$^{-/-}$ showed delayed disease onset with mean day of disease onset being 11 (Table 6), but post day 14 after immunization, *TLR23479*$^{-/-}$ mice exhibited increasing severity in disease symptoms in comparison to Wt mice (Figure 17). Median maximum score for *TLR23479*$^{-/-}$ mice was 3.5 in comparison to Wt mice which displayed 2.5 median maximum score (Table 6). The difference of median maximum scores between *TLR23479*$^{-/-}$ and Wt mice was significant (Mann-Whitney test, p value 0.005). All of the *TLR23479*$^{-/-}$ mice exhibited

paralysis of one or both hind and fore limbs in comparison to Wt mice that exhibited mostly hind limb paralysis (Figure 17).

To further assess the extent of demyelination and composition of CNS infiltrating cells, CNS of sick mice from both *TLR23479*$^{-/-}$ and Wt groups were examined histologically during the peak of the disease. Histological examination of CNS revealed a comparable extent of demyelination between the groups (Figure 18A). Myelin damage is expressed as the percentage of demyelinated area as that of total white matter in *TLR23479*$^{-/-}$ and Wt mice (Figure 18 B). Quantification of histopathological analysis revealed a higher number of infiltrating T cells (Figure 18 C and D) and macrophages in *TLR23479*$^{-/-}$ (Figure 18 E and F) in comparison to wild mice but the difference was not significant. This slight increase in the number of infiltrating T cells and macrophages reflects the disease severity observed in *TLR23479*$^{-/-}$. Similarly, axonal damage remained comparable between the groups (Figure 18 I and J). Also, no significant difference was observed regarding number of infiltrating B cells (Figure 18 G and H).

Therefore, histological examination of the CNS did not reveal significant differences either in myelin damage or infiltration by T cells, macrophages and axonal damage between the sick *TLR23479*$^{-/-}$ and Wt mice.

**A**

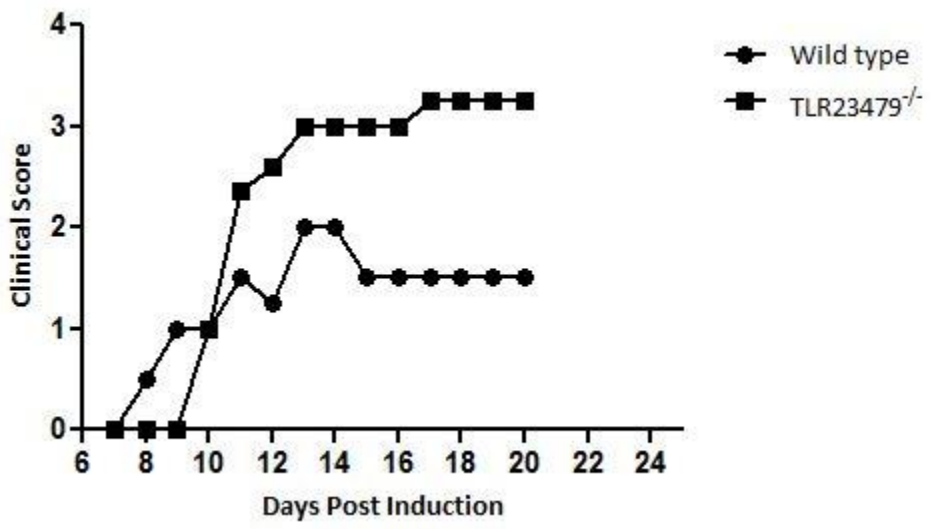


**B**

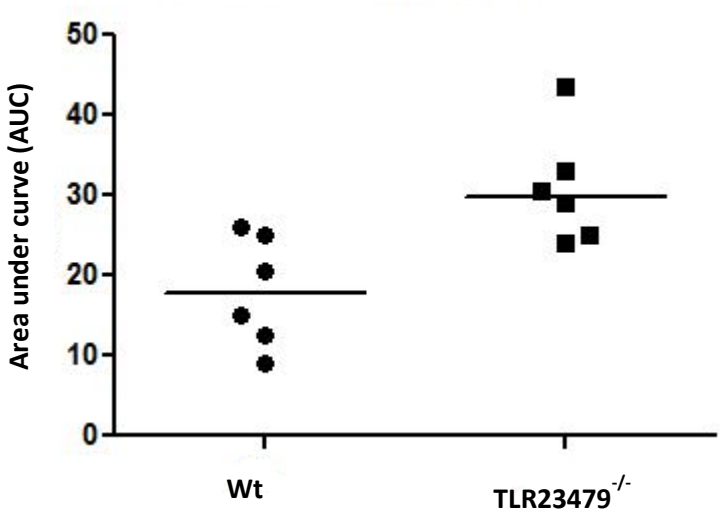


**Figure 17 . Active EAE induction in *TLR23479*$^{-/-}$ mice.** A) Both *TLR23479*$^{-/-}$ (squares) and Wt (dots) female mice, 6 mice in *TLR23479*$^{-/-}$ group and 6 mice in Wt group were immunized with MOG peptide , CFA and PT and were scored daily for EAE clinical signs. Each data point represents median per day from all the mice in that group. All *TLR23479*$^{-/-}$ and Wt mice developed EAE clinical signs with 100% disease incidence. B) Area under the curve (AUC) for each mouse was calculated during the EAE disease course and the middle line represents median. AUC was used to measure the overall disease severity between Wt and *TLR23479*$^{-/-}$ .Using Mann-Whitney U test, a significant difference was found between the groups in disease severity ($p < 0.05$). Experiment was performed thrice. Repetition of the experiment is shown in appendix II.

**Table 6. Table summarizing the requirement of TLRs 2, 3, 4, 7 and 9 for active EAE induction.** A) Data pooled in from three independent experiments. In total, 16 mice were used for analysis per group (Wt and *TLR23479*$^{-/-}$). In Wt group, out of 16 mice only 15 mice were sick with disease incidence of 93% and in *TLR23479*$^{-/-}$ group all the 16 mice developed EAE with disease incidence of 100%. Mean day of disease onset was calculated by taking mean of the first day of disease onset. Mean day of maximum score was calculated by taking the mean of the day when each mouse displayed its maximum clinical score during EAE disease course. To calculate mean day of disease onset and mean day of maximum score, only scores sick mice were included. B) Median of maximal score was calculated by taking maximum score displayed by each mouse during the EAE disease course. To calculate median of maximal score, only maximum score of sick mice was included.

**A**

| Genotype | Incidence % | Mean day of disease onset | Mean day of maximum score |
|---|---|---|---|
| **TLR23479$^{-/-}$** | **100%** | **11** | **18** |
| **Wt** | **93%** | **9** | **14** |

**B**

| Genotype | Median of maximal score |
|---|---|
| **TLR23479$^{-/-}$** | **3.5 (16/16)** |
| **Wt** | **2.5 (15/16)** |

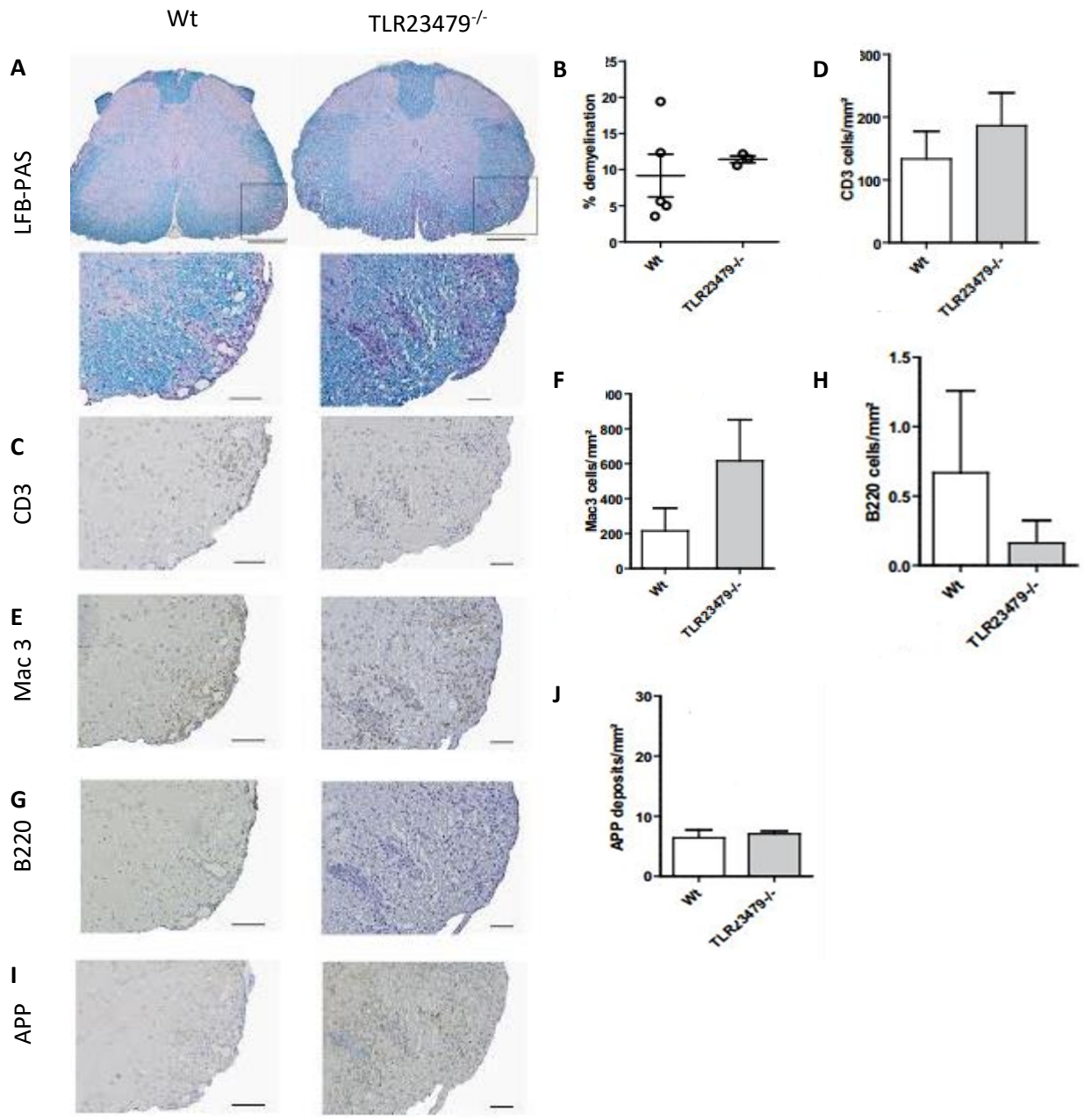
Wt
TLR23479-/-
A
LFB-PAS
B
% demyelination
D
CD3 cells/mm²
C
CD3
F
Mac3 cells/mm²
H
B220 cells/mm²
E
Mac 3
G
B220
J
APP deposits/mm²
I
APP
Wt
TLR23479-/-

**Figure 18. Histological analysis of CNS tissue from *TLR23479*$^{-/-}$ and Wt sick mice examined at the peak of the disease.** Spinal cord sections were stained with Luxol fast blue (LFB) to assess the extent of demyelination (A), CD3 to assess T cell infiltration (C), Mac 3 for macrophage infiltration and microglial population (E), B220 for B cells (G) and amyloid precursor protein (APP) (I) to assess the extent of axonal damage. Scale bars shown are 100µm. On the right is the statistical quantification of extent of demyelination, cell infiltration and axonal damage (B, D, F, G, H, I). Data is expressed as mean + SD. Note: Histological analysis of *TLR9*$^{-/-}$, *TLR379*$^{-/-}$ , *TLR23479*$^{-/-}$ and Wt mice was performed in parallel but for narration purpose they are represented separately.

### *3.4.1* *TLR23479*$^{-/-}$ splenocytes exhibited reduced *in vitro* MOG peptide specific T cell proliferation

As we did not observe a major difference in the extent of demyelination and T cell infiltration in the CNS between *TLR23479*$^{-/-}$ and Wt mice during EAE, we next wanted to investigate the *ex vivo* the MOG peptide specific T cell proliferation, for which we used thymidine incorporation assay. Spleens were harvested from both *TLR23479*$^{-/-}$ and wildtype mice post immunization on day 14 and as well from non-immunized mice from both groups that served as negative controls. Splenocytes from both immunized and non-immunized mice were stimulated with $MOG_{35-55}$ peptide. After 48 h of stimulation, tritiated thymidine was added for the last 24 h of culture. After 72 hours, proliferative responses were measured by 3H thymidine incorporation. We observed that *ex vivo* $MOG_{35-55}$ peptide induced T cell proliferation was reduced in *TLR23479*$^{-/-}$ immunized mice in comparison to the Wt immunized mice (Figure 19).

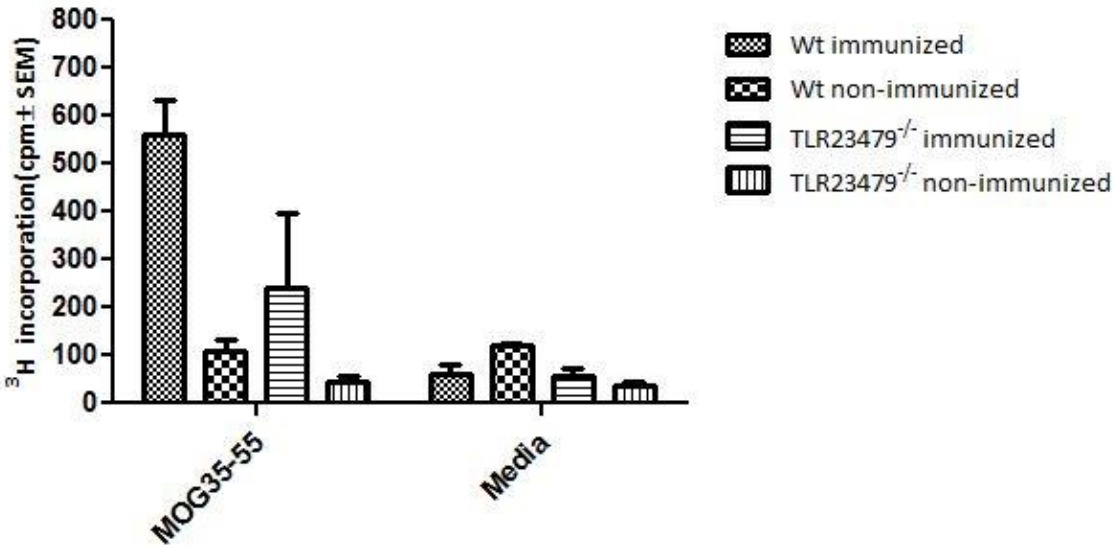


**Figure 19. In vitro MOG peptide specific T cell proliferation assay.**

Splenocytes from both *TLR23479*$^{-/-}$ and Wt immunized and non-immunized mice were harvested on day 14 post immunization and stimulated with MOG peptide for 48 h and cells cultured just with media without MOG peptide served as negative control. After 48 h of stimulation, tritiated thymidine was added for the last 24 h of culture. Data representative of two independent experiments with n=2 mice per group.

### 3.4.2 No major difference in mRNA expression levels of inflammatory cytokines during disease onset as well as during peak of disease between *TLR23479*$^{-/-}$ and Wt mice

Because neuroinflammation in EAE is mostly driven by IFNγ, IL17 (Fletcher et al., 2010), an GMCSF (Kroenke et al., 2010) producing CD4$^{+}$ T cells we next analyzed the relative mRNA expression of these proinflammatory cytokines in *TLR23479*$^{-/-}$ and Wt mice during the course of EAE. With this analysis, we aimed to decipher how combined deficiencies of TLRs 2, 3, 4, 7 and 9 would influence the expression of IFNγ, IL17 and GMCSF during the course of EAE. Further, we also analyzed the relative mRNA expression of IL10, which is a known immunosuppressive cytokine and has protective role in EAE (Cua et al., 2001). Analysis was performed during the disease onset phase on day 7 and during the peak of the disease on day 15 post immunization. Total RNA was isolated from brain, spinal cord, inguinal lymph nodes, superficial cervical lymph

nodes and spleen and cDNA was prepared and subsequently used for qPCR analysis to measure the expression levels of IFNγ, IL17, GMCSF and IL10.

We observed that during the disease onset phase i.e. on day 7, mRNA expression levels of proinflammatory cytokines - IFNγ, GMCSF and immunosuppressive cytokine IL10 levels remained comparable between *TLR23479*$^{-/-}$ and Wt mice in inguinal lymph nodes, spleen, brain, and superficial cervical lymph nodes (Figure 20). In spinal cord, Wt mice displayed increased mRNA expression levels of IL17 in comparison to *TLR23479*$^{-/-}$(Figure 20). Similarly, during the peak of the disease i.e. on day 15 even though *TLR23479*$^{-/-}$ mice displayed more severe EAE clinical signs (Figure 17, Table 6) mRNA expression levels of pro-inflammatory cytokines IFNγ, and GMCSF remained comparable between Wt and *TLR23479*$^{-/-}$ sick mice (Figure 21). Moreover, IL10 expression levels remained comparable between the two groups (Figure 21).

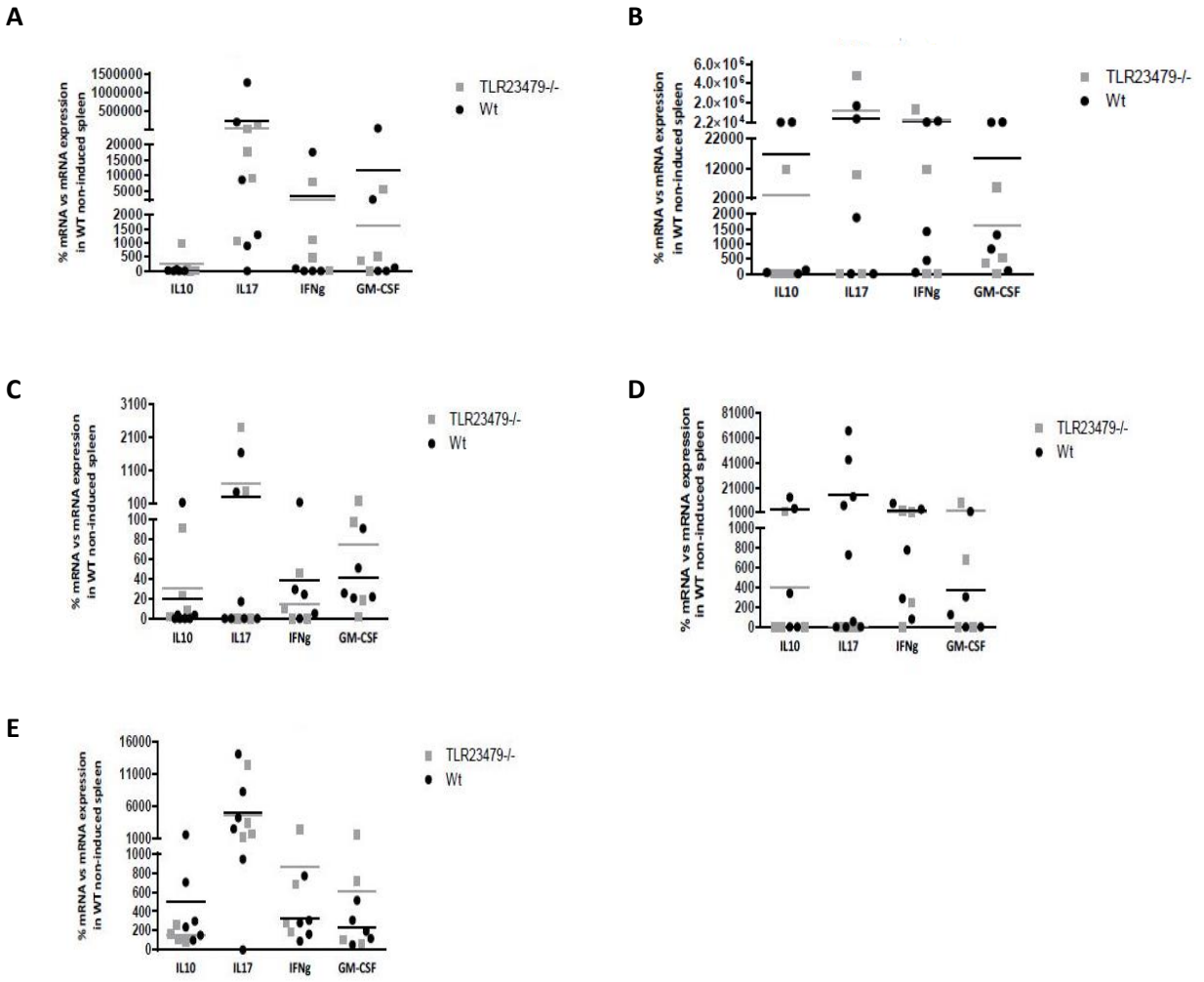


**Figure 20 mRNA expression levels of IFNγ, IL17, GMCSF and IL10 cytokines on day 7 post immunization.** *TLR23479*$^{-/-}$ and Wt mice were immunized with as described earlier and on day 7 post immunization, total RNA was extracted from inguinal lymph nodes (A), spleen (B), brain (C), spinal cord (D) and superficial cervical lymph nodes (E) of *TLR23479*$^{-/-}$ and Wt mice . cDNA was prepared and mRNA expression was assessed by qPCR. Each single value represents mean. Data was pooled from two independent experiments.

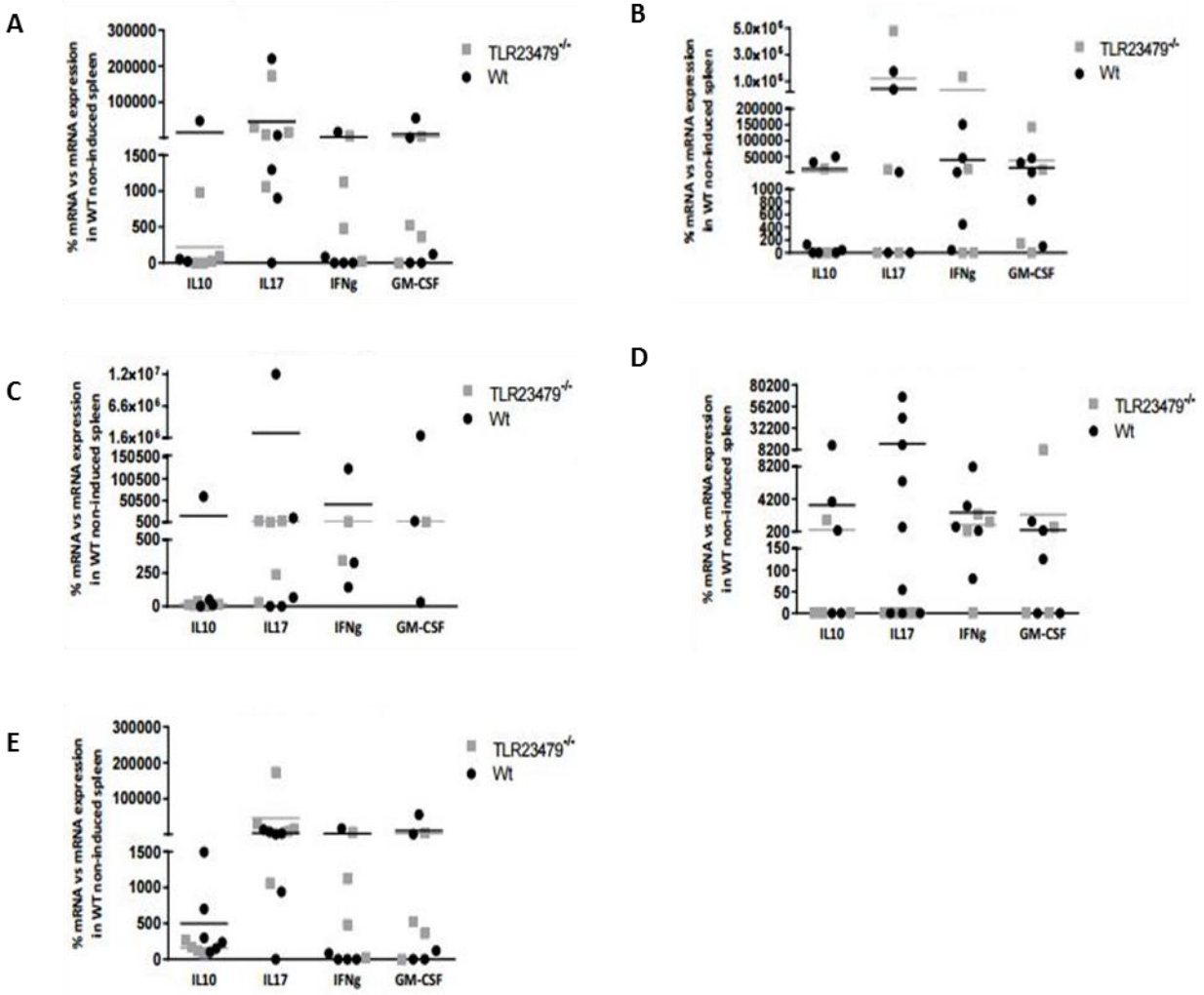


**Figure 21. mRNA expression levels of IFNγ, IL17, GMCSF and IL10 cytokines on day 15 post immunization.** *TLR23479*$^{-/-}$ and Wt mice were immunized with MOG peptide and on day 15 post immunization, total RNA was extracted from inguinal lymph nodes (A), spleen (B), brain (C), spinal cord (D) and superficial cervical lymph nodes (E) of TLR23479$^{-/-}$ and Wt mice. cDNA was prepared and mRNA expression was assessed by qPCR. mRNA expression levels were normalized to those of β-actin, as the house-keeper gene, and spleen from a wildtype non-induced mouse was used as reference. Each single value represents percentage mRNA expression levels for 1 mouse (average of technical triplicates). Data was pooled from two independent experiments.

### 3.4.3 Splenocytes and lymph node cells from *TLR23479*$^{-/-}$ mice produce more IFNγ upon *in vitro* stimulation

TLRs 2, 3, 4,7,9 are expressed by T cells (Cole et al., 2010), we aimed to investigate if combined deficiencies of TLRs influence *in vitro* production of IFNγ and IL17 from CD4$^{+}$ T cells. For this, we harvested spleen and lymph nodes from naïve *TLR23479*$^{-/-}$ and Wt mice and single cell suspension was prepared. Cells were stimulated with PMA/Ionomycin for 4.5 hr and Golgi stop was added to inhibit protein secretion. After stimulation, cells were stained with anti-CD4 antibody and cells were fixed and permeabilized and further stained with anti-IFNγ and anti-IL17 antibodies and FACS analysis was done.

We observed that upon stimulation in vitro, CD4$^{+}$ T cells from *TLR23479*$^{-/-}$ spleen and lymph nodes produced significantly more IFNγ in comparison to Wt mice whereas IL17 production was not detectable (Figure 22 and Figure 23). This is in contradiction to mRNA expression results obtained during EAE disease onset and also during peak of the disease as we did not observe any enhanced mRNA expression of IFNγ in *TLR23479*$^{-/-}$ mice in comparison to Wt. Although both these experimental setups were different, in that during EAE disease course we primarily measured the immune responses brought forth by immunization with MOG peptide which is more of an antigen specific *in vivo* stimulation and *in vitro* stimulation experiment, we measured the cytokine production ability from CD4$^{+}$ T cells after PMA/Ionomycin stimulation.

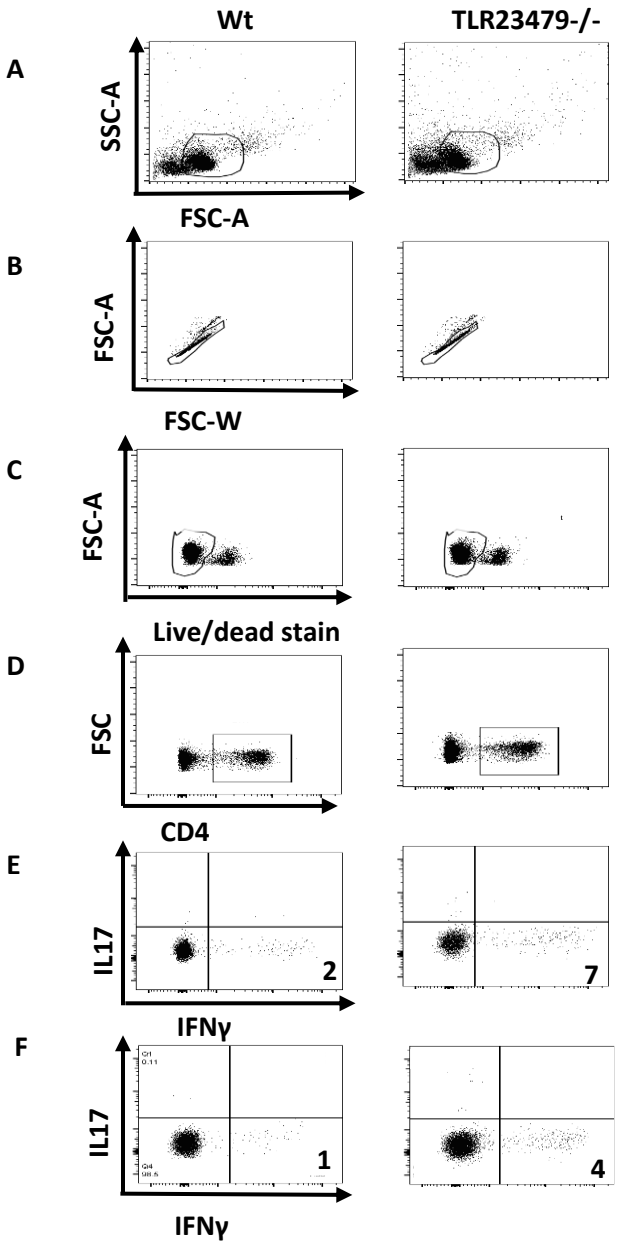


**Figure 22. FACS analysis of *in vitro* production of IFNγ and IL17 from CD4$^+$ T cells of *TLR23479*$^{-/-}$ and Wt mice.** A-C represent gating strategy for selection of lymphocytes, exclusion of doublets as well as dead cells from analysis. D represents gating strategy for selection of CD4$^+$ T cells, E represents IFNγ and IL17 production from CD4$^+$ T cells from spleen and F represents IFNγ and IL17 production from CD4+ T cells from lymph nodes. Data is representative of one sample from each TLR23479$^{-/-}$ and Wt groups.

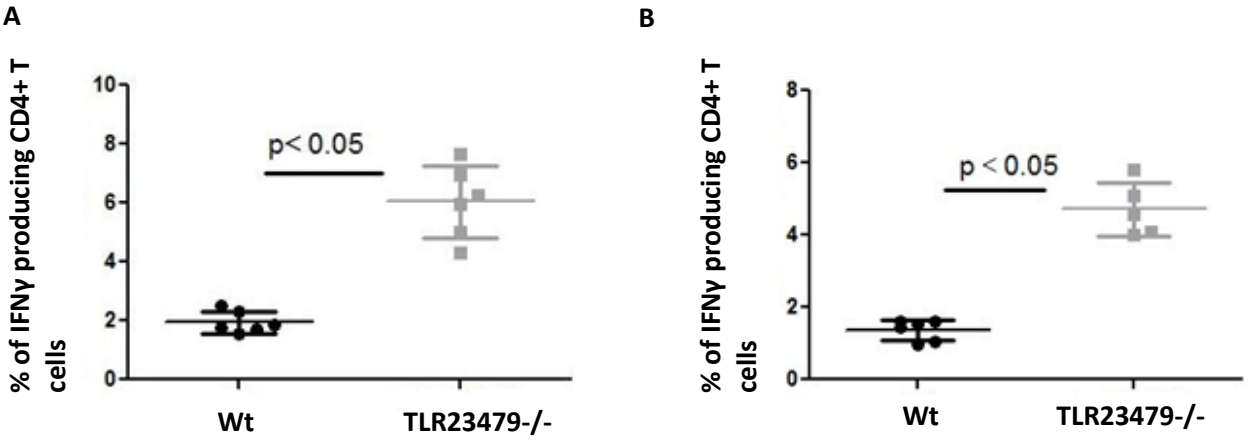


**Figure 23. In vitro-stimulated CD4+ T cells from *TLR23479*$^{-/-}$ spleen and lymph nodes produce more IFNγ**

Cells were stimulated in vitro with PMA/Ionomycin and IFNγ and IL17 cytokine production was analyzed by FACS as described in figure 22. The percentage of CD4$^{+}$ T cells producing IFNγ are compared between *TLR23479*$^{-/-}$ spleen (A), lymph nodes (B) with that of Wt spleen (A) and lymph nodes (B). Each dot (Wt) and square (*TLR23479*$^{-/-}$) represent one mouse with n= 6 per group. (t-test two tailed analysis was performed and the difference was significant at p< 0.05). Experiment was performed once.

### 3.4.4 Naïve CD4$^{+}$ T cells from *TLR23479*$^{-/-}$ mice exhibit slightly impaired *in vitro* differentiation into Th1, Th17, TR1 and iTreg subsets.

As mentioned before TLRs are expressed by broad range of non-immune and immune cells including T cells. TLR 2, TLR 3, TLR4, TLR7 and TLR 9 are expressed by T cells (Cole et al., 2010). It has been previously reported that direct activation of TLRs in T cells influences T cell differentiation into various Th subsets (Liu et al., 2010a) (Rahman et al., 2009). Therefore, we aimed to investigate the impact of combined TLR deficiencies on naïve T cell differentiation. We specifically investigated in vitro naïve CD4 T cells into Th1, Th17, type 1 regulatory T cells (TR1) and *in vitro*-induced Foxp3$^{+}$ regulatory T cells (iTregs). Th1 and Th17 subsets produce IFNγ and IL17 cytokines respectively, both subsets known to be pathogenic in EAE (Fletcher et al., 2010). TR1 cells produce IL10 and IFNγ. IL10 is a known immunosuppressive cytokine and is suggested to be protective in EAE (Bettelli et al., 1998). Foxp3$^{+}$ iTregs are also suggested to be protective in EAE. Because of these reasons, we aimed at investigating how TLR deficiencies in T cells would

impact naïve T cell *in vitro* differentiation, which would be a T cell intrinsic effect. For this, we harvested spleen and total lymph nodes from *TLR23479*$^{-/-}$ and Wt mice. Single cell suspension was prepared and $CD4^+$ $CD44^-$ $CD62L^+$ naïve T cells were isolated using Miltenyi MACS system. Cells were cultured in Th1, Th17, TR1 and iTreg skewing conditions for 72 h. After incubation, cells were stimulated with PMA/Ionomycin for 4.5 h. Post stimulation, cells were surface-stained for CD4 and intracellularly for IFNγ, IL17 and IL10. Intranuclear staining was performed for FOXP3. We observed that *in vitro* differentiation of naïve T cell into Th17, TR1 and iTreg phenotypes was reduced in *TLR23479*$^{-/-}$ group in comparison to the Wt mice (Figure 24). T cell in vitro differentiation into Th1 phenotype was also reduced in *TLR23479*$^{-/-}$ group in comparison to the Wt mice but the difference was not significant. Earlier, we observed that splenocytes from *TLR23479*$^{-/-}$ upon *in vitro* stimulation produce more IFNγ in comparison to Wt mice (Figure 23). However, naïve T cell *in vitro* differentiation was performed without APCs whereas *in vitro* stimulation experiments included them. Therefore, the slight decrease we see in naïve T cell differentiation into Th1 and significant difference in skewing towards Th17, TR1 and iTregs phenotypes in vitro in *TLR23479*$^{-/-}$ cells is an effect that is solely T cell intrinsic.

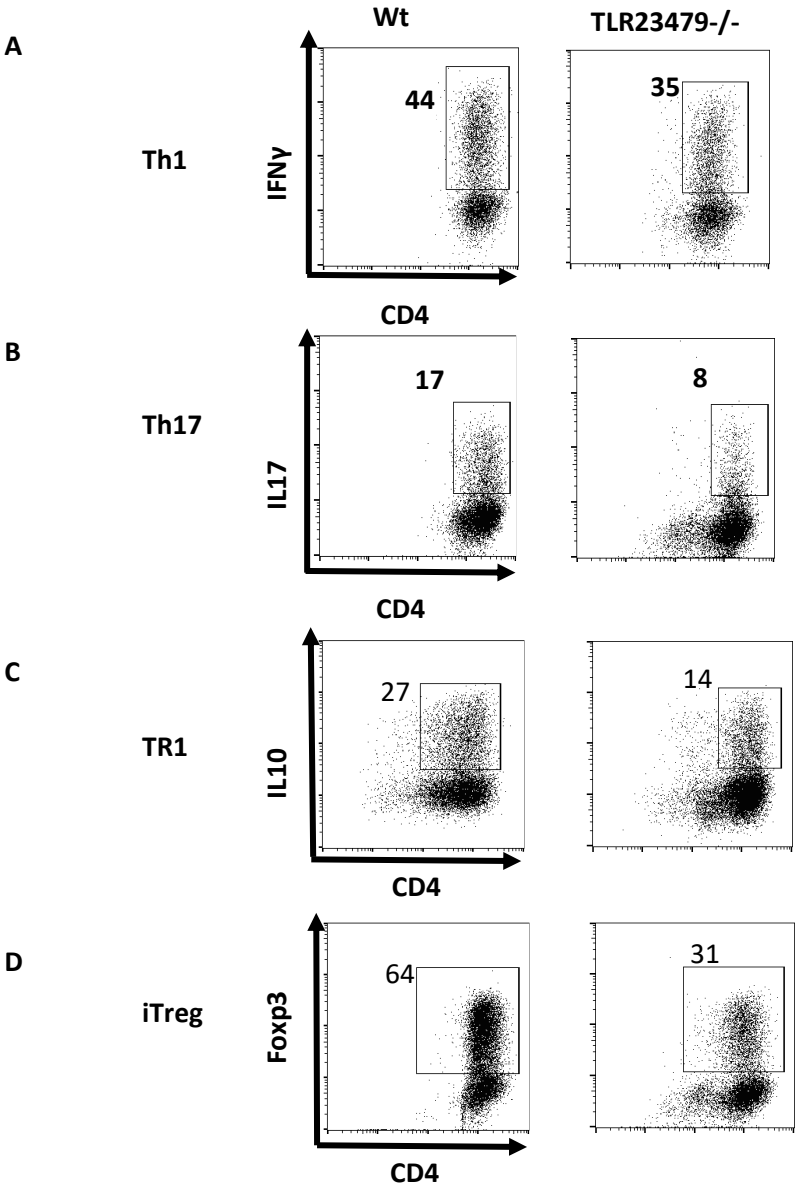
A
Th1
Wt
TLR23479-/-
44
35
IFNγ
CD4
B
Th17
17
8
IL17
CD4
C
TR1
27
14
IL10
CD4
D
iTreg
64
31
Foxp3
CD4

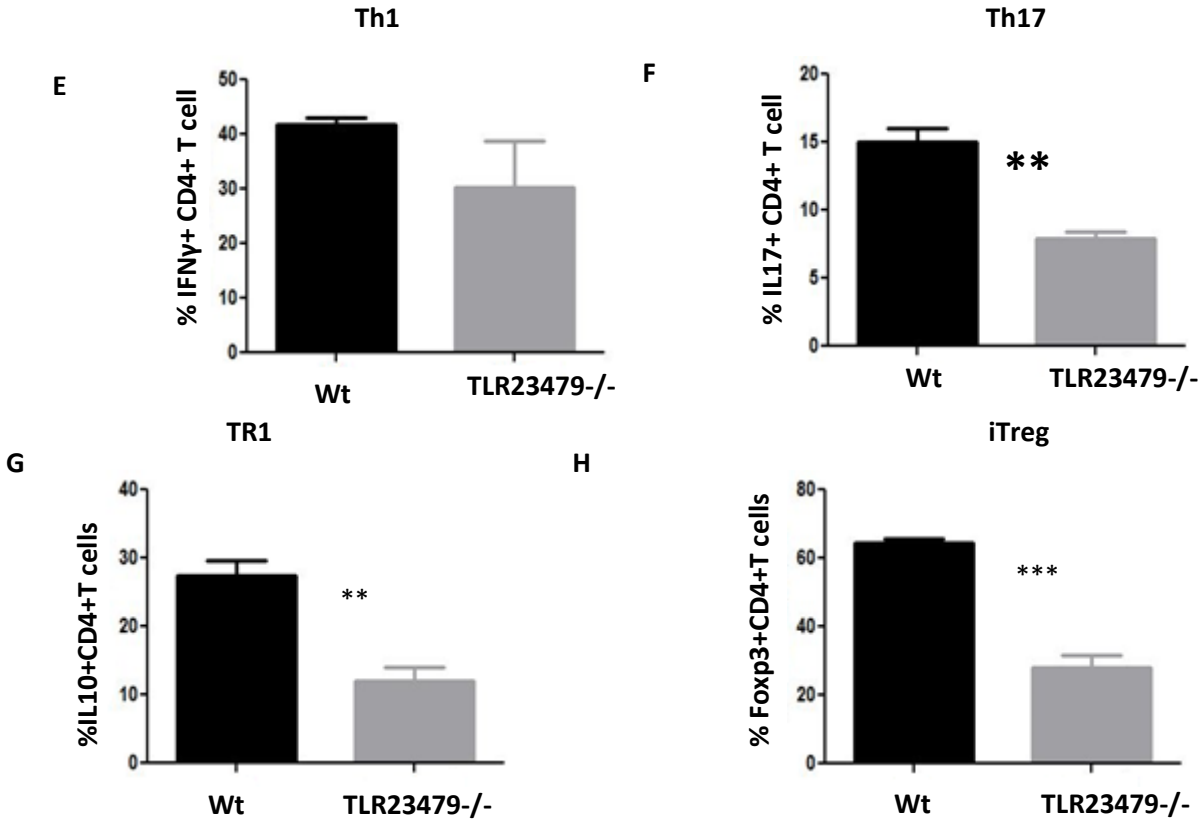


**Figure 24 FACS analysis of in vitro differentiation of naïve CD4⁺ T cells.** Spleen and total lymph nodes were harvested from TLR23479$^{-/-}$ and Wt mice. CD4$^{+}$ CD44$^{-}$CD62L$^{+}$ naïve T cells were isolated and were cultured in Th1, Th17, TR1 and iTreg skewing conditions for 72 hours, post incubation cells were stimulated with PMA/ionomycin for 4.5 h and later cells were stained and FACS analysis was performed. Gating strategy mentioned in figure 22 is used to select lymphocytes, exclude doublets and dead cells. A) IFNγ$^{+}$ CD4$^{+}$ T cells, B) IL17$^{+}$ CD4$^{+}$ T cells, C) IL10$^{+}$ CD4$^{+}$ T cells and D) Foxp3$^{+}$ CD4$^{+}$ T cells. Data represents one sample from each group with n=3 mice per group. E-H) Mean percentage of the indicated cytokine producing CD4$^{+}$ T cells ± SEM. Data represented is from one experiment. Unpaired t –test was performed. ** $p<0.01$.

## 3.5 Is IFNβ production impaired in *TLR23479*$^{-/-}$ in comparison to Wt mice?

We observed that *TLR23479*$^{-/-}$ mice are highly susceptible to EAE induction with 100 % disease incidence and that they exhibit more severe EAE clinical signs in comparison to the Wt mice (Figure 17). But the histological analysis of *TLR23479*$^{-/-}$ and Wt sick mice did not reveal major differences in terms of extent of demyelination and infiltration by T cells (Figure 18). Further, we also did not observe a difference in mRNA expression levels of pro-inflammatory cytokines

between *TLR23479*$^{-/-}$ and Wt mice (Figure 20 and 21). We next hypothesized if IFNβ production was impaired in *TLR23479*$^{-/-}$, which could explain the severe EAE clinical symptoms seen in the quintuple knockout mice in comparison to the Wt mice. Signaling through TLRs 3 & 4 via TRIF leads to the production of IFNβ by activating IRF3 (Troutman et al., 2012) . Similarly, signaling through TLRs 7 and 9 via MyD88 leads to production of IFNβ in pDCs by activating IRF7 (Newton and Dixit, 2012). As mentioned earlier, IFNβ treatment has been shown to be protective in EAE (Axtell et al., 2010) as well as is used in treating MS patients (Weinstock-Guttman et al., 2008). Wt mice treated with IFNβ exhibited less severe EAE clinical severity in comparison to non-treated group (Harari et al., 2014). Similarly, both *TRIF*$^{-/-}$ and *IFNAR*$^{-/-}$ mice exhibit severe EAE in comparison to the Wt mice (Guo et al., 2008). Therefore, we hypothesized that combined deficiency of TLRs 3, 4, 7 & 9 could lead to decreased IFNβ production which might be responsible for clinical severity exhibited by *TLR23479*$^{-/-}$ in comparison to Wt mice. In order to investigate our hypothesis, we performed experiments to visualize the *in vivo* expression of IFNβ during EAE initial disease course and measured mRNA levels of IFN α/β pathway related genes during both initial and effector phases of EAE as described in the following sections.

### 3.5.1 IFNβ induction at the site of immunization during initial phase of EAE

In our initial experimental approach, we wanted to investigate the *in vivo* expression of endogenous IFNβ during the initial phase of EAE i.e. from day 0 – day 10, as Wt mice treated with IFNβ during the initial disease priming phase resulted in reduced EAE clinical severity (Axtell et al., 2010). For this, we used Δβ−luc reporter mice in which luciferase activity is driven by IFNβ promoter (Lienenklaus et al., 2009) . Δβ−luc mice were immunized with MOG peptide and PT. IFNβ reporter gene activity was visualized post immunization at various time intervals (0h, 6h, 12h, 24h, and day2-day10) by *in vivo* imaging, which revealed IFNβ induction at the site of immunization from 6h post immunization. IFNβ induction intensity of the reporter signal was fairly consistent at the site of immunization until the end of observation i.e. day 10 with high intensity being observed around day 5 (Figure 25). This might suggest a crucial role for IFNβ production during the initial disease priming phase. This experiment was done in collaboration with Prof.Ulrich Kalinke lab at TWINCORE facility, Center for experimental and clinical infection research, Hannover.

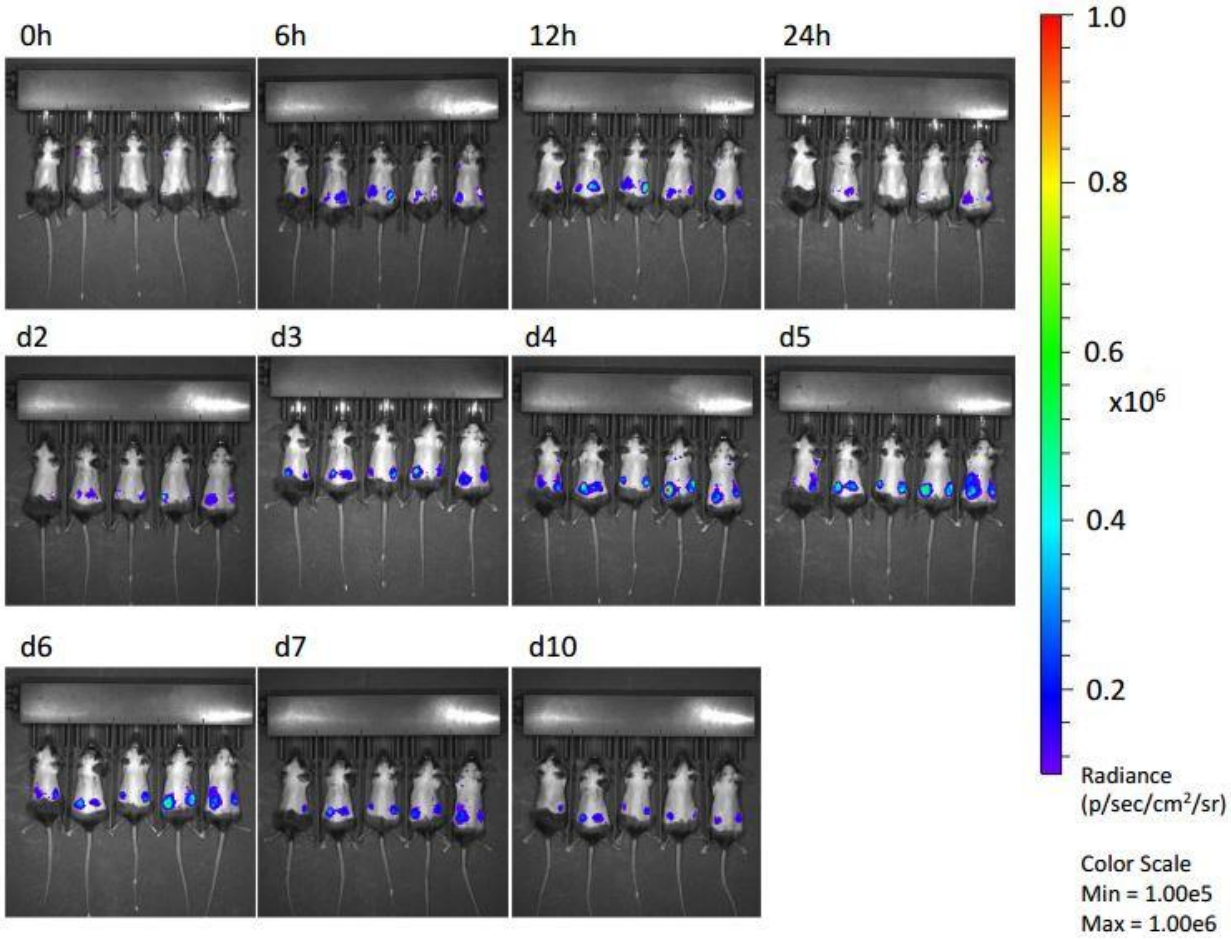


**Figure 25.Luciferase gene expression in Δβ−luc mice immunized with MOG peptide and PT.** Reporter gene expression was visualized at various time points post immunization (d denotes days post immunization). Experiment was performed once with five mice as shown.

### 3.5.2 Granulocytes are the major cell type present at the site of immunization.

After observing IFNβ induction at the site of immunization using Δβ−luc reporter mice, we analyzed the cellular composition at the site of immunization. For this, wildtype mice were immunized with MOG peptide and the site of immunization was dissected on day 5 as we saw stronger IFNβ induction intensity at this point in *in vivo* imaging experiment done with Δβ−luc mice **(Figure 25)** and cells were stained with anti-CD45, CD4, CD8, CD11c, CD11b, GR1 and CD19 antibodies. Cell populations that were CD45 negative were excluded from FACS analysis to

exclude any contaminating skin cells from analysis. We observed that the site of immunization was mostly comprised of $CD11b^+$ $GR1^+$ granulocytes followed by lower fraction of $CD11c^+$ $CD11b^+$ dendritic cells (Figure 26).

Higher number of granulocytes at the site of immunization is the result of CFA which is used for preparing MOG emulsion and serves the purpose of adjuvant, activating the innate immune system. It has been previously reported that granulocytes especially neutrophils along with APCs are recruited to the site of immunization when CFA is used (Awate et al., 2013; Yang et al., 2010).

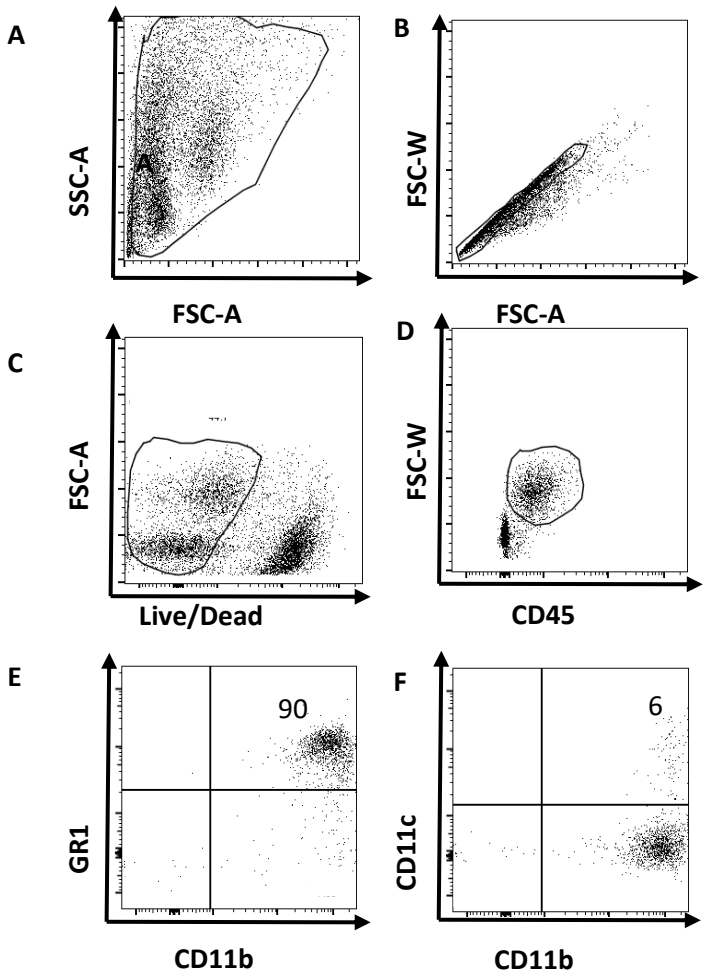


**Figure 26 . Gating Strategy for FACS analysis of cellular populations at site of immunization.** (A) (B) singlet gating, (C) Live/dead gating, (D) $CD45^+$ cells gating, (E) $CD11b^+$ $GR1^+$ granulocytes and (F) $CD11b^+$ $CD11c^+$ dendritic cells. Data representative of one sample from two independent experiments.

### 3.5.3 No difference in relative mRNA expression of IFNβ between *TLR23479*$^{-/-}$ and Wt mice at the site of immunization

For a more quantitative measurement and comparison of IFNβ induction at the site of immunization between *TLR23479*$^{-/-}$ and Wt controls, both groups were immunized with MOG peptide as described and on day 3 post immunization, the immunization site was dissected and processed for qPCR analysis. Briefly, cell suspension was used for isolating CD45$^{+}$ cells using magnetic CD45 microbeads (Miltenyi Biotech) to exclude any skin cells from analysis. Total RNA was extracted from CD45$^{+}$ cells and cDNA was prepared and used for qPCR analysis to measure the expression levels of IFNα/β pathway related genes namely IFNβ, MX1 – biomarker for IFNβ activity (Petry et al., 2006) and IRF7 – regulator of IFNα response (Haller et al., 2006). We did not observe major differences in IFNβ and IRF7 expression levels between the two genotypes (Figure 27) As overall, we did not observe a striking difference between IFNβ levels between *TLR23479*$^{-/-}$ and Wt mice at the site of immunization, we further investigated the expression of IFNα/β pathway related genes during the course of EAE in periphery and in CNS.

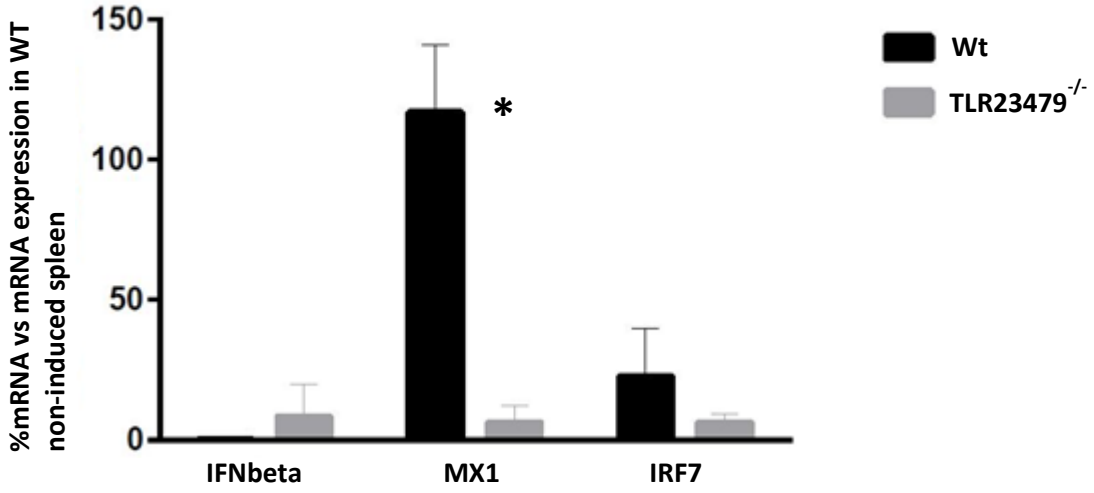


**Figure 27. mRNA expression of IFNα/β pathway related genes from cells isolated from the site of immunization.** Both Wt and *TLR23479*$^{-/-}$ mice were immunized with MOG peptide and PT. 3 days later the immunization site was dissected and qPCR was performed. Overall, a significant difference was observed in expression level of MX1 between both the groups (two-tailed t-test with 95% confidence interval). Data represented is from one experiment with n=5 mice per group.

### 3.5.4 No major difference in relative mRNA expression of IFNβ during the disease onset

To investigate the expression of levels of IFNβ in periphery and in the CNS just before the disease onset, both *TLR23479*$^{-/-}$ and Wt mice were immunized with MOG peptide and euthanized on day 7 post immunization. Total RNA was extracted from peripheral organs (spleen, inguinal lymph nodes) and from CNS (cortex, spinal cord) and superficial cervical lymph nodes. cDNA was prepared and was used to analyze the expression levels of IFNβ, MX1 and IRF7 by qPCR using β-actin as housekeeping gene. We did not observe a difference in the expression levels of IFNβ in periphery and in CNS between *TLR23479*$^{-/-}$ and Wt (Figure 28).

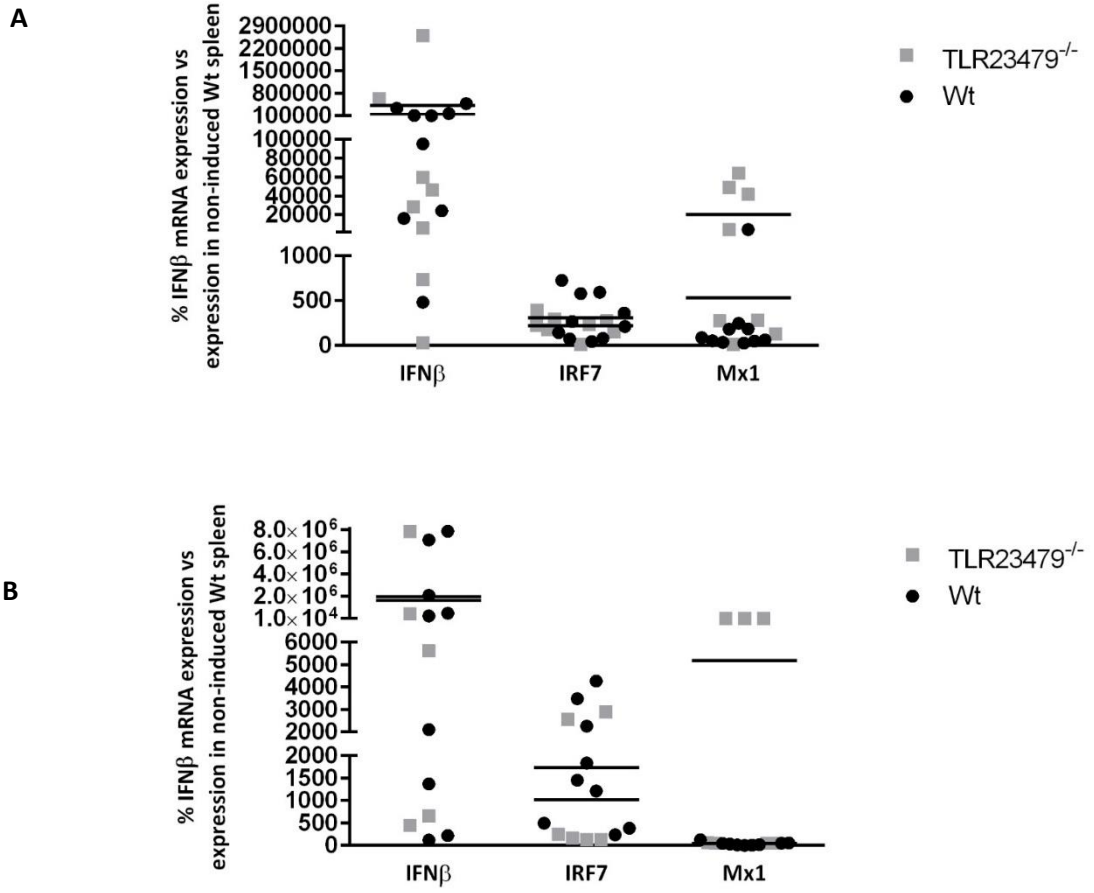

C

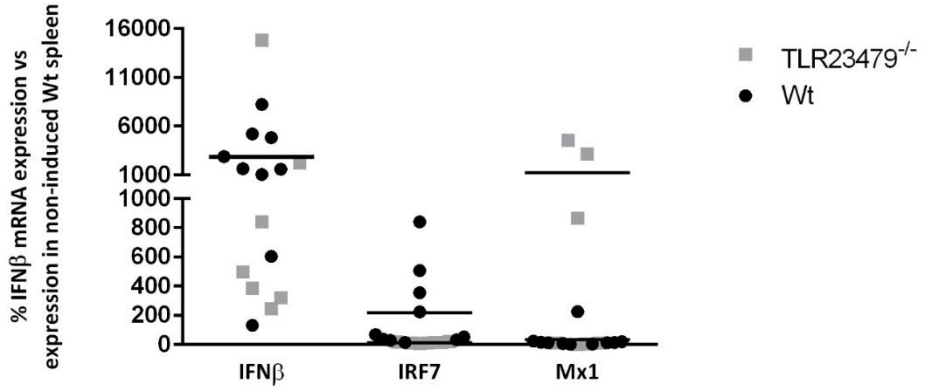
% IFNβ mRNA expression vs expression in non-induced Wt spleen
16000
11000
6000
1000
1000
800
600
400
200
0
IFNβ
IRF7
Mx1
TLR23479-/-
Wt

D

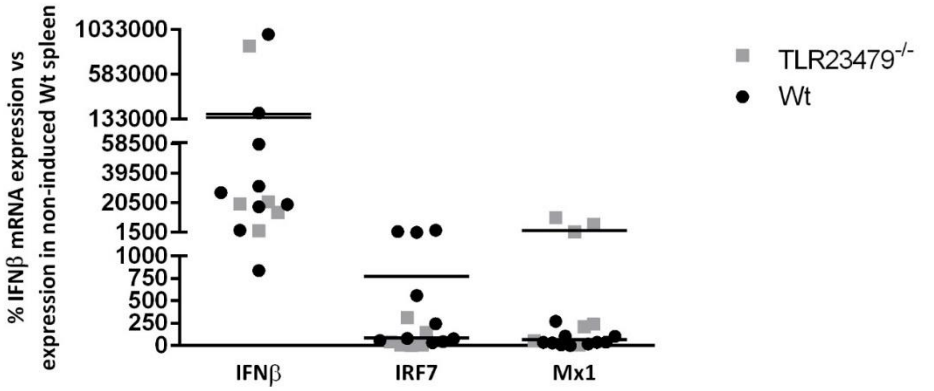
% IFNβ mRNA expression vs expression in non-induced Wt spleen
1033000
583000
133000
58500
39500
20500
1500
1000
750
500
250
0
IFNβ
IRF7
Mx1
TLR23479-/-
Wt

E

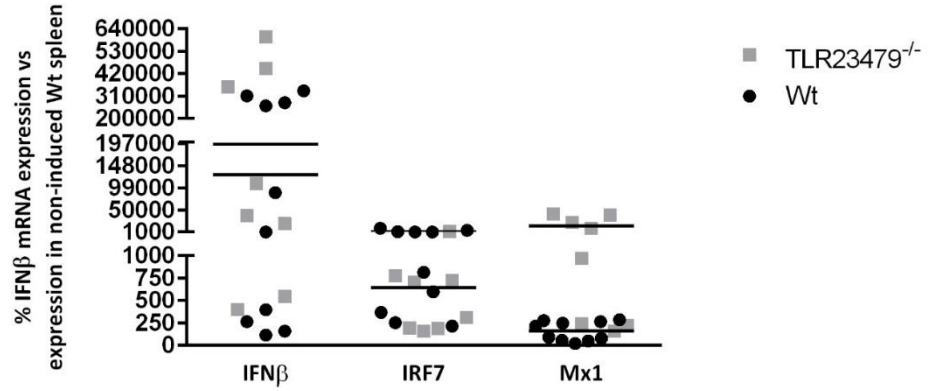
% IFNβ mRNA expression vs expression in non-induced Wt spleen
640000
530000
420000
310000
200000
197000
148000
99000
50000
1000
1000
750
500
250
0
IFNβ
IRF7
Mx1
TLR23479-/-
Wt

**Figure 28. IFNα/β related gene expression levels on day 7 post immunization.** TLR23479$^{-/-}$ and Wt mice were immunized with MOG peptide, PT ,CFA and on day 7 post immunization, total RNA was extracted from inguinal lymph nodes (A), spleen (B), brain (C), spinal cord (D) and superficial cervical lymph nodes (E) of TLR23479$^{-/-}$ and Wt mice . cDNA was prepared and mRNA expression was assessed by qPCR. mRNA expression levels were normalized to those of β-actin, as the house-keeper gene, and spleen from a wildtype non-induced mouse was used as reference. Each single value represents percentage mRNA expression levels for 1 mouse (average of technical triplicates). Data pooled from two independent experiments.

### 3.5.5 No major difference in relative mRNA expression levels of IFNβ during the peak of the disease

As we could not observe a significant difference in the expression levels of IFNβ and IRF7 between *TLR23479*$^{-/-}$ and Wt mice during the disease onset phase, we further investigated the expression levels of IFNα/β pathway related genes during the peak of the disease, on day 15. Both *TLR23479*$^{-/-}$ and Wt mice were immunized with MOG peptide and mice were observed daily for EAE clinical signs. On day 15, during the disease peak, sick mice from both groups were euthanized and total RNA was extracted from spleen, inguinal lymph nodes, brain, superficial cervical lymph nodes and spinal cord. qPCR analysis was performed to analyze expression levels of IFNβ, IRF7 and MX1 using β-actin as housekeeping gene. We did not observe a difference in expression of IFNβ, IRF7 and MX1 between *TLR23479*$^{-/-}$ and Wt controls (Figure 29).

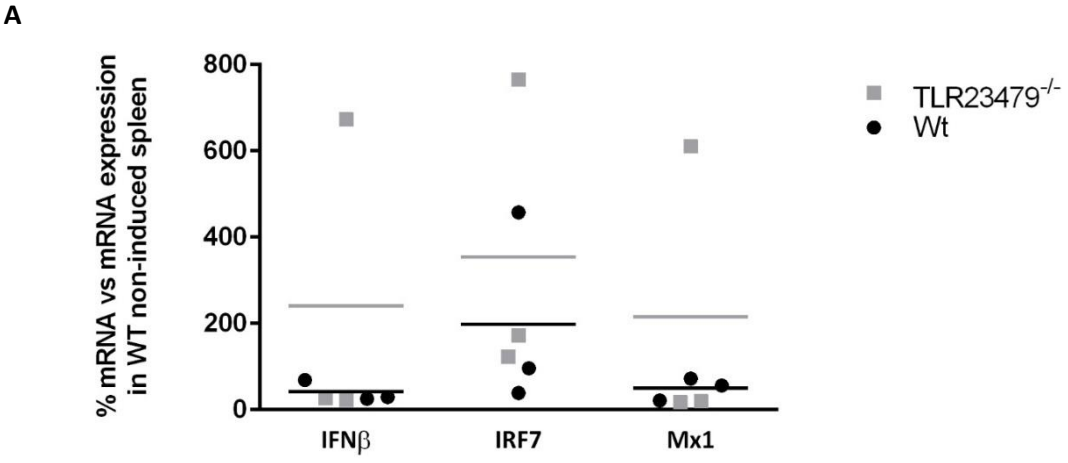

B

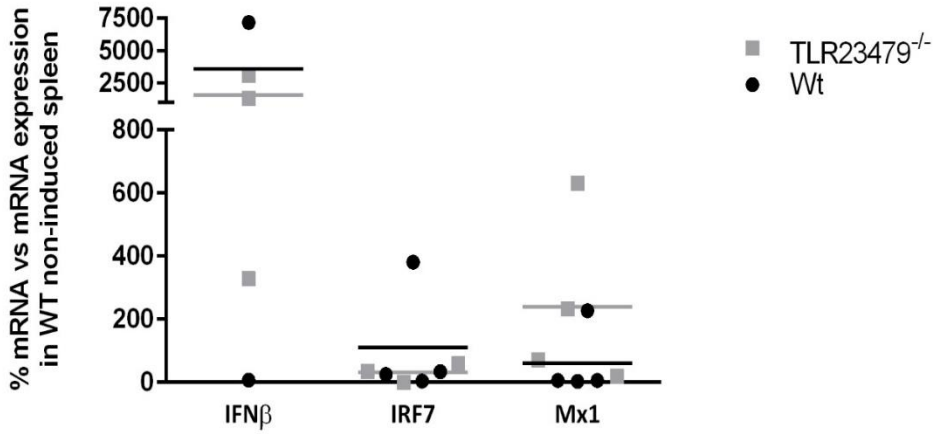
% mRNA vs mRNA expression in WT non-induced spleen
7500
5000
2500
800
600
400
200
0
IFNβ
IRF7
Mx1
TLR23479-/-
Wt

C

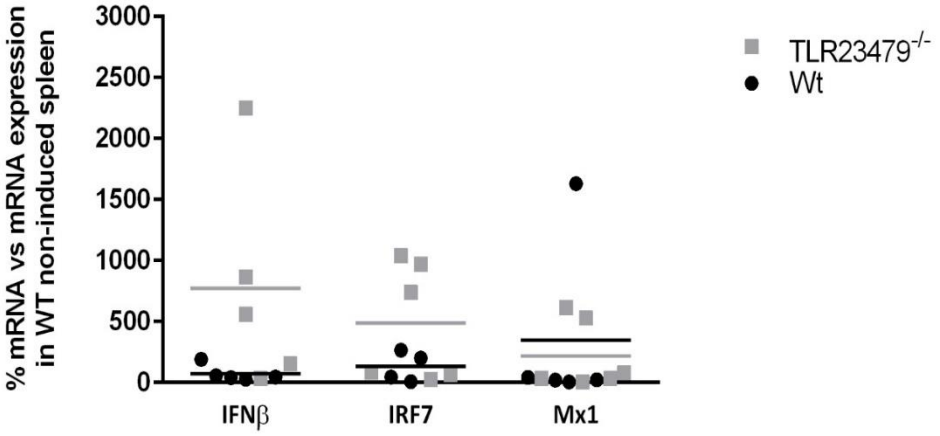
% mRNA vs mRNA expression in WT non-induced spleen
3000
2500
2000
1500
1000
500
0
IFNβ
IRF7
Mx1
TLR23479-/-
Wt

D

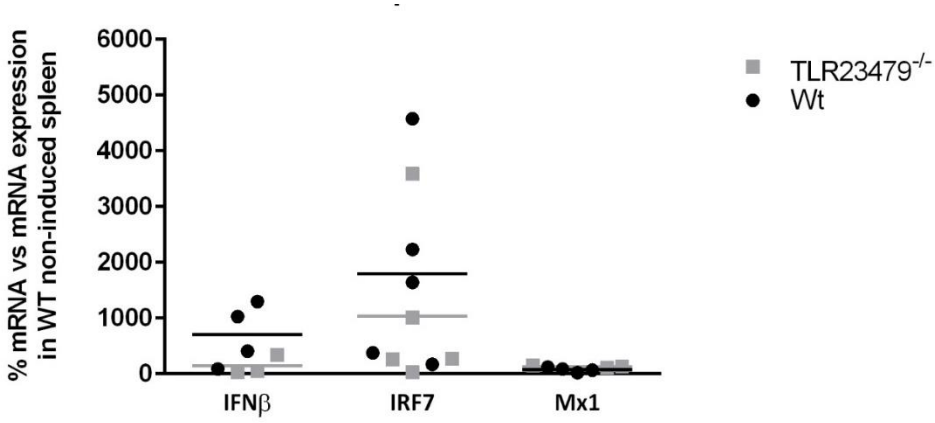
% mRNA vs mRNA expression in WT non-induced spleen
6000
5000
4000
3000
2000
1000
0
IFNβ
IRF7
Mx1
TLR23479-/-
Wt

**E**

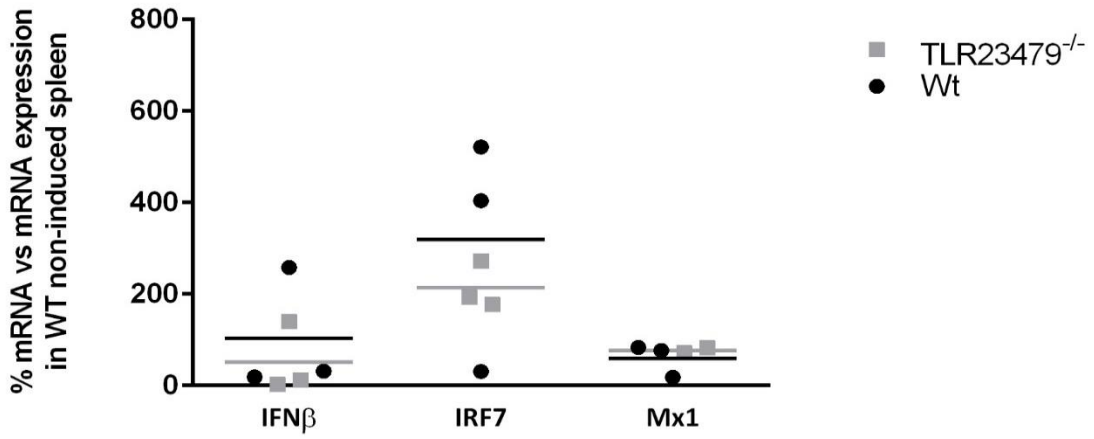


**Figure 29 IFNα/β related gene expression levels on day 15 post immunization.** *TLR23479*$^{-/-}$ and Wt mice were immunized with MOG peptide, CFA and PT. On day 15 post immunization, total RNA was extracted from inguinal lymph nodes (A), spleen (B), brain (C), spinal cord (D) and superficial cervical lymph nodes (E) of TLR23479$^{-/-}$ and Wt mice . cDNA was prepared and mRNA expression was assessed by qPCR. mRNA expression levels were normalized to those of β-actin, as the house-keeper gene, and spleen from a Wt non-induced mouse was used as reference. Each single value represents percentage mRNA expression levels for 1 mouse (average of technical triplicates). Data pooled from two independent experiments.

## 3.6 *TLR3*$^{-/-}$ deficient mice display resistance to EAE induction

As mentioned previously, signaling through TLR3 via TRIF leads to activation of IRF3 leading to IFNβ production (Troutman et al., 2012). So far, to our knowledge there are no reports about the role of TLR3 in active EAE. Therefore, to investigate the role of TLR3 in active EAE model, we immunized both male and female *TLR3*$^{-/-}$ and Wt mice with MOG peptide and observed mice daily for EAE clinical signs. We observed that the clinical disease symptoms commenced around day 10 in case of female Wt controls with 100% disease incidence and with median maximal clinical score of 3 (Figure 30, Table 7). In contrast, *TLR3*$^{-/-}$ female mice were mostly resistant to EAE induction as only 5 out of 21 mice developed EAE clinical signs with an incidence of 23% and median maximal clinical score being 2.5 (Table 7). In Wt male mice, disease symptoms commenced around day 9 with 100% incidence and median maximum clinical score of 2.75 whereas male *TLR3*$^{-/-}$ mice were mostly resistant to EAE induction (Figure 31). Only 2 out of 10, *TLR3*$^{-/-}$ male mice developed EAE with disease incidence of 20% and median maximum clinical

score of 2 (Figure 31, Table 8). Therefore, both male and female *TLR3*$^{-/-}$ mice seem to be resistant to EAE induction although this resistance is lost in both *TLR23479*$^{-/-}$ and *TLR379*$^{-/-}$ mice as these mice were highly susceptible to EAE.

A

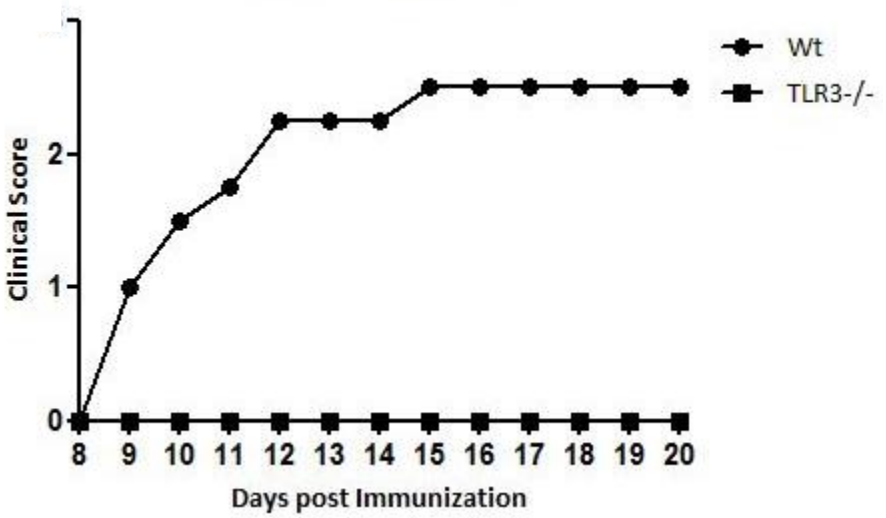


B

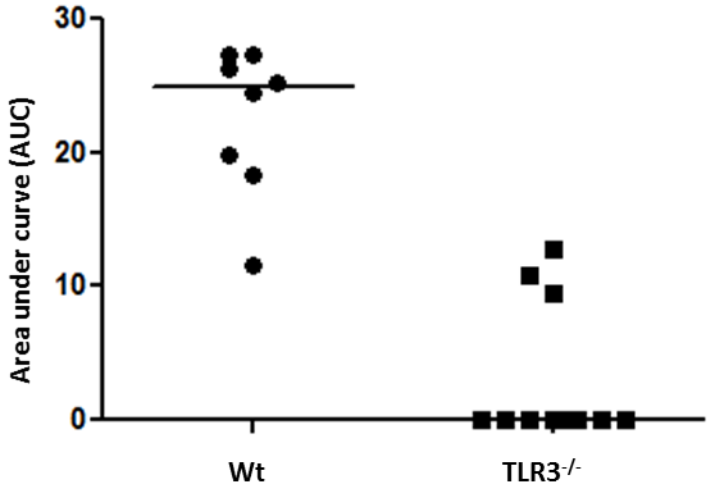

**Figure 30. Active EAE induction in *TLR3*$^{-/-}$ female mice.** A) Both *TLR3*$^{-/-}$ (squares) and Wt (dots) female mice, 11 mice in *TLR3*$^{-/-}$ group and 8 mice in Wt group were immunized with MOG peptide, CFA, PT and were scored daily for EAE clinical signs. Each data point represents median per day from all the mice in that group. All Wt mice developed EAE clinical signs with 100% disease incidence and only 3 *TLR3*$^{-/-}$ mice developed EAE clinical signs out of 11 with disease incidence of 27% B) Area under the curve (AUC) for each mouse was calculated during the EAE disease course and the middle line represents median. AUC was used to measure the overall disease severity between Wt and *TLR3*$^{-/-}$ .Using Mann-Whitney U test, a significant difference was found between the groups in disease severity ($p < 0.05$). Experiment was performed thrice. Repetition of the experiment is shown in appendix III.

**Table 7.Table summarizing the requirement of TLR3 in EAE (female mice).** A) Data pooled in from three independent experiments. Both Wt and *TLR3*$^{-/-}$ female mice were immunized with MOG peptide, CFA, PT and were scored daily for EAE clinical signs. In total, 18 mice were used for analysis in Wt group and 21 in *TLR3*$^{-/-}$ group. In Wt group, all 18 mice developed EAE clinical signs with disease incidence of 100% and in *TLR3*$^{-/-}$ group, only 5 mice out of 21 developed EAE clinical signs with disease incidence of 23%. Mean day of disease onset was calculated by taking mean of the first day of disease onset. Mean day of maximum score was calculated by taking the mean of the day when each mouse displayed its maximum clinical score during EAE disease course. To calculate mean day of disease onset and mean day of maximum score, only scores of sick mice were included. B) Median of maximal score was calculated by taking maximum score displayed by each mouse during the EAE disease course. To calculate median of maximal score, only maximum score of sick mice was included.

**A**

| Genotype | Incidence % | Mean day of disease onset | Mean day of maximum score |
|---|---|---|---|
| **TLR3$^{-/-}$** | **23%** | **14** | **16** |
| **Wt** | **100%** | **10** | **14** |

**B**

| Genotype | Median of maximal score |
|---|---|
| **TLR3$^{-/-}$** | **2.5(5/21)** |
| **Wt** | **3(18/18)** |

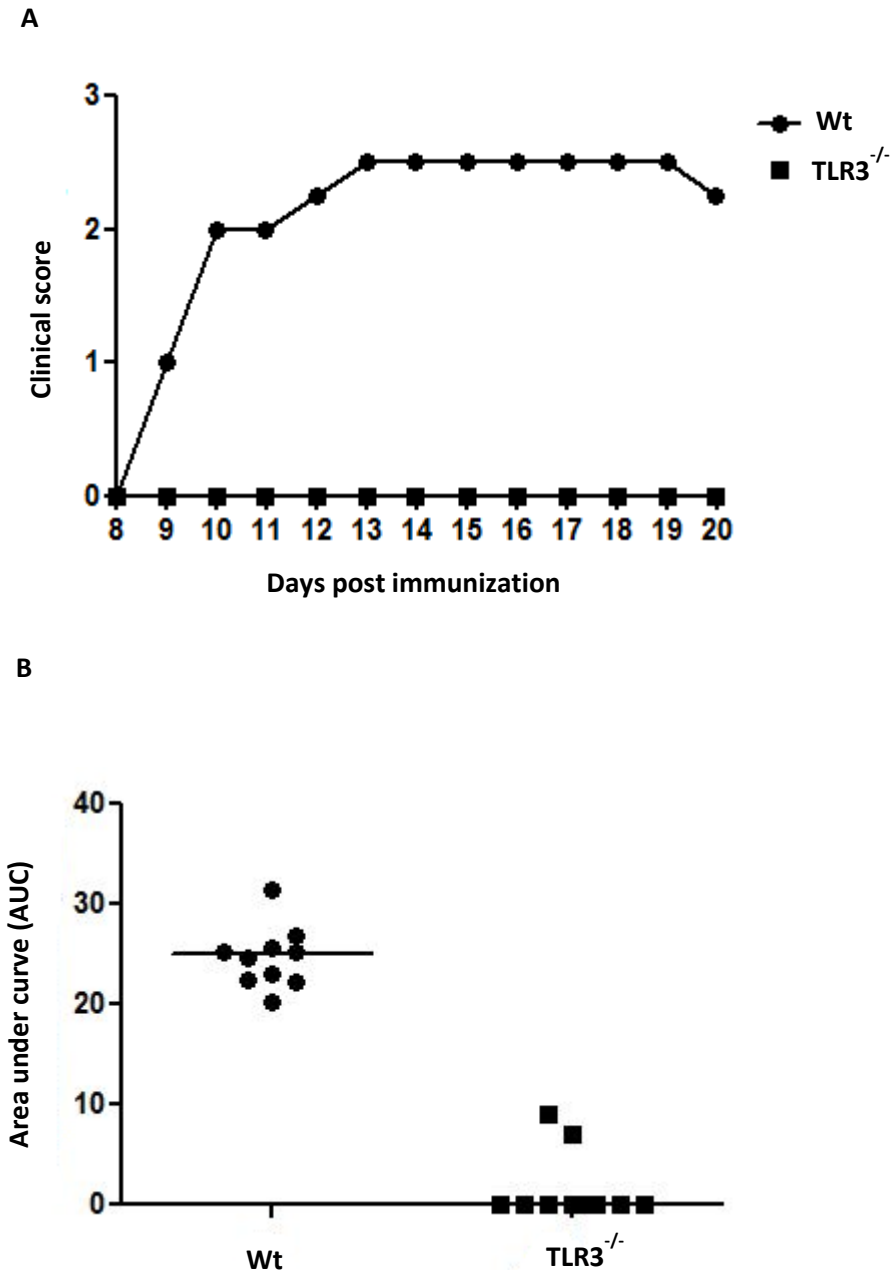


**Figure 31. Active EAE induction in *TLR3*$^{-/-}$ male mice.** A) Both *TLR3*$^{-/-}$ (squares) *and* Wt (dots) male mice, 10 mice per group were immunized with MOG peptide, PT, CFA and were scored daily for EAE clinical signs. Each data point represents median per day from ten mice. All Wt mice developed EAE clinical signs with 100% disease incidence. Out of 10, only 2 *TLR3*$^{-/-}$ mice developed EAE clinical signs with 20% disease incidence. B) Area under the curve (AUC) for each mouse was calculated during the EAE disease course and the middle line represents median. AUC was used to measure the overall disease severity

between Wt and *TLR3*$^{-/-}$ .Using Mann-Whitney U test, a significant difference was found between the groups in disease severity ($p < 0.05$). Experiment was performed once.

**Table 8. Table summarizing the requirement of TLR3 in EAE (male mice).** A) Both *TLR3*$^{-/-}$ and Wt male mice, 10 mice per group were immunized with MOG peptide and were scored daily for clinical signs. All Wt mice developed EAE clinical signs with 100% disease incidence. Out of 10, only 2 *TLR3*$^{-/-}$ mice developed EAE clinical signs with 20% disease incidence. Mean day of disease onset was calculated by taking mean of the first day of disease onset. Mean day of maximum score was calculated by taking the mean of the day when each mouse displayed its maximum clinical score during EAE disease course. To calculate mean day of disease onset and mean day of maximum score, only scores sick mice were included. B) Median of maximal score was calculated by taking maximum score displayed by each mouse during the EAE disease course. To calculate median of maximal score, only maximum score of sick mice was included.

**A**

| Genotype | Incidence % | Mean day of disease onset | Mean day of maximum score |
|---|---|---|---|
| ***TLR3***$^{-/-}$ | **20%** | **14** | **14** |
| **Wt** | **100%** | **9** | **14** |

**B**

| Genotype | Median of maximal score |
|---|---|
| ***TLR3***$^{-/-}$ | **1.75 (2/10)** |
| **Wt** | **2.75 (10/10)** |

# 4 Discussion

MS is a complex disorder of the central nervous system which is demyelinating and inflammatory in nature with unknown disease etiology (Stadelmann et al., 2011). First description of MS was documented in 1868 by Jean-Martin Charcot (Kumar et al., 2011). From that period onwards, our knowledge about MS has rapidly grown. Research knowledge coming from MS patient case studies as well as from animal models of MS have provided us with greater insights into the complex pathology lying behind MS. Many MS disease modulating drugs are currently available although many of them only aid with temporary management of the disease. Yet, in spite of all the progress, there is a great dearth in our knowledge of what exactly causes or triggers MS. Though a single causative agent has not been identified, many research studies have clearly confirmed that both genetic susceptibility and environmental factors can trigger MS (Libbey and Fujinami, 2010). Among environmental factors, infectious agents have been highly implicated as the possible culprits in triggering self-reactive T cells and thus orchestrating the myelin attack and bringing forth MS clinical symptoms. Some of these infectious agents that are being implicated in MS pathology include Epstein - Barr virus (EBV), Chlamydia pneumoniae and human herpes virus-6 (HHV-6) (Pawate and Sriram, 2010).

One of the early steps in case of an infection with pathogens is the innate recognition of microbial invasion by the immune system which is pivotal for mounting an immune attack against the invading infectious agents (Mogensen, 2009). This process involves recognition of PAMPs from invading pathogens by PRRs and TLRs being the most prominent PRRs have gained considerable attention regarding their role in initiating and supporting the progression of many autoimmune disorders including MS (Mills, 2011). Apart from aiding the innate immune system in the recognition of invading pathogens, TLRs also play a crucial role in defining adaptive immune responses by inducing the secretion of cytokines that drive naïve Th cell differentiation into various subsets such as Th1, Th2 and Th17 among others (Jin et al., 2012). For example, activation of TLR signaling in DCs induces production of cytokines such as IL12, IL6 and TGFβ that are needed for differentiation of naïve T cell to Th1( IL12) or Th17 (IL6 + TGFβ) phenotypes, both

of these subsets are pathogenic in EAE as well as in MS (Mills, 2011). Therefore, modulating TLR signaling holds good promise for developing therapeutic drugs for treating MS.

So far, various research groups have investigated the role of individual TLRs in EAE but the results have been inconsistent. One of the main reasons for this could be that immunization protocols used for disease induction vary between the research groups. In the current project, we planned to decipher the requirement of TLRs in EAE using combinatorial TLR deficiency approach. We aimed at investigating the combined deficiencies of various TLRs based on their location, ligand recognition and earlier significant reports from individual TLR requirement studies in EAE. Therefore, we have investigated the role of TLRs in active EAE model using *TLR9*$^{-/-}$, *TLR3*$^{-/-}$, *TLR379*$^{-/-}$ and *TLR23479*$^{-/-}$ mice.

In our initial experiments, we assessed the requirement of TLR9 for EAE induction and how its deficiency impacts disease course and severity. As mentioned earlier, TLR 9 is located within the endosomal and recognizes CpG DNA from microbes (Akira and Takeda, 2004). TLR9 activation in pDCs results in production of IFNα via MyD88-dependent pathway (Fuchsberger et al., 2005). CFA used for preparing MOG emulsion for EAE induction consists of heat-killed Mycobacterium tuberculosis whose CpG DNA is recognized by TLR9. Therefore, we wanted to investigate the requirement of TLR9 that recognizes adjuvant components. We observed that the induction of active EAE is not dependent on TLR9. *TLR9*$^{-/-}$ mice were highly susceptible to disease induction and showed a trend of more severe EAE in comparison to the Wt mice but the difference between the maximal scores of the two groups was not significant. The results we observed for *TLR9*$^{-/-}$ deficiency in active EAE were similar to the ones observed by Marta et al. but are in contrast to reports from Prinz et al. and Miranda-Hernandez et al.. As mentioned, this contradiction in outcome could result from the different immunization protocols used. In their experiments, both groups immunized mice twice with MOG peptide, first immunization was done on day 0 followed by a second immunization on day 7 and reported that deficiency of TLR9 exerted a protective effect as *TLR9*$^{-/-}$ mice in their experiments developed less severe EAE clinical signs in comparision to the wild type mice (Miranda-Hernandez et al., 2011; Prinz et al., 2006). Here we have applied the more traditional protocol of EAE induction by immunizing mice only once with MOG peptide. Our results were similar to those observed by Marta et al. even though they had immunized mice with MOG protein instead of peptide. Consistently all reports showed that *TLR9*$^{-/-}$ mice were not

completely resistant to EAE induction, only the extent of disease severity varied. This clearly suggests that *TLR9*$^{-/-}$ is dispensable for EAE induction despite the fact that CFA is required for successful EAE induction in C57bl/6 background (McCarthy et al., 2012) and that TLR9 recognizes mycobacterial components in CFA. This suggests the presence of other redundant mechanisms to faciliate the adjuvant action of CFA in the absence of TLR9.

We next investigated the impact of combined deficiencies of endosomal TLRs on active EAE induction and disease progression. TLRs 3, 7 and 9 are localized in endosomal cellular compartments and recognize nucleic acids. Under steady state conditions, synthesis of TLRs occurs in endoplasmic reticulum (ER) and are trafficked to either cell surface or to endosomal compartments via ER-Golgi complex secretory pathway (Lee and Barton, 2014). Trafficking of endosomal TLRs is highly regulated and controlled in order to prevent them from recognizing self-nucleic acids. Further, self-nucleic acids released from dying cells are destroyed by enzymes such as DNaseI before they reach endolysosomes (Barbalat et al., 2011) whereas microbial nucleic acids reach endolysosomes via mechanisms such as autophagy (Saitoh and Miyake, 2009). But when these regulatory mechanisms are breached, it was shown to lead to autoimmunity (Barbalat et al., 2011; Lee and Barton, 2014). Endosomal TLRs have been highly implicated in many autoimmune disorders such as systemic lupus erythematosus (SLE). In SLE, tolerance to the self-nucleic acids is lost leading to production of auto-antibodies against self-DNA (Barbalat et al., 2011). As mentioned earlier, infectious agents, especially viruses have been implicated as possible causative agents in MS (Fujinami et al., 2006) and because endosomal TLRs 3 and 7 recognize double and single stranded RNA from viruses respectively and as TLR9 recognizes CpG moieties from bacterial DNA (Takeda et al., 2003), endosomal TLRs might play a crucial role in MS. Yet, so far there are no reports on the impact of combined deficiency of endosomal TLRs in EAE. Therefore, we have investigated the requirement of endosomal TLRs for EAE induction and how it impacts disease course. We observed that endosomal TLRs are not required for active EAE induction. Moreover, *TLR379*$^{-/-}$ mice developed more severe disease symptoms in comparison to the wild type mice. However, histological analysis of sick mice at the peak of the disease revealed comparable extent of demyelination and infiltration by T cells in the CNS between *TLR379*$^{-/-}$ and wild type groups. Exhibition of more severe clinical signs by *TLR379*$^{-/-}$ mice suggests a protective role for endosomal TLRs in active EAE.

Next, we aimed at investigating the requirement of TLR signaling for active EAE induction using *TLR23479*$^{-/-}$ mice. As mentioned earlier, using *TLR23479*$^{-/-}$ mice it is possible to investigate the role of a major number of TLRs in EAE giving us insights into requirement of the TLR signaling for EAE induction. In *TLR23479*$^{-/-}$ mice, not only TLR 2 ,3 , 4, 7 and 9 signaling is disabled but also that of TLRs 1 and 6 because of their dependency on TLR2 for heterodimer formation. We initiated our EAE induction experiments in *TLR23479*$^{-/-}$ mice with the hypothesis that the TLR quintuple knockout mice would be resistant to EAE induction. This hypothesis was based on the earlier reports from various groups which clearly confirmed that *MyD88*$^{-/-}$ mice are completely resistant to EAE (Marta et al., 2008; Prinz et al., 2006) TLRs 1, 2, 4, 7, 9 utilize MyD88 adaptor protein for downstream signaling and TLR3 utilizes only TRIF adaptor protein whereas TLR4 can utilize both MyD88 and TRIF for its downstream signaling (Akira and Takeda, 2004).

We observed that combined deficiencies of multiple TLRs did not protect mice from developing EAE clinical signs. It was surprising to see that the absence of multiple TLRs could not account for the EAE resistant phenotype exhibited by *MyD88*$^{-/-}$ mice. *TLR23479*$^{-/-}$ mice were highly susceptible to disease induction and exhibited more severe disease clinical signs in comparison to wild type mice. However, histological analysis of sick *TLR23479*$^{-/-}$ and wild type mice at the peak disease did not reveal any major differences in the extent of demyelination and infiltration by T cells between the two groups. Furthermore, relative mRNA expression levels of inflammatory cytokines IFNγ, IL17 and GMCSF in the periphery and in the CNS during EAE disease course remained comparable between *TLR23479*$^{-/-}$ and wild type mice. Therefore, our initial hypothesis that *TLR23479*$^{-/-}$ mice would be resistant to EAE induction was proven wrong. Yet, it was intriguing that *TLR23479*$^{-/-}$ mice were susceptible to EAE and developed more severe EAE symptoms in comparison to the wild type mice. Even though our wild type mice were not bred in our facility and were purchased from Harlan, mice were ordered at the age of 4-5 weeks and were co-housed with *TLR23479*$^{-/-}$ for at least 5 weeks in our animal facility under SPF conditions before EAE induction. Co-housing was done in order to facilitate the transfer of gut microbiota. In spite of that, *TLR23479*$^{-/-}$ mice still developed higher clinical score in comparison to the wild type mice with EAE clinical scores of 3.5-4 with complete hind and forelimb paralysis.

As we observed that combined deficiencies of TLRs 2, 3, 4, 7 and 9 does not account for disease resistance phenotype exhibited by *MyD88*$^{-/-}$ mice, we next questioned if lack of signaling through

TRIF adaptor protein renders *TLR23479*$^{-/-}$ mice highly susceptible and more prone to disease severity. As mentioned earlier, signaling through TRIF results in the induction of IFNβ (O'Neill and Bowie, 2007) which has been reported to be beneficial in EAE (Axtell et al., 2010). Moreover, *TRIF*$^{-/-}$ and *IFNAR*$^{-/-}$ mice have been reported to be susceptible to EAE induction and to exhibit more disease severity in comparison to wild type mice (Guo et al., 2008). So based on this previous reports, we next hypothesized that lack or reduced production of IFNβ in *TLR23479*$^{-/-}$ mice renders them susceptible to both disease induction and severity. In our initial experiments to test this hypothesis, we induced EAE in Δβ−luc reporter mice in which luciferase activity is driven by IFNβ promoter. Thus, by measuring luciferase activity by *in vivo* imaging it is possible to read out IFNβ induction intensity. We observed that 6h after induction, a consistent induction of IFNβ was observed at the site of injection until the end of observation i.e. day 10 post induction. Next, we wanted to investigate if production of IFNβ at the site of injection varies between *TLR23479*$^{-/-}$ and wild type mice and if this could account for the disease severity in quintuple mice during EAE. To test this, we isolated cells from the site of immunization on day 3 post induction and extracted total RNA and performed qPCR analysis to measure the mRNA expression levels of IFN pathway related genes, IFNβ and IRF7 and that of MX1, a biomarker of IFNβ activity (Petry et al., 2006). We observed no difference in the mRNA expression levels of IFNβ and IRF7 between *TLR23479*$^{-/-}$ and wild type mice at the site of immunization. Further, we measured IFNβ and IRF7 mRNA levels during both disease priming phase i.e. on day 7 and as well as at the peak of the disease when mice exhibited severe EAE clinical signs in periphery as well as in the CNS and in both the situations, we found comparable mRNA expression levels for IFNβ and IRF7 between *TLR23479*$^{-/-}$ and wild type mice. These observations proved our hypothesis wrong.

Our observations that IFNβ expression levels remained comparable between *TLR23479*$^{-/-}$ and wild type mice during the course of EAE lead us to question the requirement of TLR3 in active EAE. As mentioned earlier, TLR3 signals through TRIF adaptor protein instead of MyD88 (Akira and Takeda, 2004) and its signaling results in the induction of IFNβ. Also, both *TRIF*$^{-/-}$ and *IFNAR*$^{-/-}$ mice are susceptible to EAE and develop more severe disease symptoms in comparison to the wild type mice (Guo et al., 2008). However, to the best of our knowledge, so far there are no reports about the impact of TLR3 deficiency on active EAE induction and disease course. Treating mice with TLR3 ligand poly I: C has been reported to attenuate EAE disease severity by inducing IFN-β production (Touil et al., 2006) and other previous studies have shown protective role for IFN-β

in EAE. Therefore, we expected *TLR3*$^{-/-}$ mice to exhibit more severe EAE clinical signs. We observed that *TLR3*$^{-/-}$ mice were resistant to EAE induction although this protection was not complete. Wild type mice were all highly susceptible to EAE induction but *TLR3*$^{-/-}$ mice displayed very low disease incidence of about 23%, whereas 100% disease incidence was observed in the wild type group. Moreover, a delayed onset of disease by 4 days was seen in *TLR3*$^{-/-}$ mice that developed EAE clinical signs. Yet, disease severity of sick *TLR3*$^{-/-}$ mice remained comparable to that of wild type. TLR3 signaling through TRIF leads to IFNβ production (Perry et al., 2005) and IFNβ has a protective role in EAE (Axtell et al., 2010) . Thus, our findings are surprising and complex to interpret. However, previously it has been reported that *IRF3*$^{-/-}$ mice also display partial disease resistance with low disease incidence as is the case with *TLR3*$^{-/-}$ mice. *IRF3*$^{-/-}$ mice exhibit impaired Th17 differentiation *in vitro* and further less IL17 production was observed in CNS of sick *IRF3*$^{-/-}$ in comparison to wild type mice (Fitzgerald et al., 2014). IRF3 is a transcription factor that is activated by TLR3 signaling via TRIF inducing IFNβ production (Troutman et al., 2012). Further, deficiency of TBK1 in T cells resulted in EAE disease resistance. TBK1 is downstream of TRIF and association of TRIF with TBK1 promotes its kinase activity resulting in phosphorylation and activation of IRF3 (Sato et al., 2003). Ablation of TBK1 in T cells though did not hinder T cell activation nor differentiation but rather prevented effector T cell egress from lymph nodes thus dampening the CNS infiltration by T cells (Yu et al., 2014). Therefore, different EAE phenotypes observed upon the deficiencies of various molecules involved in TLR3 signaling via TRIF makes it very complex and convoluted to come to a conclusion about the requirement of TRIF signaling pathway in EAE.

# 5 Conclusion and future scope

We have shown that TLR9 which recognizes CpG DNA from mycobacterial components in CFA is dispensable for EAE induction. Similarly, we have shown that endosomal TLRs 3, 7 and 9 that recognize nucleic acids are also dispensable for EAE induction. Further, combined deficiency of endosomal TLRs along with surface receptors 2 and 4 did not protect *TLR23479*$^{-/-}$ mice from developing EAE clinical signs, even though these receptors mostly signal through MyD88 and mice deficient in MyD88 are resistant to EAE. Further, we have shown that IFNβ mRNA expression levels remained comparable between *TLR23479*$^{-/-}$ and wild type sick mice during the

course of EAE both in periphery and in CNS suggesting that despite lack of TRIF signaling through TLRs 3 and 4 in *TLR23479*$^{-/-}$ mice, IFNβ is still being produced and therefore disease severity is not correlated to its absence. This assumption is made based on the previous reports that suggested that *TRIF*$^{-/-}$ and *IFNAR*$^{-/-}$ mice develop more severe EAE clinical signs in comparison to the wild type mice and that IFNβ is protective in MS and used as a treatment option.

MyD88 adaptor protein is not just utilized by TLRs for its downstream signaling but also by members of IL1R family including IL1R, IL18R and IL33R (ST2) (Arend et al., 2008) and by double stranded (ds) DNA censors namely asparate-glutamate-alanine-histidine box motif DEAH-box helicase 36 (dhx36) and DEAH-box helicase 9 (dhx9) (Kim et al., 2010). Not much is known about the role of dhx36 and dhx9 in EAE. However, the role of IL1R family members has been investigated in EAE. It has been previously reported that *IL1R*$^{-/-}$ show resistance to EAE induction but not a complete resistance (Lukens et al., 2012), *IL18R*$^{-/-}$ mice have been reported to be EAE resistant but *IL18*$^{-/-}$ mice were susceptible (Gutcher et al., 2006) making it complex to understand the disconnection as no other ligand has been so far reported for IL18R other than IL18. In contrast, *IL33R*$^{-/-}$ mice have been reported to develop more severe EAE clinical signs in comparison to wild type (Jiang et al., 2012). Over all, it appears that EAE resistance phenotype exhibited by *MyD88*$^{-/-}$ mice might not be an individual effect of either IL1R, IL18R or IL33R deficiency but rather a combined deficiency of all the three IL1R family members. As a future perspective, investigating the requirement of IL1R family members using *IL1R/IL18R/IL33R*$^{-/-}$ mice and single and double knockouts as controls holds good promise to check if IL1R family accounts for *MyD88*$^{-/-}$ mice EAE phenotype, if so which one of them in more neat way.

We have also shown that *TLR3*$^{-/-}$ mice displayed resistance to EAE induction, although the protection was not complete as some of the *TLR3*$^{-/-}$ mice did develop EAE clinical signs with delayed onset of disease symptoms in comparison to wild type mice. Some of the *TLR3*$^{-/-}$ mice that developed EAE clinical signs displayed EAE clinical scores around 2-3.5 with both hind limbs and partial fore limb paralysis suggesting once the pathogenic T cells reach the brain, they are able to cause the CNS damage. But majority of *TLR3*$^{-/-}$ mice were resistant to disease induction suggesting a probable impairment either in initial priming of myelin reactive T cells or their homing to CNS. As future perspective, investigating how initial disease priming phase in *TLR3*$^{-/-}$ mice differs from that of wild type mice in terms of APC maturation and antigen presentation

together with T cell activation, differentiation and homing studies holds key to investigate how absence of TLR3 protects mice from developing EAE clinical signs.

# 6 References

Akira, S., Takeda, K., 2004. Toll-like receptor signalling. Nat Rev Immunol 4, 499-511.
Alexopoulou, L., Holt, A.C., Medzhitov, R., Flavell, R.A., 2001. Recognition of double-stranded RNA and activation of NF-kappaB by Toll-like receptor 3. Nature 413, 732-738.
Andersson, A., Covacu, R., Sunnemark, D., Danilov, A.I., Dal Bianco, A., Khademi, M., Wallstrom, E., Lobell, A., Brundin, L., Lassmann, H., Harris, R.A., 2008. Pivotal advance: HMGB1 expression in active lesions of human and experimental multiple sclerosis. J Leukoc Biol 84, 1248-1255.
Arend, W.P., Palmer, G., Gabay, C., 2008. IL-1, IL-18, and IL-33 families of cytokines. Immunol Rev 223, 20-38.
Awate, S., Babiuk, L.A., Mutwiri, G., 2013. Mechanisms of action of adjuvants. Front Immunol 4, 114.
Axtell, R.C., de Jong, B.A., Boniface, K., van der Voort, L.F., Bhat, R., De Sarno, P., Naves, R., Han, M., Zhong, F., Castellanos, J.G., Mair, R., Christakos, A., Kolkowitz, I., Katz, L., Killestein, J., Polman, C.H., de Waal Malefyt, R., Steinman, L., Raman, C., 2010. T helper type 1 and 17 cells determine efficacy of interferon-beta in multiple sclerosis and experimental encephalomyelitis. Nat Med 16, 406-412.
Balashov, K.E., Aung, L.L., Vaknin-Dembinsky, A., Dhib-Jalbut, S., Weiner, H.L., 2010. Interferon-beta inhibits toll-like receptor 9 processing in multiple sclerosis. Ann Neurol 68, 899-906.
Barbalat, R., Ewald, S.E., Mouchess, M.L., Barton, G.M., 2011. Nucleic acid recognition by the innate immune system. Annu Rev Immunol 29, 185-214.
Basu, J., Shin, D.M., Jo, E.K., 2012. Mycobacterial signaling through toll-like receptors. Front Cell Infect Microbiol 2, 145.
Becher, B., Durell, B.G., Noelle, R.J., 2002. Experimental autoimmune encephalitis and inflammation in the absence of interleukin-12. J Clin Invest 110, 493-497.
Bettelli, E., Das, M.P., Howard, E.D., Weiner, H.L., Sobel, R.A., Kuchroo, V.K., 1998. IL-10 is critical in the regulation of autoimmune encephalomyelitis as demonstrated by studies of IL-10- and IL-4-deficient and transgenic mice. J Immunol 161, 3299-3306.
Bittner, S., Afzali, A.M., Wiendl, H., Meuth, S.G., 2014. Myelin oligodendrocyte glycoprotein (MOG35-55) induced experimental autoimmune encephalomyelitis (EAE) in C57BL/6 mice. J Vis Exp.
Botos, I., Segal, D.M., Davies, D.R., 2011. The structural biology of Toll-like receptors. Structure 19, 447-459.
Bsibsi, M., Ravid, R., Gveric, D., van Noort, J.M., 2002. Broad expression of Toll-like receptors in the human central nervous system. J Neuropathol Exp Neurol 61, 1013-1021.
Buchholz, B.M., Bauer, A.J., 2010. Membrane TLR signaling mechanisms in the gastrointestinal tract during sepsis. Neurogastroenterol Motil 22, 232-245.
Carty, M., Goodbody, R., Schroder, M., Stack, J., Moynagh, P.N., Bowie, A.G., 2006. The human adaptor SARM negatively regulates adaptor protein TRIF-dependent Toll-like receptor signaling. Nat Immunol 7, 1074-1081.
Cole, J.E., Georgiou, E., Monaco, C., 2010. The expression and functions of toll-like receptors in atherosclerosis. Mediators Inflamm 2010, 393946.
Compston, A., Coles, A., 2002. Multiple sclerosis. Lancet 359, 1221-1231.
Conrad, M.L., Ferstl, R., Teich, R., Brand, S., Blumer, N., Yildirim, A.O., Patrascan, C.C., Hanuszkiewicz, A., Akira, S., Wagner, H., Holst, O., von Mutius, E., Pfefferle, P.I., Kirschning, C.J., Garn, H., Renz, H., 2009.

Maternal TLR signaling is required for prenatal asthma protection by the nonpathogenic microbe Acinetobacter lwoffii F78. J Exp Med 206, 2869-2877.
Constantinescu, C.S., Farooqi, N., O'Brien, K., Gran, B., 2011. Experimental autoimmune encephalomyelitis (EAE) as a model for multiple sclerosis (MS). Br J Pharmacol 164, 1079-1106.
Corthay, A., 2009. How do regulatory T cells work? Scand J Immunol 70, 326-336.
Cua, D.J., Hutchins, B., LaFace, D.M., Stohlman, S.A., Coffman, R.L., 2001. Central nervous system expression of IL-10 inhibits autoimmune encephalomyelitis. J Immunol 166, 602-608.
Cusick, M.F., Libbey, J.E., Fujinami, R.S., 2012. Molecular mimicry as a mechanism of autoimmune disease. Clin Rev Allergy Immunol 42, 102-111.
Denic, A., Johnson, A.J., Bieber, A.J., Warrington, A.E., Rodriguez, M., Pirko, I., 2011. The relevance of animal models in multiple sclerosis research. Pathophysiology 18, 21-29.
Dyment, D.A., Ebers, G.C., Sadovnick, A.D., 2004. Genetics of multiple sclerosis. Lancet Neurol 3, 104-110.
Enevold, C., Oturai, A.B., Sorensen, P.S., Ryder, L.P., Koch-Henriksen, N., Bendtzen, K., 2010. Polymorphisms of innate pattern recognition receptors, response to interferon-beta and development of neutralizing antibodies in multiple sclerosis patients. Mult Scler 16, 942-949.
Engelhardt, B., 2006. Molecular mechanisms involved in T cell migration across the blood-brain barrier. J Neural Transm (Vienna) 113, 477-485.
Ercolini, A.M., Miller, S.D., 2009. The role of infections in autoimmune disease. Clin Exp Immunol 155, 1-15.
Erny, D., Hrabe de Angelis, A.L., Jaitin, D., Wieghofer, P., Staszewski, O., David, E., Keren-Shaul, H., Mahlakoiv, T., Jakobshagen, K., Buch, T., Schwierzeck, V., Utermohlen, O., Chun, E., Garrett, W.S., McCoy, K.D., Diefenbach, A., Staeheli, P., Stecher, B., Amit, I., Prinz, M., 2015. Host microbiota constantly control maturation and function of microglia in the CNS. Nat Neurosci 18, 965-977.
Fischer, M., Ehlers, M., 2008. Toll-like receptors in autoimmunity. Ann N Y Acad Sci 1143, 21-34.
Fitzgerald, D.C., O'Brien, K., Young, A., Fonseca-Kelly, Z., Rostami, A., Gran, B., 2014. Interferon regulatory factor (IRF) 3 is critical for the development of experimental autoimmune encephalomyelitis. J Neuroinflammation 11, 130.
Fitzner, D., Simons, M., 2010. Chronic progressive multiple sclerosis - pathogenesis of neurodegeneration and therapeutic strategies. Curr Neuropharmacol 8, 305-315.
Fletcher, J.M., Lalor, S.J., Sweeney, C.M., Tubridy, N., Mills, K.H., 2010. T cells in multiple sclerosis and experimental autoimmune encephalomyelitis. Clin Exp Immunol 162, 1-11.
Frohman, E.M., Racke, M.K., Raine, C.S., 2006. Multiple sclerosis--the plaque and its pathogenesis. N Engl J Med 354, 942-955.
Fuchsberger, M., Hochrein, H., O'Keeffe, M., 2005. Activation of plasmacytoid dendritic cells. Immunol Cell Biol 83, 571-577.
Fujinami, R.S., von Herrath, M.G., Christen, U., Whitton, J.L., 2006. Molecular mimicry, bystander activation, or viral persistence: infections and autoimmune disease. Clin Microbiol Rev 19, 80-94.
Gold, R., Linington, C., Lassmann, H., 2006. Understanding pathogenesis and therapy of multiple sclerosis via animal models: 70 years of merits and culprits in experimental autoimmune encephalomyelitis research. Brain 129, 1953-1971.
Goldenberg, M.M., 2012. Multiple sclerosis review. P T 37, 175-184.
Goverman, J., 2009. Autoimmune T cell responses in the central nervous system. Nat Rev Immunol 9, 393-407.
Guo, B., Chang, E.Y., Cheng, G., 2008. The type I IFN induction pathway constrains Th17-mediated autoimmune inflammation in mice. J Clin Invest 118, 1680-1690.
Gutcher, I., Urich, E., Wolter, K., Prinz, M., Becher, B., 2006. Interleukin 18-independent engagement of interleukin 18 receptor-alpha is required for autoimmune inflammation. Nat Immunol 7, 946-953.

Haller, O., Kochs, G., Weber, F., 2006. The interferon response circuit: induction and suppression by pathogenic viruses. Virology 344, 119-130.
Hansen, B.S., Hussain, R.Z., Lovett-Racke, A.E., Thomas, J.A., Racke, M.K., 2006. Multiple toll-like receptor agonists act as potent adjuvants in the induction of autoimmunity. J Neuroimmunol 172, 94-103.
Harari, D., Kuhn, N., Abramovich, R., Sasson, K., Zozulya, A.L., Smith, P., Schlapschy, M., Aharoni, R., Koster, M., Eilam, R., Skerra, A., Schreiber, G., 2014. Enhanced in vivo efficacy of a type I interferon superagonist with extended plasma half-life in a mouse model of multiple sclerosis. J Biol Chem 289, 29014-29029.
Haussleiter, I.S., Brune, M., Juckel, G., 2009. Psychopathology in multiple sclerosis: diagnosis, prevalence and treatment. Ther Adv Neurol Disord 2, 13-29.
Hayashi, T., Yao, S., Crain, B., Chan, M., Tawatao, R.I., Gray, C., Vuong, L., Lao, F., Cottam, H.B., Carson, D.A., Corr, M., 2012. Treatment of autoimmune inflammation by a TLR7 ligand regulating the innate immune system. PLoS One 7, e45860.
Hemmi, H., Kaisho, T., Takeuchi, O., Sato, S., Sanjo, H., Hoshino, K., Horiuchi, T., Tomizawa, H., Takeda, K., Akira, S., 2002. Small anti-viral compounds activate immune cells via the TLR7 MyD88-dependent signaling pathway. Nat Immunol 3, 196-200.
Hemmi, H., Takeuchi, O., Kawai, T., Kaisho, T., Sato, S., Sanjo, H., Matsumoto, M., Hoshino, K., Wagner, H., Takeda, K., Akira, S., 2000. A Toll-like receptor recognizes bacterial DNA. Nature 408, 740-745.
Hirotani, M., Niino, M., Fukazawa, T., Kikuchi, S., Yabe, I., Hamada, S., Tajima, Y., Sasaki, H., 2010. Decreased IL-10 production mediated by Toll-like receptor 9 in B cells in multiple sclerosis. J Neuroimmunol 221, 95-100.
Honda, K., Sakaguchi, S., Nakajima, C., Watanabe, A., Yanai, H., Matsumoto, M., Ohteki, T., Kaisho, T., Takaoka, A., Akira, S., Seya, T., Taniguchi, T., 2003. Selective contribution of IFN-alpha/beta signaling to the maturation of dendritic cells induced by double-stranded RNA or viral infection. Proc Natl Acad Sci U S A 100, 10872-10877.
Hoshino, K., Takeuchi, O., Kawai, T., Sanjo, H., Ogawa, T., Takeda, Y., Takeda, K., Akira, S., 1999. Cutting edge: Toll-like receptor 4 (TLR4)-deficient mice are hyporesponsive to lipopolysaccharide: evidence for TLR4 as the Lps gene product. J Immunol 162, 3749-3752.
Hou, B., Reizis, B., DeFranco, A.L., 2008. Toll-like receptors activate innate and adaptive immunity by using dendritic cell-intrinsic and -extrinsic mechanisms. Immunity 29, 272-282.
Hurwitz, B.J., 2009. The diagnosis of multiple sclerosis and the clinical subtypes. Ann Indian Acad Neurol 12, 226-230.
Iwasaki, A., Medzhitov, R., 2004. Toll-like receptor control of the adaptive immune responses. Nat Immunol 5, 987-995.
Jiang, H.R., Milovanovic, M., Allan, D., Niedbala, W., Besnard, A.G., Fukada, S.Y., Alves-Filho, J.C., Togbe, D., Goodyear, C.S., Linington, C., Xu, D., Lukic, M.L., Liew, F.Y., 2012. IL-33 attenuates EAE by suppressing IL-17 and IFN-gamma production and inducing alternatively activated macrophages. Eur J Immunol 42, 1804-1814.
Jin, B., Sun, T., Yu, X.H., Yang, Y.X., Yeo, A.E., 2012. The effects of TLR activation on T-cell development and differentiation. Clin Dev Immunol 2012, 836485.
Johnson, T.P., Tyagi, R., Patel, K., Schiess, N., Calabresi, P.A., Nath, A., 2013. Impaired toll-like receptor 8 signaling in multiple sclerosis. J Neuroinflammation 10, 74.
Kakalacheva, K., Munz, C., Lunemann, J.D., 2011. Viral triggers of multiple sclerosis. Biochim Biophys Acta 1812, 132-140.
Kamradt, T., Mitchison, N.A., 2001. Tolerance and autoimmunity. N Engl J Med 344, 655-664.
Kawai, T., Akira, S., 2010. The role of pattern-recognition receptors in innate immunity: update on Toll-like receptors. Nat Immunol 11, 373-384.

Kawasaki, T., Kawai, T., 2014. Toll-like receptor signaling pathways. Front Immunol 5, 461.
Kerfoot, S.M., Long, E.M., Hickey, M.J., Andonegui, G., Lapointe, B.M., Zanardo, R.C., Bonder, C., James, W.G., Robbins, S.M., Kubes, P., 2004. TLR4 contributes to disease-inducing mechanisms resulting in central nervous system autoimmune disease. J Immunol 173, 7070-7077.
Kim, T., Pazhoor, S., Bao, M., Zhang, Z., Hanabuchi, S., Facchinetti, V., Bover, L., Plumas, J., Chaperot, L., Qin, J., Liu, Y.J., 2010. Aspartate-glutamate-alanine-histidine box motif (DEAH)/RNA helicase A helicases sense microbial DNA in human plasmacytoid dendritic cells. Proc Natl Acad Sci U S A 107, 15181-15186.
Klein, L., Kyewski, B., Allen, P.M., Hogquist, K.A., 2014. Positive and negative selection of the T cell repertoire: what thymocytes see (and don't see). Nat Rev Immunol 14, 377-391.
Koblansky, A.A., Jankovic, D., Oh, H., Hieny, S., Sungnak, W., Mathur, R., Hayden, M.S., Akira, S., Sher, A., Ghosh, S., 2013. Recognition of profilin by Toll-like receptor 12 is critical for host resistance to Toxoplasma gondii. Immunity 38, 119-130.
Kragt, J., van Amerongen, B., Killestein, J., Dijkstra, C., Uitdehaag, B., Polman, C., Lips, P., 2009. Higher levels of 25-hydroxyvitamin D are associated with a lower incidence of multiple sclerosis only in women. Mult Scler 15, 9-15.
Kroenke, M.A., Chensue, S.W., Segal, B.M., 2010. EAE mediated by a non-IFN-gamma/non-IL-17 pathway. Eur J Immunol 40, 2340-2348.
Kroner, A., Vogel, F., Kolb-Maurer, A., Kruse, N., Toyka, K.V., Hemmer, B., Rieckmann, P., Maurer, M., 2005. Impact of the Asp299Gly polymorphism in the toll-like receptor 4 (tlr-4) gene on disease course of multiple sclerosis. J Neuroimmunol 165, 161-165.
Kumar, D.R., Aslinia, F., Yale, S.H., Mazza, J.J., 2011. Jean-Martin Charcot: the father of neurology. Clin Med Res 9, 46-49.
Kuokkanen, E., Sustar, V., Mattila, P.K., 2015. Molecular control of B cell activation and immunological synapse formation. Traffic 16, 311-326.
Lalive, P.H., Benkhoucha, M., Tran, N.L., Kreutzfeldt, M., Merkler, D., Santiago-Raber, M.L., 2014. TLR7 signaling exacerbates CNS autoimmunity through downregulation of Foxp3+ Treg cells. Eur J Immunol 44, 46-57.
Lassmann, H., Bruck, W., Lucchinetti, C.F., 2007. The immunopathology of multiple sclerosis: an overview. Brain Pathol 17, 210-218.
Lee, B.L., Barton, G.M., 2014. Trafficking of endosomal Toll-like receptors. Trends Cell Biol 24, 360-369.
Lee, C.C., Avalos, A.M., Ploegh, H.L., 2012. Accessory molecules for Toll-like receptors and their function. Nat Rev Immunol 12, 168-179.
Lee, Y.K., Menezes, J.S., Umesaki, Y., Mazmanian, S.K., 2011. Proinflammatory T-cell responses to gut microbiota promote experimental autoimmune encephalomyelitis. Proc Natl Acad Sci U S A 108 Suppl 1, 4615-4622.
Li, B., Baylink, D.J., Deb, C., Zannetti, C., Rajaallah, F., Xing, W.R., Walter, M.H., Lau, K.H.W., Qin, X.Z., 2013. 1,25-Dihydroxyvitamin D3 Suppresses TLR8 Expression and TLR8-Mediated Inflammatory Responses in Monocytes In Vitro and Experimental Autoimmune Encephalomyelitis In Vivo. Plos One 8.
Libbey, J.E., Fujinami, R.S., 2010. Potential triggers of MS. Results Probl Cell Differ 51, 21-42.
Lienenklaus, S., Cornitescu, M., Zietara, N., Lyszkiewicz, M., Gekara, N., Jablonska, J., Edenhofer, F., Rajewsky, K., Bruder, D., Hafner, M., Staeheli, P., Weiss, S., 2009. Novel reporter mouse reveals constitutive and inflammatory expression of IFN-beta in vivo. J Immunol 183, 3229-3236.
Litman, G.W., Rast, J.P., Fugmann, S.D., 2010. The origins of vertebrate adaptive immunity. Nat Rev Immunol 10, 543-553.
Liu, G., Zhang, L., Zhao, Y., 2010a. Modulation of immune responses through direct activation of Toll-like receptors to T cells. Clin Exp Immunol 160, 168-175.

Liu, J., Xu, C., Hsu, L.C., Luo, Y., Xiang, R., Chuang, T.H., 2010b. A five-amino-acid motif in the undefined region of the TLR8 ectodomain is required for species-specific ligand recognition. Mol Immunol 47, 1083-1090.
Loma, I., Heyman, R., 2011. Multiple sclerosis: pathogenesis and treatment. Curr Neuropharmacol 9, 409-416.
Ludwin, S., Jacobson, S., 2011. Epstein-Barr Virus and MS:Causality or Association? Int MS J 17, 39-43.
Lukens, J.R., Barr, M.J., Chaplin, D.D., Chi, H., Kanneganti, T.D., 2012. Inflammasome-derived IL-1beta regulates the production of GM-CSF by CD4(+) T cells and gammadelta T cells. J Immunol 188, 3107-3115.
Lunemann, J.D., Kamradt, T., Martin, R., Munz, C., 2007. Epstein-barr virus: environmental trigger of multiple sclerosis? J Virol 81, 6777-6784.
Marta, M., Andersson, A., Isaksson, M., Kampe, O., Lobell, A., 2008. Unexpected regulatory roles of TLR4 and TLR9 in experimental autoimmune encephalomyelitis. Eur J Immunol 38, 565-575.
McCarthy, D.P., Richards, M.H., Miller, S.D., 2012. Mouse models of multiple sclerosis: experimental autoimmune encephalomyelitis and Theiler's virus-induced demyelinating disease. Methods Mol Biol 900, 381-401.
McKay, K.A., Kwan, V., Duggan, T., Tremlett, H., 2015. Risk factors associated with the onset of relapsing-remitting and primary progressive multiple sclerosis: a systematic review. Biomed Res Int 2015, 817238.
Medzhitov, R., Janeway, C., Jr., 2000. Innate immunity. N Engl J Med 343, 338-344.
Miller, S.D., Karpus, W.J., Davidson, T.S., 2010. Experimental autoimmune encephalomyelitis in the mouse. Curr Protoc Immunol Chapter 15, Unit 15 11.
Mills, K.H., 2011. TLR-dependent T cell activation in autoimmunity. Nat Rev Immunol 11, 807-822.
Miranda-Hernandez, S., Baxter, A.G., 2013. Role of toll-like receptors in multiple sclerosis. Am J Clin Exp Immunol 2, 75-93.
Miranda-Hernandez, S., Gerlach, N., Fletcher, J.M., Biros, E., Mack, M., Korner, H., Baxter, A.G., 2011. Role for MyD88, TLR2 and TLR9 but not TLR1, TLR4 or TLR6 in experimental autoimmune encephalomyelitis. J Immunol 187, 791-804.
Mogensen, T.H., 2009. Pathogen recognition and inflammatory signaling in innate immune defenses. Clin Microbiol Rev 22, 240-273, Table of Contents.
Munz, C., Lunemann, J.D., Getts, M.T., Miller, S.D., 2009. Antiviral immune responses: triggers of or triggered by autoimmunity? Nat Rev Immunol 9, 246-258.
Netea, M.G., Van der Meer, J.W., Sutmuller, R.P., Adema, G.J., Kullberg, B.J., 2005. From the Th1/Th2 paradigm towards a Toll-like receptor/T-helper bias. Antimicrob Agents Chemother 49, 3991-3996.
Newton, K., Dixit, V.M., 2012. Signaling in innate immunity and inflammation. Cold Spring Harb Perspect Biol 4.
Nielsen, N.M., Westergaard, T., Rostgaard, K., Frisch, M., Hjalgrim, H., Wohlfahrt, J., Koch-Henriksen, N., Melbye, M., 2005. Familial risk of multiple sclerosis: a nationwide cohort study. Am J Epidemiol 162, 774-778.
Noppert, S.J., Fitzgerald, K.A., Hertzog, P.J., 2007. The role of type I interferons in TLR responses. Immunol Cell Biol 85, 446-457.
Noseworthy, J.H., Lucchinetti, C., Rodriguez, M., Weinshenker, B.G., 2000. Multiple sclerosis. N Engl J Med 343, 938-952.
Nothelfer, K., Sansonetti, P.J., Phalipon, A., 2015. Pathogen manipulation of B cells: the best defence is a good offence. Nat Rev Microbiol 13, 173-184.
O'Brien, K., Fitzgerald, D., Rostami, A., Gran, B., 2010. The TLR7 agonist, imiquimod, increases IFN-beta production and reduces the severity of experimental autoimmune encephalomyelitis. J Neuroimmunol 221, 107-111.

O'Gorman, C., Lucas, R., Taylor, B., 2012. Environmental risk factors for multiple sclerosis: a review with a focus on molecular mechanisms. Int J Mol Sci 13, 11718-11752.
O'Neill, L.A., Bowie, A.G., 2007. The family of five: TIR-domain-containing adaptors in Toll-like receptor signalling. Nat Rev Immunol 7, 353-364.
O'Neill, L.A., Golenbock, D., Bowie, A.G., 2013. The history of Toll-like receptors - redefining innate immunity. Nat Rev Immunol 13, 453-460.
Ohashi, P.S., 2002. T-cell signalling and autoimmunity: molecular mechanisms of disease. Nat Rev Immunol 2, 427-438.
Oldenburg, M., Kruger, A., Ferstl, R., Kaufmann, A., Nees, G., Sigmund, A., Bathke, B., Lauterbach, H., Suter, M., Dreher, S., Koedel, U., Akira, S., Kawai, T., Buer, J., Wagner, H., Bauer, S., Hochrein, H., Kirschning, C.J., 2012. TLR13 recognizes bacterial 23S rRNA devoid of erythromycin resistance-forming modification. Science 337, 1111-1115.
Olson, J.K., Miller, S.D., 2004. Microglia initiate central nervous system innate and adaptive immune responses through multiple TLRs. J Immunol 173, 3916-3924.
Parkin, J., Cohen, B., 2001. An overview of the immune system. Lancet 357, 1777-1789.
Pawate, S., Sriram, S., 2010. The role of infections in the pathogenesis and course of multiple sclerosis. Ann Indian Acad Neurol 13, 80-86.
Pender, M.P., Burrows, S.R., 2014. Epstein-Barr virus and multiple sclerosis: potential opportunities for immunotherapy. Clin Transl Immunology 3, e27.
Pennock, N.D., White, J.T., Cross, E.W., Cheney, E.E., Tamburini, B.A., Kedl, R.M., 2013. T cell responses: naive to memory and everything in between. Adv Physiol Educ 37, 273-283.
Perry, A.K., Chen, G., Zheng, D., Tang, H., Cheng, G., 2005. The host type I interferon response to viral and bacterial infections. Cell Res 15, 407-422.
Petry, H., Cashion, L., Szymanski, P., Ast, O., Orme, A., Gross, C., Bauzon, M., Brooks, A., Schaefer, C., Gibson, H., Qian, H., Rubanyi, G.M., Harkins, R.N., 2006. Mx1 and IP-10: biomarkers to measure IFN-beta activity in mice following gene-based delivery. J Interferon Cytokine Res 26, 699-705.
Pieper, K., Grimbacher, B., Eibel, H., 2013. B-cell biology and development. J Allergy Clin Immunol 131, 959-971.
Pradhan, V.D., Das, S., Surve, P., Ghosh, K., 2012. Toll-like receptors in autoimmunity with special reference to systemic lupus erythematosus. Indian J Hum Genet 18, 155-160.
Prinz, M., Garbe, F., Schmidt, H., Mildner, A., Gutcher, I., Wolter, K., Piesche, M., Schroers, R., Weiss, E., Kirschning, C.J., Rochford, C.D., Bruck, W., Becher, B., 2006. Innate immunity mediated by TLR9 modulates pathogenicity in an animal model of multiple sclerosis. J Clin Invest 116, 456-464.
Racke, M.K., 2009. Immunopathogenesis of multiple sclerosis. Ann Indian Acad Neurol 12, 215-220.
Rahman, A.H., Taylor, D.K., Turka, L.A., 2009. The contribution of direct TLR signaling to T cell responses. Immunol Res 45, 25-36.
Riera Romo, M., Perez-Martinez, D., Castillo Ferrer, C., 2016. Innate immunity in vertebrates: an overview. Immunology.
Rioux, J.D., Abbas, A.K., 2005. Paths to understanding the genetic basis of autoimmune disease. Nature 435, 584-589.
Saitoh, S., Miyake, K., 2009. Regulatory molecules required for nucleotide-sensing Toll-like receptors. Immunol Rev 227, 32-43.
Saresella, M., Gatti, A., Tortorella, P., Marventano, I., Piancone, F., La Rosa, F., Caputo, D., Rovaris, M., Biasin, M., Clerici, M., 2014. Toll-like receptor 3 differently modulates inflammation in progressive or benign multiple sclerosis. Clin Immunol 150, 109-120.
Sato, S., Sugiyama, M., Yamamoto, M., Watanabe, Y., Kawai, T., Takeda, K., Akira, S., 2003. Toll/IL-1 receptor domain-containing adaptor inducing IFN-beta (TRIF) associates with TNF receptor-associated

factor 6 and TANK-binding kinase 1, and activates two distinct transcription factors, NF-kappa B and IFN-regulatory factor-3, in the Toll-like receptor signaling. J Immunol 171, 4304-4310.
Sato, Y., Goto, Y., Narita, N., Hoon, D.S., 2009. Cancer Cells Expressing Toll-like Receptors and the Tumor Microenvironment. Cancer Microenviron 2 Suppl 1, 205-214.
Scheikl, T., Pignolet, B., Mars, L.T., Liblau, R.S., 2010. Transgenic mouse models of multiple sclerosis. Cell Mol Life Sci 67, 4011-4034.
Severa, M., Rizzo, F., Giacomini, E., Annibali, V., Gafa, V., Romano, S., Buscarinu, M.C., Fornasiero, A., Salvetti, M., Coccia, E.M., 2015. IFN-beta Therapy Regulates TLR7-Mediated Response in Plasmacytoid Dendritic Cells of Multiple Sclerosis Patients Influencing an Anti-Inflammatory Status. J Interferon Cytokine Res 35, 668-681.
Sfriso, P., Ghirardello, A., Botsios, C., Tonon, M., Zen, M., Bassi, N., Bassetto, F., Doria, A., 2010. Infections and autoimmunity: the multifaceted relationship. J Leukoc Biol 87, 385-395.
Shaw, P.J., Barr, M.J., Lukens, J.R., McGargill, M.A., Chi, H., Mak, T.W., Kanneganti, T.D., 2011. Signaling via the RIP2 adaptor protein in central nervous system-infiltrating dendritic cells promotes inflammation and autoimmunity. Immunity 34, 75-84.
Sheedy, F.J., O'Neill, L.A., 2007. The Troll in Toll: Mal and Tram as bridges for TLR2 and TLR4 signaling. J Leukoc Biol 82, 196-203.
Shirani, A., Tremlett, H., 2010. The effect of smoking on the symptoms and progression of multiple sclerosis: a review. J Inflamm Res 3, 115-126.
Simpson, S., Jr., Blizzard, L., Otahal, P., Van der Mei, I., Taylor, B., 2011. Latitude is significantly associated with the prevalence of multiple sclerosis: a meta-analysis. J Neurol Neurosurg Psychiatry 82, 1132-1141.
Singh, M.K., Scott, T.F., LaFramboise, W.A., Hu, F.Z., Post, J.C., Ehrlich, G.D., 2007. Gene expression changes in peripheral blood mononuclear cells from multiple sclerosis patients undergoing beta-interferon therapy. J Neurol Sci 258, 52-59.
Sloane, J.A., Batt, C., Ma, Y., Harris, Z.M., Trapp, B., Vartanian, T., 2010. Hyaluronan blocks oligodendrocyte progenitor maturation and remyelination through TLR2. Proc Natl Acad Sci U S A 107, 11555-11560.
Spiller, S., Dreher, S., Meng, G., Grabiec, A., Thomas, W., Hartung, T., Pfeffer, K., Hochrein, H., Brade, H., Bessler, W., Wagner, H., Kirschning, C.J., 2007. Cellular recognition of trimyristoylated peptide or enterobacterial lipopolysaccharide via both TLR2 and TLR4. J Biol Chem 282, 13190-13198.
Stadelmann, C., Wegner, C., Bruck, W., 2011. Inflammation, demyelination, and degeneration - recent insights from MS pathology. Biochim Biophys Acta 1812, 275-282.
Steinman, L., Zamvil, S., 2003. Transcriptional analysis of targets in multiple sclerosis. Nat Rev Immunol 3, 483-492.
Storey, M., Jordan, S., 2008. An overview of the immune system. Nurs Stand 23, 47-56; quiz 58, 60.
Sweeney, C.M., Lonergan, R., Basdeo, S.A., Kinsella, K., Dungan, L.S., Higgins, S.C., Kelly, P.J., Costelloe, L., Tubridy, N., Mills, K.H., Fletcher, J.M., 2011. IL-27 mediates the response to IFN-beta therapy in multiple sclerosis patients by inhibiting Th17 cells. Brain Behav Immun 25, 1170-1181.
Takeda, K., Kaisho, T., Akira, S., 2003. Toll-like receptors. Annu Rev Immunol 21, 335-376.
Thompson, M.R., Kaminski, J.J., Kurt-Jones, E.A., Fitzgerald, K.A., 2011. Pattern recognition receptors and the innate immune response to viral infection. Viruses 3, 920-940.
Touil, T., Fitzgerald, D., Zhang, G.X., Rostami, A., Gran, B., 2006. Cutting Edge: TLR3 stimulation suppresses experimental autoimmune encephalomyelitis by inducing endogenous IFN-beta. J Immunol 177, 7505-7509.
Trapp, B.D., Nave, K.A., 2008. Multiple sclerosis: an immune or neurodegenerative disorder? Annu Rev Neurosci 31, 247-269.

Trivedi, S., Greidinger, E.L., 2009. Endosomal Toll-like receptors in autoimmunity: mechanisms for clinical diversity. Therapy 6, 433-442.
Troutman, T.D., Bazan, J.F., Pasare, C., 2012. Toll-like receptors, signaling adapters and regulation of the pro-inflammatory response by PI3K. Cell Cycle 11, 3559-3567.
Turvey, S.E., Broide, D.H., 2010. Innate immunity. J Allergy Clin Immunol 125, S24-32.
Urcelay, E., Blanco-Kelly, F., de Las Heras, V., de la Concha, E.G., Arroyo, R., Martinez, A., 2007. TLR4 haplotypes in multiple sclerosis: a case-control study in the Spanish population. J Neuroimmunol 192, 215-218.
Vanderlugt, C.L., Miller, S.D., 2002. Epitope spreading in immune-mediated diseases: implications for immunotherapy. Nat Rev Immunol 2, 85-95.
Watters, T.M., Kenny, E.F., O'Neill, L.A., 2007. Structure, function and regulation of the Toll/IL-1 receptor adaptor proteins. Immunol Cell Biol 85, 411-419.
Weiner, H.L., Selkoe, D.J., 2002. Inflammation and therapeutic vaccination in CNS diseases. Nature 420, 879-884.
Weinstock-Guttman, B., Ramanathan, M., Zivadinov, R., 2008. Interferon-beta treatment for relapsing multiple sclerosis. Expert Opin Biol Ther 8, 1435-1447.
Werling, D., Jungi, T.W., 2003. TOLL-like receptors linking innate and adaptive immune response. Vet Immunol Immunopathol 91, 1-12.
Wingerchuk, D.M., 2012. Smoking: effects on multiple sclerosis susceptibility and disease progression. Ther Adv Neurol Disord 5, 13-22.
Yang, C.W., Strong, B.S., Miller, M.J., Unanue, E.R., 2010. Neutrophils influence the level of antigen presentation during the immune response to protein antigens in adjuvants. J Immunol 185, 2927-2934.
Yarovinsky, F., Zhang, D., Andersen, J.F., Bannenberg, G.L., Serhan, C.N., Hayden, M.S., Hieny, S., Sutterwala, F.S., Flavell, R.A., Ghosh, S., Sher, A., 2005. TLR11 activation of dendritic cells by a protozoan profilin-like protein. Science 308, 1626-1629.
Yu, J., Zhou, X., Nakaya, M., Jin, W., Cheng, X., Sun, S.C., 2014. T cell-intrinsic function of the noncanonical NF-kappaB pathway in the regulation of GM-CSF expression and experimental autoimmune encephalomyelitis pathogenesis. J Immunol 193, 422-430.
Yu, P., Lubben, W., Slomka, H., Gebler, J., Konert, M., Cai, C., Neubrandt, L., Prazeres da Costa, O., Paul, S., Dehnert, S., Dohne, K., Thanisch, M., Storsberg, S., Wiegand, L., Kaufmann, A., Nain, M., Quintanilla-Martinez, L., Bettio, S., Schnierle, B., Kolesnikova, L., Becker, S., Schnare, M., Bauer, S., 2012. Nucleic acid-sensing Toll-like receptors are essential for the control of endogenous retrovirus viremia and ERV-induced tumors. Immunity 37, 867-879.

# 7 Appendix I

## 7.1 EAE induction in *TLR379*$^{-/-}$ (Experiment II):

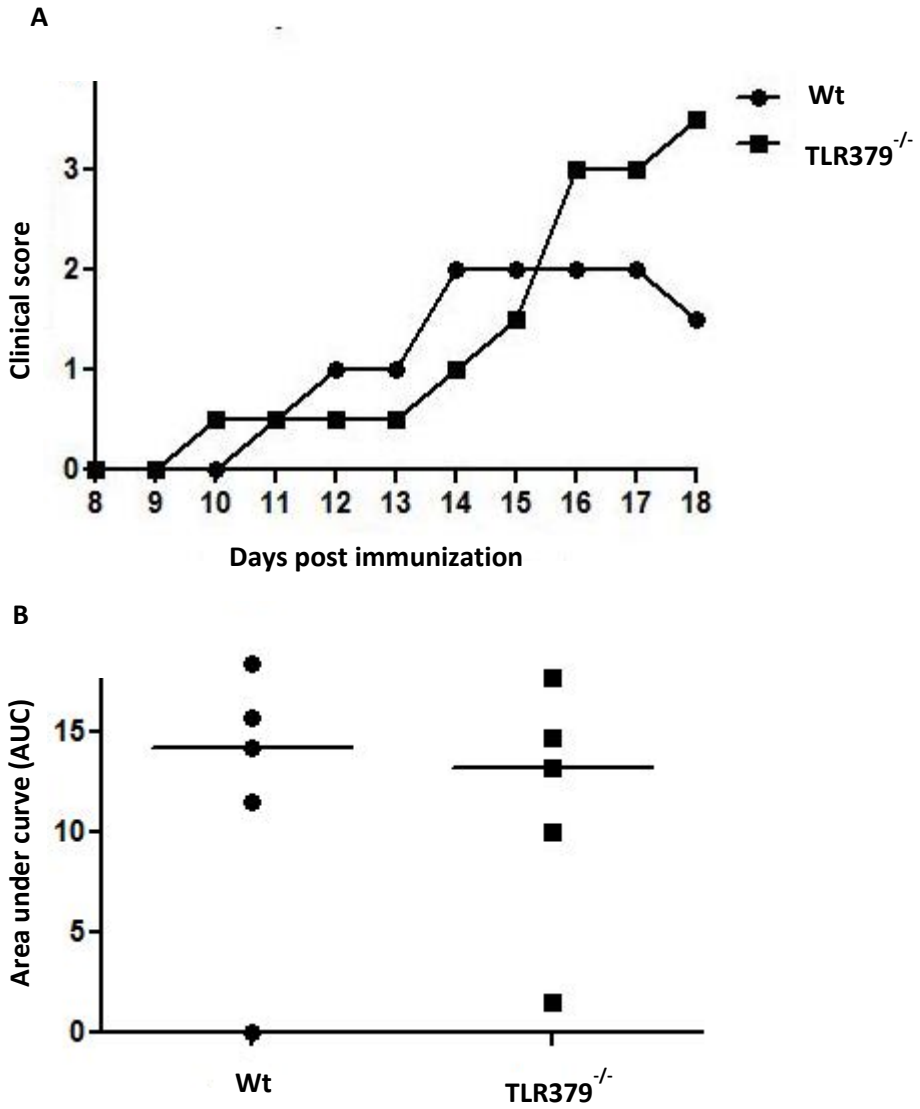


**Figure 32. Active EAE induction in *TLR379*$^{-/-}$, experiment II.**A) Both *TLR379*$^{-/-}$ (squares) and Wt (dots) female mice, 5 mice in each group were immunized with MOG peptide, CFA, PT and were scored daily

for EAE clinical signs. Each data point represents median per day from all the mice in that group. All *TLR379*$^{-/-}$ mice developed EAE clinical signs with 100% disease incidence and only 4 mice out of 5 developed EAE clinical signs in Wt group. B) Area under the curve (AUC) for each mouse was calculated during the EAE disease course and the middle line represents median. AUC was used to measure the overall disease severity between Wt and *TLR379*$^{-/-}$ . Using Mann-Whitney U test, no significant difference was found between the groups in disease severity at $p < 0.05$.

## 7.2 EAE induction in *TLR379*$^{-/-}$ (Experiment III):

**A**

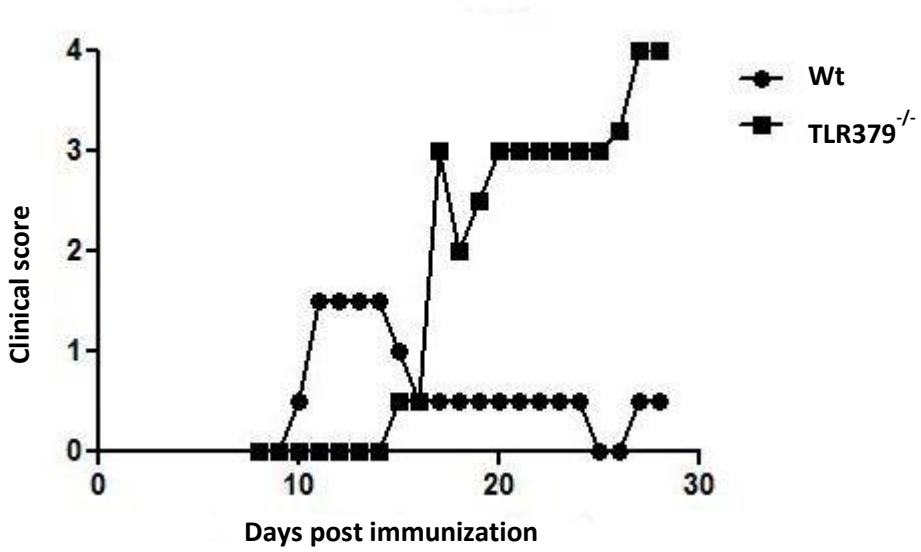

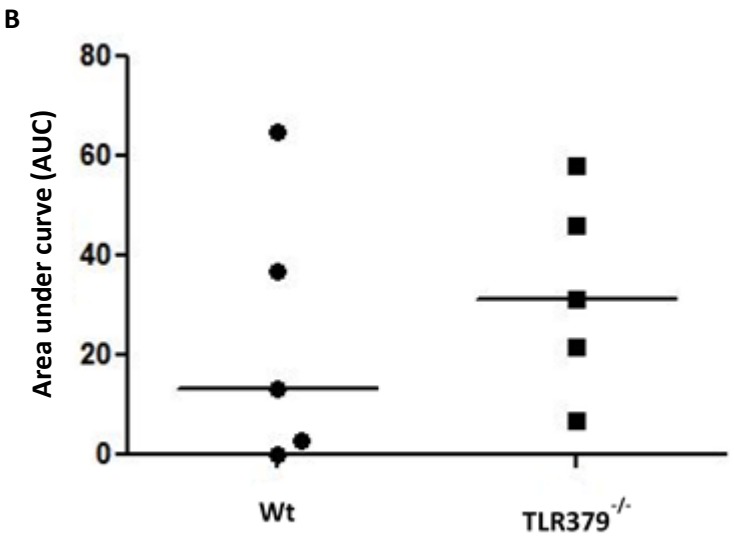


**Figure 33. Active EAE induction in *TLR379*$^{-/-}$, experiment III**. A) Both *TLR379*$^{-/-}$ (squares) and Wt (dots) female mice, 5 mice in each group were immunized with MOG peptide, CFA, PT and were scored daily for EAE clinical signs. Each data point represents median per day from all the mice in that group. All *TLR379*$^{-/-}$ mice developed EAE clinical signs with 100% disease incidence and only 4 mice out of 5 developed EAE clinical signs in Wt group with disease incidence of 80%. B) Area under the curve (AUC) for each mouse was calculated during the EAE disease course and the middle line represents median. AUC was used to measure the overall disease severity between Wt and *TLR379*$^{-/-}$ .Using Mann-Whitney U test, no significant difference was found between the groups in disease severity at $p < 0.05$.

## *7.3* Area under curve analysis, data pooled from all three active EAE induction experiments in *TLR379*$^{-/-}$ and Wt control groups.

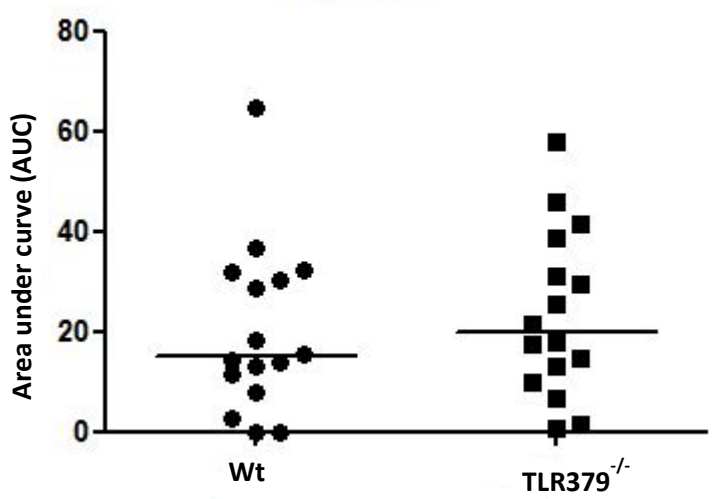

**Figure 34. Area under curve analysis, data pooled from all the three active EAE induction experiments in TLR379$^{-/-}$** Data pooled in from all the three active EAE induction experiments in *TLR379$^{-/-}$*. Both Wt (dots) and *TLR379$^{-/-}$ (Squares)* female mice were immunized with MOG peptide, CFA, PT and were scored daily for EAE clinical signs. In total from all the three experiments, 16 mice from Wt and 16 mice from *TLR379$^{-/-}$* group were used for analysis. In *TLR379$^{-/-}$* group, all 16 mice developed EAE clinical signs with disease incidence of 100% and in Wt group, only 14 mice out of 16 developed EAE clinical signs with disease incidence of 87%. Area under the curve (AUC) for each mouse was calculated during the EAE disease course and the middle line represents median. AUC was used to measure the overall disease severity between Wt and *TLR379$^{-/-}$* groups. Using Mann-Whitney U test, no significant difference was found between the groups in disease severity at $p<0.05$.

# 8 Appendix II

## 8.1 EAE induction in *TLR23479*$^{-/-}$ (Experiment II):

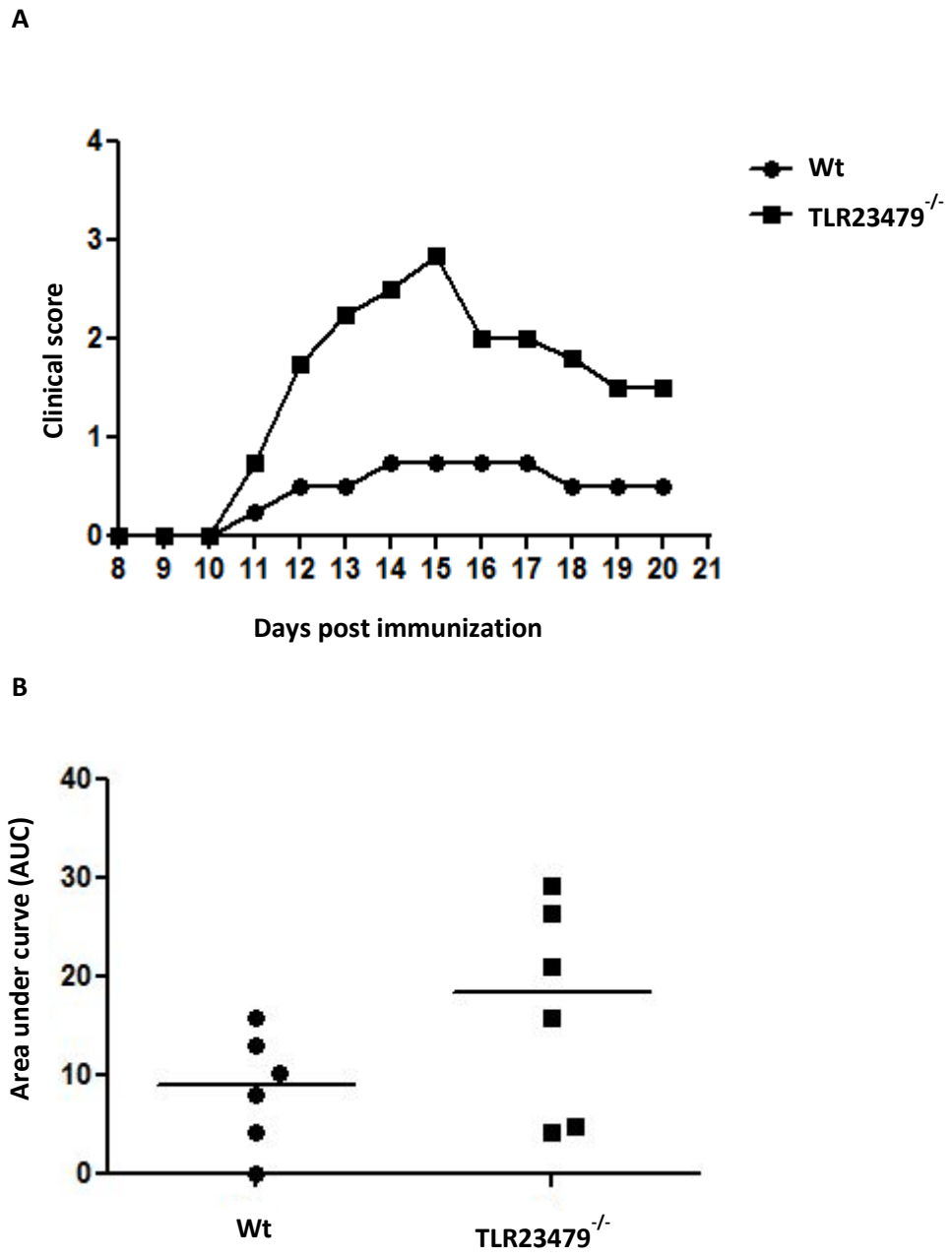


**Figure 35. Active EAE induction in *TLR23479*$^{-/-}$, Experiment II**. A) Both *TLR23479*$^{-/-}$ (squares) and Wt (dots) female mice, 6 mice in each group were immunized with MOG peptide, CFA, PT and were scored

daily for EAE clinical signs. Each data point represents median per day from all the mice in that group. All *TLR23479*$^{-/-}$ mice developed EAE clinical signs with 100% disease incidence and only 5 mice out of 6 developed EAE clinical signs in Wt group with disease incidence of 83%. B) Area under the curve (AUC) for each mouse was calculated during the EAE disease course and the middle line represents median. AUC was used to measure the overall disease severity between Wt and *TLR23479*$^{-/-}$ .Using Mann-Whitney U test, no significant difference was found between the groups in disease severity at $p < 0.05$.

## 8.2 EAE induction in *TLR23479*$^{-/-}$ (Experiment III):

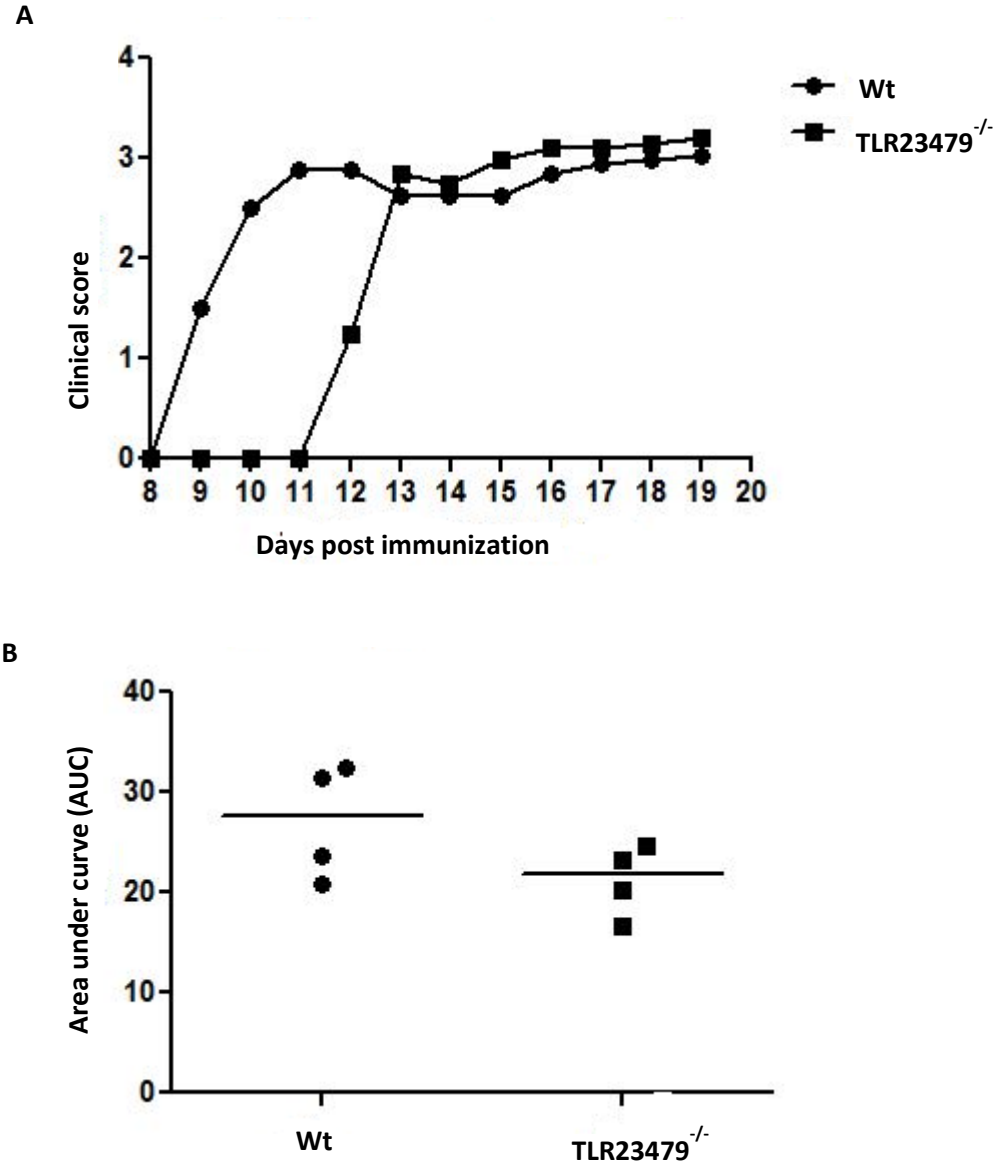

**Figure 36. Active EAE induction in *TLR23479$^{-/-}$*, experiment III.** A) Both *TLR23479$^{-/-}$* (squares) and Wt (dots) female mice, 4 mice in each group were immunized with MOG peptide, CFA, PT and were scored daily for EAE clinical signs. Each data point represents median per day from all the mice in that group. All *TLR23479$^{-/-}$* and Wt mice developed EAE clinical signs with 100% disease incidence. B) Area under the curve (AUC) for each mouse was calculated during the EAE disease course and the middle line represents median. AUC was used to measure the overall disease severity between Wt and *TLR23479$^{-/-}$* .Using Mann-Whitney U test, no significant difference was found between the groups in disease severity at $p < 0.05$.

## 8.3 Area under curve analysis, data pooled in from all the three active EAE inductions in *TLR23479$^{-/-}$* and Wt control groups.

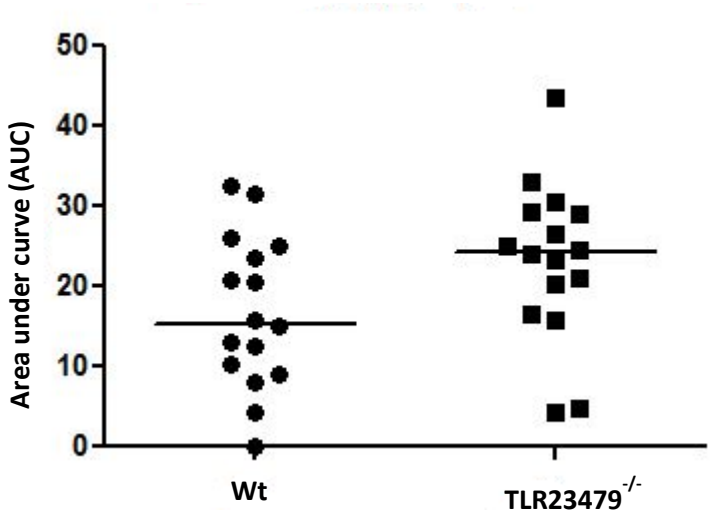


**Figure 37. Area under curve analysis, data pooled in from all the three active EAE inductions in *TLR23479$^{-/-}$* and Wt mice.** Data pooled in from all the three active EAE induction experiments in *TLR23479$^{-/-}$*. Both Wt (dots) and *TLR23479$^{-/-}$* (Squares) female mice were immunized with MOG peptide, CFA, PT and were scored daily for EAE clinical signs. In total from all the three experiments, 16 mice from Wt and 16 mice from *TLR23479$^{-/-}$* group were used for analysis. In *TLR23479$^{-/-}$* group, all 16 mice developed EAE clinical signs with disease incidence of 100% and in Wt group, only 15 mice out of 16 developed EAE clinical signs with disease incidence of 93%. Area under the curve (AUC) for each mouse was calculated during the EAE disease course and the middle line represents median. AUC was used to measure the overall disease severity between Wt and *TLR23479$^{-/-}$* groups. Using Mann-Whitney U test, no significant difference was found between the groups in disease severity at $p<0.05$.

# 9 Appendix III

## 9.1 Active EAE induction in *TLR3*$^{-/-}$ female mice (Experiment II):

**A**

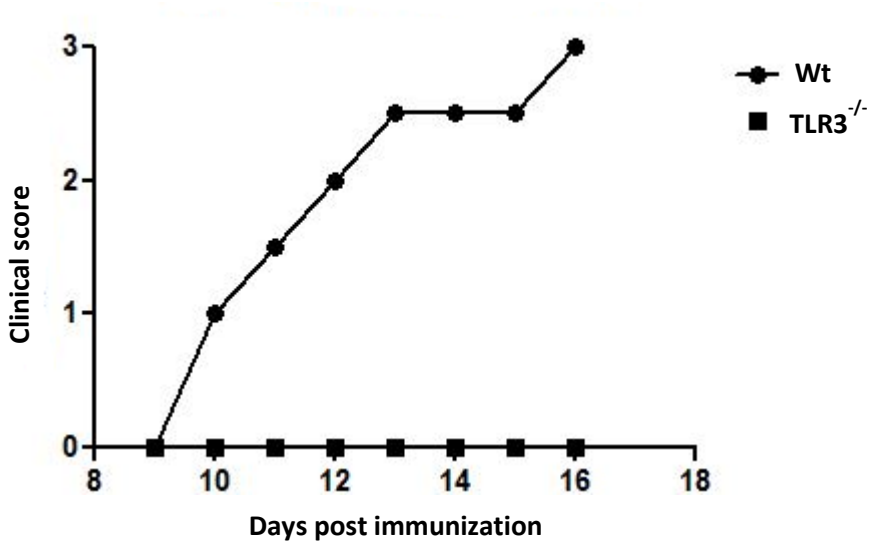


**B**

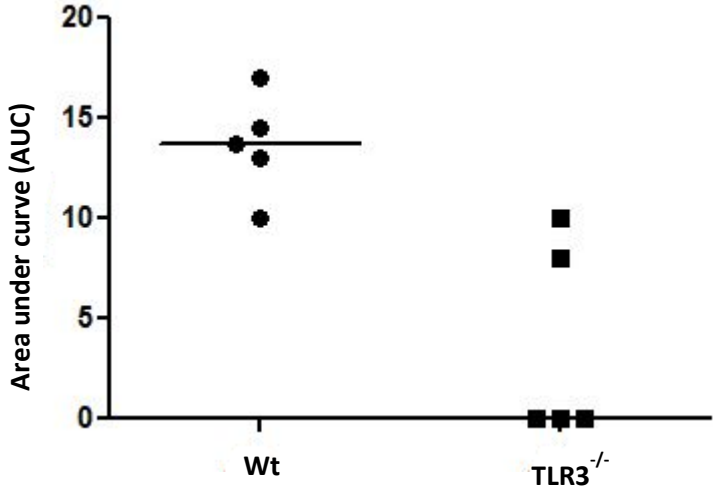

**Figure 38.Active EAE induction in *TLR3*$^{-/-}$, Experiment II**: A) Both *TLR3*$^{-/-}$ (squares) and Wt (dots) female mice, 5 mice in each group were immunized with MOG peptide, CFA, PT and were scored daily for EAE clinical signs. Each data point represents median per day from all the mice in that group. All Wt mice developed EAE clinical signs with 100% disease incidence. In *TLR3*$^{-/-}$ group, out of 5 mice only 2 mice developed EAE clinical signs with disease incidence of 40% B) Area under the curve (AUC) for each mouse was calculated during the EAE disease course and the middle line represents median. AUC was used to measure the overall disease severity between Wt and *TLR3*$^{-/-}$ .Using Mann-Whitney U test, a significant difference was found between the groups in disease severity at $p < 0.05$.

## 9.2 Active EAE induction in *TLR3*$^{-/-}$ female mice (Experiment III)

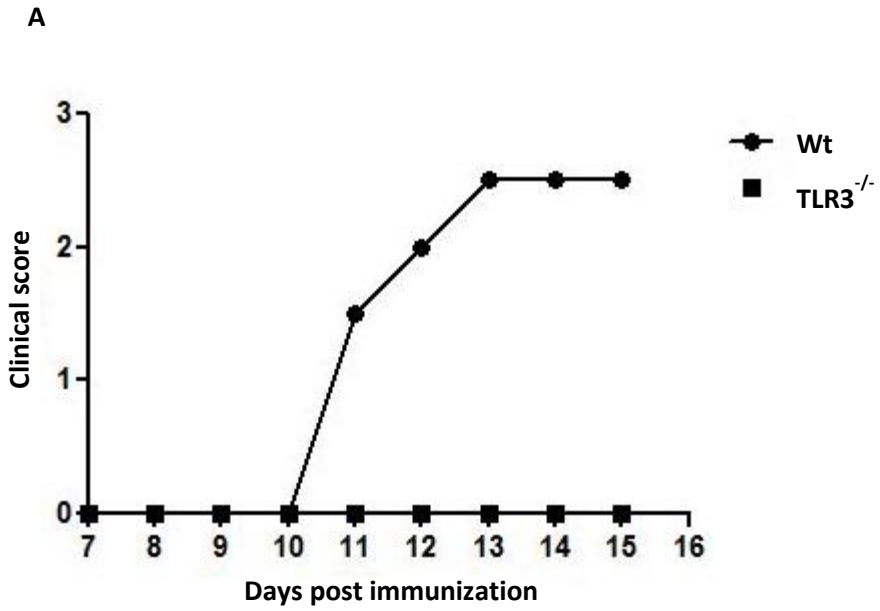

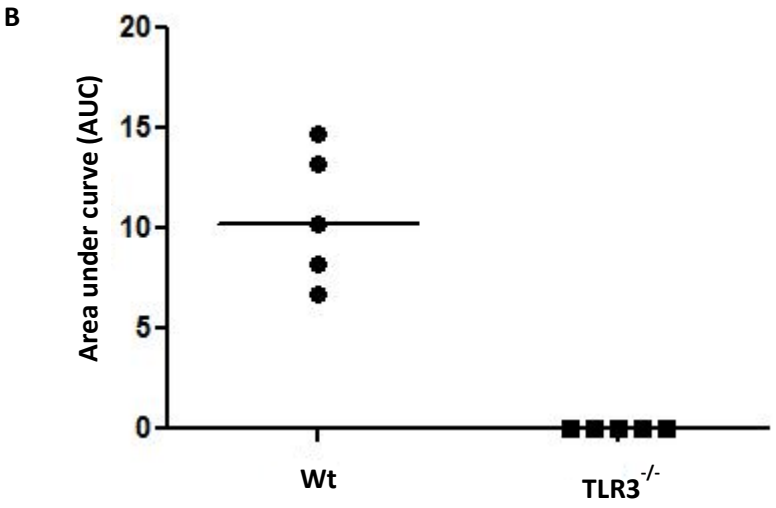


**Figure 39 Active EAE induction in *TLR3*$^{-/-}$ mice, Experiment III.** A) Both *TLR3*$^{-/-}$ (squares) and Wt (dots) female mice, 5 mice in each group were immunized with MOG peptide, CFA, PT and were scored daily for EAE clinical signs. Each data point represents median per day from all the mice in that group. All Wt mice developed EAE clinical signs with 100% disease incidence. In *TLR3*$^{-/-}$ group, none of the five mice developed EAE B) Area under the curve (AUC) for each mouse was calculated during the EAE disease course and the middle line represents median. AUC was used to measure the overall disease severity between Wt and *TLR3*$^{-/-}$ . Using Mann-Whitney U test, a significant difference was found between the groups in disease severity at $p<0.05$.

## 9.3 Area under curve analysis, data pooled in from all the three active EAE induction experiments in *TLR3*$^{-/-}$ and Wt female mice

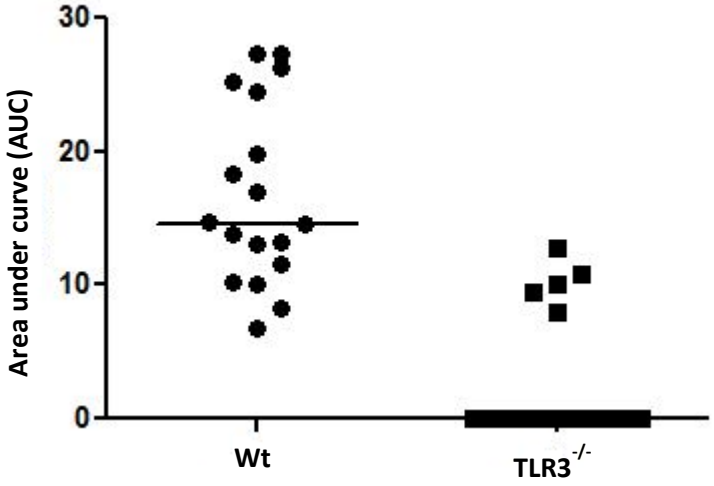

**Figure 40. Area under curve analysis, data pooled in from all the three active EAE induction experiments in *TLR3*$^{-/-}$ and Wt female mice**. Data pooled in from all the three active EAE induction experiments in *TLR3*$^{-/-}$. Both Wt (dots) and *TLR3*$^{-/-}$ (Squares) female mice were immunized with MOG peptide, CFA, PT and were scored daily for EAE clinical signs. In total from all the three experiments, 18 mice from Wt and 21 mice from *TLR3*$^{-/-}$ group were used for analysis. In Wt group, all 18 mice developed EAE clinical signs with disease incidence of 100% and in *TLR3*$^{-/-}$ group, only 5 mice out of 21 developed EAE clinical signs with disease incidence of 23%. Area under the curve (AUC) for each mouse was calculated during the EAE disease course and the middle line represents median. AUC was used to measure the overall disease severity between Wt and *TLR3*$^{-/-}$ groups. Using Mann-Whitney U test, a significant difference was found between the groups in disease severity at $p<0.05$.

# 10 ACKNOWLEDGEMENTS

The memories of attending DAAD PhD fellowship interview in New Delhi are still fresh in my mind. It's been 6 years from then and it's been a life changing experience. I will be ever grateful to German Academic Exchange Service (DAAD) for the PhD fellowship. Without that financial aid this thesis would not have been possible. Through DAAD I have met some wonderful people and had a great time in Germany.

First and foremost, I would like to thank my supervisor Prof.Thorsten Buch for his constant support, encouragement and motivation. I thank him for his time, guidance and valuable discussions. I would like to thank him for the opportunities he provided that helped me grow.

I would like to thank my thesis committee members, Prof.Clarissa Prazeres da Costa and Prof. Martin Klingenspor for their support and valuable comments.

I would like to thank the collaborators and people who contributed towards this thesis work. Firstly, I would like to thank Nora Hagemeyer, Prinz lab at University of Freiburg for performing histology. I thank Katharina Borst, Prof.Ulrich Kalinke lab, Twincore facility, Hannover for performing experiments with Δβ−luc mice. I thank Raphaela Semper for performing ELISA. I thank Filipa Marques Ferreira, my fellow lab mate for help with experiments and for performing qPCR analysis.

Its great pleasure to thank my fellow lab mates both in Munich and Zurich. I extend special thanks to Martin Skerhut for help with animal experiments. I thank Ravindra, Jane, Lynsey, Olivia, Silvia, Karin, Sabine and Filipa for their constant support and stimulating discussions.

I thank my friends in Munich and Zurich for always being there for me and for being my family in a foreign country.

Finally, I thank my parents for their phenomenal support, love and confidence they have shown in me. I am indebted to them for all the affection and constant encouragement that helped me stay calm in rough times. I thank my brother and sister for helping me to keep my spirits high and for all the funny conversations that made life pretty awesome thing.